CIVIL ENGINEERING STUDIES
STRUCTURAL RESEARCH SERIES NO. 139

STRENGTH IN SHEAR OF PRESTRESSED CONCRETE BEAMS WITHOUT WEB REINFORCEMENT

A Thesis
by
M. A. SOZEN

Issued as a Part
of the
SIXTH PROGRESS REPORT
of the
INVESTIGATION OF PRESTRESSED CONCRETE
FOR HIGHWAY BRIDGES

AUGUST, 1957
UNIVERSITY OF ILLINOIS
URBANA, ILLINOIS

STRENGTH IN SHEAR OF PRESTRESSED CONCRETE BEAMS WITHOUT WEB REINFORCEMENT

A Thesis by
M. A. Sozen

Issued as a Part of the Sixth Progress Report of the
INVESTIGATION OF PRESTRESSED CONCRETE
FOR HIGHWAY BRIDGES

Conducted by
THE ENGINEERING EXPERIMENT STATION
UNIVERSITY OF ILLINOIS

In Cooperation With
THE DIVISION OF HIGHWAYS
STATE OF ILLINOIS
and
U. S. DEPARTMENT OF COMMERCE
BUREAU OF PUBLIC ROADS

Urbana, Illinois
August 1957

TABLE OF CONTENTS

TABLE OF CONTENTS (Continued)

LIST OF TABLES

LIST OF FIGURES

LIST OF FIGURES (Continued)

LIST OF FIGURES (Continued)

LIST OF FIGURES (Continued)

I. INTRODUCTION

1. Object and Scope

The experimental studies described in this report were undertaken to obtain information about the behavior of simply-supported prestressed concrete beams with straight tension reinforcement only. Since beams are seldom subjected to flexure alone, and since beams with straight tension reinforcement only are extremely vulnerable to the effects of inclined tensile stresses, the investigation was mainly concerned with "shear" strength. The beams were loaded to failure under one or two concentrated loads within four to six hours. Studies of the effects of the following primary variables were included in the test program: (1) Shape of cross-section, (2) prestress level, (3) length of shear span, (4) amount of longitudinal reinforcement, and (5) concrete strength.

These tests were planned and carried out primarily to serve as a basis for the planning of investigations of beams with various types of web reinforcement. They were started by E. M. Zwoyer in 1952. His observations from tests of rectangular beams led to the formulation of the shear-compression hypothesis (1,2)*. Tests of rectangular beams were followed by tests of I-beams with two different web thicknesses. The results from all beams tested in the course of this investigation are presented and discussed in this report with emphasis on inclined tension cracking. An empirical expression for the inclined tension cracking load is offered, and the shear-compression hypothesis is restated to reflect the observed phenomenon more closely.

2. Outline of Tests

This report is based on the results of tests on 99 simply-supported prestressed concrete beams. The overall cross-sectional dimensions for all the beams

---

* Numbers in parentheses refer to entries in the Bibliography at the end of this volume.

were 6 by 12 in. All beams, except four rectangular beams which were tested over a seven-foot span, had nine-foot spans. Only straight longitudinal tension reinforcement was used. The series comprised 43 rectangular beams, 33 I-beams with 3-inch thick webs, and 23 I-beams with 1 3/4-inch thick webs. The properties of all specimens are listed in Table 1. The ranges of the variables are given below:

Rectangular Beams

Bond:

Post-tensioned and grouted.....35 beams

Pretensioned..... 8 beams

Prestress:

90,000 to 140,000 psi.....21 beams

35,000 to 90,000 psi.....14 beams

Zero to 35,000 psi..... 8 beams

Longitudinal Reinforcement Ratio: 0.10 to 0.96 per cent

Concrete Strength: 2600 to 6220 psi

Shear Span:

54 in..... 4 beams

36 in.....35 beams

24 in..... 4 beams

I-beams with Three-inch Thick Webs

Bond: All beams pretensioned

Prestress:

90,000 to 140,000 psi.....19 beams

35,000 to 90,000 psi..... 7 beams

Zero..... 7 beams

Longitudinal Reinforcement Ratio: 0.179 to 0.604 percent

Concrete Strength: 1750 to 8560 psi

Shear Span:

54 in..... 4 beams

36 in.....25 beams

28 in..... 4 beams

I-beams with 1 3/4-inch Thick Webs

Bond: All beams pretensioned

Prestress:

90,000 to 140,000 psi..... 9 beams

35,000 to 90,000 psi..... 8 beams

Zero..... 6 beams

Longitudinal Reinforcement Ratio: 0.181 to 0.797 percent

Concrete Strength: 2060 to 7310 psi

Shear Span: 36 in. for all beams

3. Acknowledgment

The studies reported herein were made as a part of an investigation of prestressed concrete for highway bridges conducted in the Talbot Laboratory of the Engineering Experiment Station of the University of Illinois in cooperation with the Division of Highways, State of Illinois, and the U. S. Department of Commerce, Bureau of Public Roads.

The program of the investigation has been guided by an advisory committee on which the following persons have served during the period covered by the work described in this report: E. F. Kelley, E. L. Erickson, R. Archibald, and Harold Allen, representing the Bureau of Public Roads; W. E. Chastain, Sr., W. J. Mackay, and C. E. Thunman, Jr., representing the Illinois Division of

Highways; and N. M. Newmark, C. P. Siess, I. M. Viest, and N. Khachaturian, representing the University of Illinois.

The project has been under the general direction of N. M. Newmark and the immediate direction of C. P. Siess. The work was initiated under the immediate supervision of J. H. Appleton, formerly Research Associate in Civil Engineering.

Much of the prestressing reinforcement used in this work was provided without charge by the American Steel and Wire Division of the U. S. Steel Corporation.

Appreciation is due R. J. Allen, J. H. Appleton, D. F. Billet, and E. M. Zwoyer for their contributions to the development of the prestressing and testing equipment.

Most of the rectangular beams and four I-beams were tested by Zwoyer.

The following research personnel gave valuable assistance in conducting the tests, and reducing and presenting the data: R. J. Allen, P. C. Gardner, G. Hernandez, T. J. Larsen, and R. A. Sachs.

This report was written as a thesis under the direction of Professor Siess. His suggestions and teaching are gratefully acknowledged.

4. Notation

(a) Designation of Test Specimens

Although the specimens were numbered originally according to the order of testing, for easier reference, they have been regrouped and redesignated according to the major variables. Each beam is designated by one letter and two pairs of numerals, e.g., B.12.50. The letter refers to the web thickness. The first numeral indicates the level of prestress, and the second the length of the shear span. The second pair of numerals represents the Q-value to two significant figures.

The code for the first three symbols in the designation is as follows:

Letter (B.12.50)

A.....Rectangular beam

B.....I-beam, 3-inch web

C.....I-beam, 1 3/4-inch web

First Numeral (B.12.50)

1.....90,000 to 140,000 psi prestress

2.....35,000 to 90,000 psi prestress

3.....Zero to 35,000 psi prestress

Second Numeral (B.12.50)

1.....54-in. shear span

2.....36-in. shear span

3.....28-in. shear span

4.....24-in. shear span

It should be noted here that most of the specimens at the high, medium, and low prestress levels (designated 1,2 and 3) were prestressed to about 120,000 psi, 60,000 psi, and zero, respectively. The beams with 54-in. shear spans were loaded at midspan by a single load. The others had two loads symmetrically located about midspan. The beams with 24-in. shear spans (designated 4) had a total span of seven feet. All others had a span of nine feet.

(b) Symbols

Cross-sectional Constants

A_c = gross area of cross-section

A_s = total area of reinforcement

b = top flange width

b' = web thickness

d = effective depth of the reinforcement

Loads

F_{se} = effective prestressing force

P_c = applied load at inclined tension cracking

P_u = ultimate applied load

V_c = applied shear at inclined tension cracking

M_c = applied bending moment at inclined tension cracking

M'_c = total bending moment at the loading point, corresponding to inclined tension cracking

M_u = total ultimate bending moment

M_t = total ultimate moment measured in test

C = total compressive force in the concrete

T = total tensile force in the reinforcement

Stresses

Concrete

f'_c = compressive strength determined from 6 by 12-in. control cylinders

f_{cu} = average concrete stress in compression zone at failure

f_r = modulus of rupture determined from 6 by 6 by 24-in. control beams loaded at the third-points over an 18-in. span

f_t = assumed tensile strength of concrete

E_c = assumed modulus of elasticity of concrete

v = nominal shear stress

Steel

f_{se} = effective prestress

f_{sc} = stress in reinforcement at inclined tension cracking

f_{su} = stress in reinforcement at failure of beam

f'_s = ultimate tensile strength of reinforcement

E_s = modulus of elasticity of steel

Strains

Concrete

ϵ_u = limiting strain at which concrete crushes in a beam

ϵ_c = concrete strain

ϵ_{cc} = concrete strain on top surface of beam at loading point, corresponding to inclined tension cracking

ϵ_{ce} = concrete strain at level of reinforcement, due to effective prestress

Steel

ϵ_{se} = steel strain corresponding to effective prestress

ϵ_{sc} = steel strain at inclined tension cracking

$\epsilon'_{sc} = \epsilon_{sc} - (\epsilon_{se} + \epsilon_{ce})$

ϵ_{su} = steel strain at failure of beam

$\epsilon_{sa} = \epsilon_{su} - (\epsilon_{se} + \epsilon_{ce})$ = increase in steel strain after zero concrete strain at level of reinforcement is reached

$\epsilon'_{sa} = \epsilon_{su} - \epsilon_{sc}$ = increase in steel strain after inclined tension cracking

Dimensionless Factors

$p = A_s/bd$ = reinforcement ratio

k_u = ratio of neutral axis depth at failure to effective depth

k_c = ratio of neutral axis depth at inclined tension cracking to effective depth

k_2 = ratio of depth of the compressive force to effective depth

a/d = ratio of shear span length to effective depth

F = apparent strain compatibility factor

F_1 = strain compatibility factor before inclined tension cracking

F_2 = strain compatibility factor after inclined tension cracking

$Q = pE_s/f'_c$

II. MATERIALS, FABRICATION, AND TEST SPECIMENS

5. Materials

(a) Cements. Marquette brand Type I Portland Cement was used for the post-tensioned specimens. Marquette or Atlas brand Type III Portland Cement was used for the pretensioned specimens and the grout. The types of cement used in the beams are listed in Table 2. The cement was purchased from local dealers in lots of 20 or 40 bags.

(b) Aggregates. Wabash River sand and gravel were used for all beams. Both aggregates have been used in this laboratory for many previous investigations and have passed the usual specification tests. Two types of coarse aggregate were used, one graded to 1 1/2-inch maximum size and the other to 3/8-inch maximum size. The types of coarse aggregate used in the various beams are given in Table 2.

The origin of these aggregates is an outwash of the Wisconsin glaciation. The major constituents of the gravel were limestone and dolomite with minor quantities of quartz, granite and gneiss. The sand consisted mainly of quartz. The absorption of both the fine and the coarse aggregate was about one percent by weight of surface-dry aggregate.

A fine Lake Michigan beach sand was used in the grout mixes.

(c) Concrete Mixes. Mixes were designed by the trial batch method. The proportions by weight of the batches used in each beam are given in Table 2. The figures are based on actual weights corrected for the measured amount of free moisture. The following properties of each batch, in addition to the proportions, are listed in Table 2: slump, compressive strength and modulus of rupture at time of beam test, age, type of cement, and type of aggregate.

The characteristics of the mixes made with Type III cement are summarized in Figs. 1 and 2. Interpolated seven-day compressive strengths are compared with water-cement ratio on Fig. 1. Figure 2 shows the increase with age, expressed as a ratio of the seven-day strength, for concrete batches made with Type III cement.

On Figs. 3 and 4, the moduli of rupture determined from control beams are compared with compressive strengths. The control beams were 6 by 6 in. in cross-section and were loaded at the third-points of an 18-in. span. The results for concrete with 1 1/2-in. maximum size coarse aggregate are shown on Fig. 3, and those for concrete with 3/8-in. maximum size coarse aggregate are shown on Fig. 4. As would be expected, the larger coarse aggregate yielded a higher modulus of rupture for the same concrete strength. Since a measure of the tensile strength of the concrete in each beam was necessary for the interpretation of the test results, and since the scatter in the data did not warrant use of the results of individual control beams, two expressions were selected to represent a statistical average of the accumulated data. These were as follows:

For concrete with large-size coarse aggregate:

$$f_r = \frac{3000}{2 + \frac{12,000}{f'_c}} \qquad (1)$$

For concrete with small-size coarse aggregate:

$$f_r = \frac{3000}{4 + \frac{12,000}{f'_c}} \qquad (2)$$

The values of the modulus of rupture, f_r, and compressive strength, f'_c, are all in pounds per square inch.

(d) Grout Mixes. The grout mixes had equal proportions by weight of fine Lake Michigan beach sand and Type III Portland cement. The water-cement

ratios ranged from about 0.40 to 0.55. Approximately 6 grams of aluminum powder per 100 pounds of cement was added to counteract shrinkage. The grout attained a strength of about 3000 psi as determined from 2 by 4-in. cylinders at three days.

(e) Reinforcing Wire. Single wire reinforcement from seven different lots was used. The properties of the reinforcement are listed in Table 3.

Lot I was a straightened and stress-relieved single wire reinforcement. Lots II, VI, VII, VIII and IX, were stress-relieved and not straightened. Lot III was an unstraightened galvanized wire. The galvanizing was removed with hydrochloric acid.

Information about the manufacture of the steel was made available by the American Steel and Wire Division of the United States Steel Corporation. The manufacture of the straight wire designated as Lot I involved the following steps: (1) hot rolling ingots into rods of suitable size, (2) patenting, i.e. quenching from an austenitizing temperature by immersion in hot lead, (3) wet-drawing cleaned and lime-coated rods to finished size through wire drawing soap, (4) machine straightening, and (5) stress-relieving 15 minutes at 750°F. Step (4) was omitted in the manufacture of Lots VI, VII, VIII, and IX. These unstraightened wires were stress-relieved by immersion in hot lead at a temperature of about 800°F. The time of immersion depended on the size of the wire and ranged from 5 to 15 seconds.

Lots II and III were stress-relieved wires manufactured by John A. Roebling Sons Corporation.

The unstraightened wires were received in coils about 5 ft. in diameter and weighing from 200 to 350 pounds. When uncoiled, the wires tended to describe an arc with a radius of approximately six feet. The straightened wire was received in 15-foot lengths.

In order to improve the bond, the cut lengths of wire were first wiped with a rag dipped in a weak solution of hydrochloric acid and then rusted by storing in a moist room for several days. Insulating tape was wrapped around the wire at the intended locations of electric strain gages. On being removed from the moist room, the rusted wires were cleaned with a wire brush to remove all loose rust.

The stress-strain relationships for the different lots determined from tests of samples cut from different portions of each coil are shown in Figs. 5 through 10. The deformation, up to three percent strain, was measured with an eight-inch extensometer employing a Baldwin "microformer" coil and recorded with an automatic device.

6. Description of the Specimens

(a) Post-Tensioned Rectangular Beams. The post-tensioned rectangular beams were nominally 6 by 12-in. in cross-section and 10 ft. 5 in. long. They were cast with a rectangular hole to provide a channel for the single wire reinforcement which extended in a straight line through the length of the beam. The dimensions and location of this hole in the beam are shown in Fig. 11. At about one foot away from each end of the beam, access holes were formed for grouting. After the reinforcement was tensioned, the channel was grouted. However, the end-anchorages were not released.

(b) Pretensioned Rectangular Beams. The pretensioned rectangular beams were nominally 6 by 12 in. in cross-section and 10 ft. 10 in. long. The single wire reinforcement extended in a straight line through the length of the beam. No end-anchorages were used during the tests.

(c) Pretensioned I-Beams. The nominal overall measurements for all I-beams were 6 by 12 in. by 10 ft. 10 in. The I-beams of Series B had web thicknesses

of 3 in., and the I-beams of Series C, 1 3/4 in. The nominal dimensions are shown on Fig. 12. The single wire reinforcement was straight, as in the rectangular beams. End-anchorages were used initially in some specimens; however, since no slip of the wires was observed, this precaution was abandoned. The end-blocks were about 18-in. long. All but three of the I-beams had prestressed external stirrups to prevent propagation of cracks into the end-block. Four stirrups were used on each beam. One stirrup was placed at each junction of the web and the end-block, and one immediately on the outside of each reaction block.

7. Casting and Curing

All concrete was mixed in a non-tilting drum-type mixer of 6-cu. ft. capacity. A butter mix of one cu. ft. preceded two batches of about four cu. ft. each which were used in the specimens. The mixing time for each batch was from three to six minutes. Before batching, samples of the aggregates were taken for free moisture tests. Slump was determined immediately after mixing.

Metal forms were used. A hole was formed in the lower part of the post-tensioned beams (Fig. 11) to provide a channel for the single wire reinforcement. The core form for the hole was composed of eight half-inch round steel rods, four one-inch angles, ten rubber tubes, and a sheet rubber cover made from automobile inner-tubes. The rods were spaced by steel templates at each end, and the rubber tubes were placed between and outside the rods. The angles were placed at the corners to form a nearly rectangular core. The strip of sheet rubber, about four inches wide, was then wrapped continuously around the angles and tubes. The entire core unit was placed in the beam form along with steel end-plates which slipped over the ends of the core unit and helped to support it. At about one foot from the ends of the beam, one-inch diameter access holes (Fig. 11) from the top of the beam to the grout channel were formed with short lengths of garden hose.

The reinforcement was already in the forms before the casting of the pretensioned beams. Since the clear distance between the wires was about one-half inch, the coarse aggregate used in all but four of these beams was pea gravel having a maximum size of 3/8 in.

The first batch was placed in a layer of uniform height through the beam and filled about three-quarters of the depth. The second batch was placed on top of the first batch. Consequently, all the concrete in the compression zone of the beam was from the same batch.

Four 6 by 12-in. control cylinders and one 6 by 6 by 24-in. control beam were cast from the first batch. Eight control cylinders and one beam were cast from the second batch.

The freshly cast concrete in the test beam and in the control beams and cylinders was vibrated with a high frequency internal vibrator. The tops of the test beam and control beams were troweled smooth and the cylinders were capped with a paste of neat cement four or five hours after casting. Experience indicated that it was best to loosen the sides of the forms for the I-beams about three or four hours after casting. Otherwise, the sides stuck to the beam despite the form oil and it was very difficult to remove them without damaging the beam. Several specimens were lost in this way.

The post-tensioned beams were removed from the forms the day after they were cast and stored in a constant temperature moist room for six days. After this period, they were kept in the laboratory until the time of test.

The pretensioned beams were removed from the forms after the wires were released and stored in the laboratory. The tension in the wires was released after the tests of control cylinders indicated adequate strength which usually took two to four days depending on the intended seven-day concrete strength and

the prestressing force. The tension was released by slowly loosening the nuts so that the tension in each of the wires was approximately equal at all times. Beams, in which the magnitude and/or eccentricity of the prestressing force were high enough to cause high tensile stresses at the top fiber, were prestressed externally at the top before release of the wires. The "top prestress" was removed in the very early stages of the test. In all cases, the control specimens were stored under the same conditions as the test beams.

8. Prestressing

(a) End Details of Wires

Threaded connections were used to grip the wire in the tensioning process. Specially heat-treated chasers with 24 threads to the inch were used in an automatic threading machine to cut the threads on the end three inches of the wires. Despite the heat treatment, the chasers required resharpening after threading fifteen to eighteen wires. The threads on the wires were cut to provide a medium fit with the threads in the nuts, requiring a thread slightly larger than No. 10 with a basic major diameter of 0.190 in.

The 5/8-in. long hexagonal nuts used in almost all of the specimens were specially manufactured in the laboratory machine shop. They were sub-drilled with a No. 16 tap drill and tapped with a standard No. 12, 24 threads to the inch tap. This provided a full No. 12 thread in the nuts. Nuts with a No. 10 thread required too much material to be cut from the wires to be practical. The thread cut on the wires to fit the No. 12 thread in the nuts was sufficient to develop at least 160,000 psi in the wires for several days and was considered to be the most suitable.

The nuts were made from "Buster" alloy punch and chisel steel of the following analysis range; Carbon 0.56-0.60 percent; Chromium, 1.10-1.30 per

cent; Tungsten, 2.00-2.30 per cent; Vanadium, 0.20-0.30 percent. The hardening process involved the following steps: (1) Packing in charcoal in a closed steel box, (2) heating for 20 minutes at 1200°F, (3) heating for 45-60 minutes at 1650°F, (4) oil quenching to slightly above room temperature, (5) tempering at 1000°F for 30 minutes, and (6) removal from the furnace and air cooling.

(b) Tensioning Apparatus

Post-Tensioned Beams. A 30-ton Simplex center-hole hydraulic ram operated by a 10,000-psi capacity Simplex pump was used to tension the reinforcement. Figure 14 is a photograph of the apparatus in place during the prestressing of a beam. A jacking frame bolted to the bearing plate provided a reaction for the jack; the bearing plate reacted against the beam. To tension the wires, the ram reacted against the frame and a 5/8-in. rod. The thrust was transferred from the ram to the rod through a washer and nut, and from the rod to the wire through a threaded union connection. When the wire was tensioned to the desired stress, a nut was turned up tight against one or two shims.

The bearing plates for the post-tensioned beams are shown schematically in Fig. 13, and in place on a beam in Fig. 14. The 6 by 6 by 2-in. plates were heavy enough so that a fairly uniform bearing pressure was produced on the ends of the beam. The heavy bearing plates were used in order to eliminate the need for special reinforcement near the ends of the beam, and proved to be satisfactory in this respect.

Pretensioned Beams. The same tensioning equipment was used for pretensioning the wire reinforcement as for post-tensioning. However, since the reinforcement was tensioned before the beam was cast, a reaction had to be provided for the tensioning force. The reaction consisted of the prestressing frame shown in Fig. 15. It was made from two lengths of extra heavy three-in. pipe, and two

bearing plates 6 by 2 by 21 in. The plates were provided with four rows of six 0.206-in. diameter holes spaced at 11/16-in. vertically and laterally to accommodate various positions of the wires. To tension the wires, the ram reacted against the jacking frame and a 5/8-in. rod as in the post-tensioned beams. However, instead of the thrust being absorbed by the beam through the jacking frame, it was transferred from the jacking frame to the prestressing frame which was built to fit around the form for the beam. The wires were tensioned and secured against the prestressing frame in the same manner as for post-tensioning.

(c) Measurement of Tensioning Force

The tensioning force in each wire was determined by measuring the compressive strain in small aluminum dynamometers placed on the wire between the nut and the bearing plate at the end of the beam opposite that at which the tension was applied. The dynamometers were made of 2-in. lengths of 9/16-in. or 1/2-in. aluminum rod, with 0.2-in. diameter holes drilled through their centers. Strains were measured by means of two type A7 SR-4 electric strain gages. These gages, attached to opposite sides of each dynamometer, were wired in series, giving a strain reading which was the average of the strain in the two gages. The dynamometers were calibrated using the 6000-lb range of a 120,000-lb. capacity Baldwin hydraulic testing machine. The calibrations of the dynamomters were nearly the same; the strain increment necessary to measure a tensioning stress of 120,000 psi in the 0.196-in. wires was 1500 and 2000 millionths for the 9/16-in. and 1/2-in. diameter dynamometers, respectively. This large increment of strain allowed a fairly precise measurement of stress in the wires, since the strain indicator used had a sensitivity of 2 or 3 millionths.

At the dynamometer end of the wire, the prestress was transferred from the wire to the dynamometer through a nut, and from the dynamometer to the beam

through the bearing plate. Figure 13 shows a schematic drawing of this arrangement.

(d) Tensioning Procedure

Post-Tensioned Beams. Before inserting the wires into the grout channel, one end of each wire was threaded through one of the bearing plates and secured with a nut. Then all wires were pulled through the hole in the beam at the same time. The wires were then threaded through the other bearing plate and the plates secured to the ends of the beam with a thin layer of "Hydrocal" gypsum plaster. The dynamometers were then slipped onto the wires at one end of the beam and finally the anchoring nuts were put on both ends of each wire. After taking readings on all of the strain gages, the wires were tensioned individually. The jacking frame was attached to the bearing plate and the pull-rod connected to the wire. The center-hole ram was placed over the pull-rod and each wire in turn was tensioned to the desired value of stress. The anchor nut was turned up snug against the shim, and the pressure on the ram was released. Since the beam underwent a certain amount of elastic shortening with the tensioning of the wires, the first wires to be stressed had to be retensioned if an exact value of stress was desired. However, if there were more than two rows of wires, it was very difficult to make adjustments on the interior wires after the anchorages on the other wires were in place. In such cases the wires were initially overstressed to compensate for elastic losses.

Pretensioned Beams. The reinforcement for the pretensioned beams was tensioned in the prestressing frame prior to casting the beam. The ends of the wires were slipped through the end plates of the forms and through the bearing plates of the prestressing frame. The dynamometers were then slipped onto one end of the wires and the anchoring nuts were put on both ends of each wire. Some of the wires had Type A12 or A7 SR-4 electric strain gages located at midspan. After

making strain measurements on the wires and dynamometers in an unstressed condition, the wires were tensioned individually. This procedure was identical to that of the post-tensioned beams except that the prestressing frame underwent greater elastic shortening than the post-tensioned beams and greater adjustment was required to give the wires the desired amount of initial tension. Figure 15 shows the prestressing frame and the tensioning apparatus.

Since pre-tensioned beams experienced a greater loss of prestress prior to testing than did the post-tensioned beams, it was necessary to make the initial prestress higher in order to have the same effective prestress at the time of test.

(e) Grouting

For the post-tensioned beams, following the tensioning of the reinforcement, grout was pumped into the beam to provide bond between the wires and the surrounding concrete. The grout was placed through a vertical hole located about one foot from the end of the beam as shown in Fig. 11. Pumping was continued until grout was forced out of a similar hole at the other end of the beam.

The grout pump was constructed of a 5-in. diameter steel cylinder about 30 in. long and a 1 1/2-ton hydraulic auto bumper jack. A steel plate with a hole threaded for a hose connection was welded to the lower end of the cylinder. A piston with a cupped pump leather attached was bolted to the base of the bumper jack. The jack was rigidly attached to the cover of the pump in such a manner that the plunger of the jack extended into the cylinder and drove the piston. This arrangement permitted rapid refilling of the pump. The grout was pumped through a heavy rubber hose into the beam. The capacity of the jack was such that a pressure of more than 100 psi could be developed, but the grout flowed freely and the pressure developed in the grout undoubtedly much less than 100 psi. The grout was mixed in a counter-current, horizontal, tub type mixer of 2-cu ft capacity.

III. INSTRUMENTATION, LOADING APPARATUS, AND TEST PROCEDURE

9. Electric Strain Gages

(a) Strain Gages on Reinforcing Wire

Except for a few beams where Type A12 SR-4 gages were used, strains in the wires were measured with Type A7 SR-4 electric strain gages which have a nominal gage length of 1/4 in. and a minimum trim width of 3/16 in. They were chosen for their narrow width, short length, and flexibility. The gages were placed at midspan on two or three wires located symmetrically about the center of gravity of the wire group. The surface of the wire was prepared for gage application by using fine emery cloth and acetone. The gage was mounted with Duco cement. After several hours of air drying, heat lamps were used to hasten the drying of the cement. The gages were then waterproofed using Cycleweld or Petrolastic*. The simplest and most efficient method of waterproofing was found to be the following: Before turning off the heat lamps, N. 18 Type FL solid lead wires were soldered to the terminals of the gage and firmly attached to the wire so that there would be no danger of pulling out the gage filaments during handling. While the wire was still warm, the gage was covered with a short length of insulating tape and molten Petrolastic was brushed on the gage, one layer at a time, to an average thickness of 1/4 to 3/8 in. The uninsulated parts of the leads were kept under this cover.

(b) Strain Gages on Concrete

Type A1 or A3 SR-4 electric strain gages were used to measure concrete strains in most of the specimens. These gages have a nominal gage length of 3/4 in. and a minimum trim width of 3/16 in. A portable grinder was used to grind the

---

* Asphaltic compound manufactured by Standard Oil of California.

spots where gages were to be applied. These spots were later smoothed with sand paper. Before the mounting of the gage, a thin film of Duco cement was applied and allowed to dry for about fifteen minutes. Then the gage was mounted with Duco cement. Steel weights of one pound were left on the gages for a period of one hour. A cushion of sponge rubber was placed under each weight. The Type A3 gages were much easier to apply. The gages were mounted usually 1 to 2 days before test. No waterproofing or curing was used.

From 9 to 15 strain gages were used on the top surface of each specimen. The gages were located at a 3-in. spacing near the load points and at 6 or 12 in. elsewhere. In all but a few of the specimens they were placed along the longitudinal center-line of the beams. Wherever strain distributions are presented in the text, the locations of the gages are indicated.

10. Loading Apparatus

The specimens were loaded either in a screw-type testing machine (Fig. 16) or in a specially constructed frame (Fig. 17). Most of the rectangular beams were tested in a 200,000-lb. Olsen testing machine, three in a 300,000-lb. Riehle machine, and two in the loading frame. Some of the I-beams were tested in the 200,000-lb. Olsen machine, four in the 300,000-lb. Riehle machine, and the remaider in the loading frame. The load was always applied through a 50,000-lb. elastic-ring dynamometer. For the midspan-loaded specimens, the distributing beam was omitted. The loading blocks were 6 by 6 by 2-in. steel plates. Two pieces of leather were inserted between the beam and each load block so as to leave a surface about two-inches wide along the beam center line free of contact with the steel. This was done to permit the application of electric strain gages beneath the load point. In the I-beam with high values of Q, one leather piece 4 by 4 in. was centered under the loading block to prevent transverse bending of the top flange. The bearing blocks at the reactions were also 6 by 6 by 2-in. steel plates. The

block at one end was supported on a "half-round" and that at the other end on a roller to provide for elongation of the beam during test.

11. Measurements

The load was measured by means of a 50,000-lb. elastic-ring dynamometer equipped with a 0.0001-in. dial indicator. The dynamometer calibration was 110.8 to 111 lb. per division.

Deflections were measured at midspan and at the third-points with 0.001 in. dial indicators.

Strains in the longitudinal reinforcement and on the top surface of the beam were measured by electric strain gages.

The cracks were marked on the sides of the beams after each increment of load and the number of the increment at which the crack was observed was marked on the beam beside the pertinent crack. Photographs were taken at different stages of the test to be kept as a permanent record of the development of the crack pattern.

The distance from the top of the beam to the principal inclined or vertical crack was measured for almost all beams in the final stages of the test, and mechanical measurements of strain on the sides of the beams were made for some rectangular beams. However, these data are not reported.

After completion of each test, the width of the flange, the depth of the beam and the reinforcement, and the thickness of the web in the case of I-beams were measured at the section of failure.

12. Test Procedure

Normally, the failure load was reached in 10 to 15 increments. After each increment of load, all deflection and strain measurements were taken and the cracks were marked. This took about 20 minutes. Load and mid-span deflections were measured immediately after the interruption and before the resumption of loading.

The specimens were loaded very slowly when the estimated flexural or inclined tension cracking loads were being approached. Usually the load was applied in three equal increments up to the flexural cracking load. After it was reached, the magnitude of each increment depended on the development of the crack pattern.

Loading was continued to complete failure in every case. Each test took four to six hours.

Control specimens were tested concurrently with or immediately after the beam test.

IV. BEHAVIOR OF TEST SPECIMENS

13. Load-Deflection Relationships

A very significant overall property of a structural member is its response to load which is almost completely described by the load-deflection relationship. Load-deflection curves are useful in studying behavior at working loads, estimating resistance to impulsive loads, and determining the range of safe working loads. The load-deflection curves determined from tests of reinforced or prestressed concrete beams failing in shear cannot be used directly for such purposes like those of beams failing in flexure, since part of the ductility, if any, is contributed by the opening up of the inclined tension cracks. Nevertheless, the curves are of value in evaluating and comparing "load-worthiness". The characteristics of load-deflection curves for prestressed concrete beams failing in shear have been studied only qualitatively in this report. Billet (3) has discussed deflections quantitatively for beams failing in flexure. As emphasized in later sections, beams with practical levels of prestress should not be relied on beyond inclined tension cracking, and up to this point their behavior should be reasonably similar, both qualitatively and quantitively, to comparable beams failing in flexure. After inclined tension cracks form, the prediction of the deflections of beams without web reinforcement would be very erratic and of little practical significance.

The load-deflection curves for all the specimens are presented in Figs. 18 through 31. The curves have been grouped according to web thickness, level of prestress, and type of loading. Each figure contains the data for beams having the same or similar values of these variables so that the differences of the curves reflect roughly the effects of concrete strength and amount of longitudinal steel,

except in the figure pertaining to I-beams loaded at midspan. It should be noted here that two different scales have been used in plotting these curves. Consequently, not all the curves can be compared directly with each other.

On the basis of the load-deflection curves alone, two distinctly different stages can be defined. Stage 1 corresponds to that part of the curve before flexural cracking. The two can be distinguished from each other by the shape of the load-deflection curve. In the first stage the curve is practically linear; in the second stage it is not.

The extent of the first stage depends on the compressive stress exerted by the prestressing force on the bottom beam fiber, the modulus of rupture of the concrete, and the type of loading. If the stress-strain relationships for steel and concrete are known, the flexural cracking load and the deflections up to this load can be computed on the basis of an uncracked section analysis. However, because of the inherent variations in the properties of concrete, such computations cannot be very accurate. In general, the measured and computed flexural cracking loads agreed reasonably well for beams with the high prestress level. The error in the estimates of the flexural cracking load increased with an increase in the relative contribution of the modulus of rupture to the cracking load. The deflection up to the flexural cracking load could be estimated with reasonable accuracy using a slightly modified form of Jensen's expression for the modulus of elasticity of concrete. This was

$$E_c = \frac{30,000}{6 + \frac{10}{f'_c}} \qquad (3)$$

The second stage of the load-deflection relationship is characterized by a constantly changing rate of increase of deflection with load. Except for beams with very low values of Q, the beams failing in shear seldom if ever had a flat or

nearly flat region in their load-deflection curves. The occurrence of inclined tension cracking could not be detected by any significant change in the load-deflection curves.

The differences between load-deflection curves of beams failing in shear and flexure may best be discussed in terms of specific examples. Figures 32a and 32b show such curves for rectangular beams failing in shear and flexure. The properties of the beams are listed on the figures. All four beams were loaded at the third-points over simple spans of nine feet. The load-deflection curves for beams B-23 and B-24, which failed in flexure and which had prestressed external stirrups to prevent inclined cracks, were taken from Billet (3). The observed inclined tension cracking loads are marked on curves for Beams A.12.34 and A.12.31. Both comparisons indicate essentially the same trends. Before inclined tension cracking, the only differences between the curves for beams failing in shear and flexure are those that can be attributed to differences in the concrete strength, amount and location of reinforcement, and to some slight effect of cracks in the shear span. This is brought out especially by the curves on Fig. 32a which pertain to specimens having almost identical properties. The ultimate load is less in the case of the shear failure. However, the ultimate deflection at midspan is nearly equal for both types of failure. As discussed before, the normal deflection due to bending is augmented by that due to the opening of inclined tension cracks in the case of the shear failures.

Comparisons of load-deflection curves for I-beams failing in shear and flexure are presented on Fig. 33. The load-deflection curves for beams G-4 and G-12 are taken from tests of I-beams with conventional vertical web reinforcement carried out by G. Hernandez. The curves for I-beams with three-inch webs on Fig.

32a indicate that in the second stage, Beam B.12.35 deflects at a significantly faster rate than G-12 in which the inclined cracks were restrained by the stirrups. The ultimate load for B.12.35 was less than that for G-12, but the ultimate deflections were comparable. A more interesting comparison is shown on Fig. 33b. Both beams G-4 and C.12.44 were I-beams with 1.75-in. webs. Beam G-4 had conventional U-stirrups as web reinforcement. Besides having no web reinforcement, beam C.12.44 did not have the prestressed external stirrups near the support which were used in the I-beam tests. Its failure was simultaneous with the formation of the inclined tension crack. Needless to say, in such cases the load-deflection curves for shear failures are hardly comparable to those for flexural failures.

The effect of prestress level on the load-deflection curves of rectangular beams failing in shear are illustrated on Fig. 34a. As the prestress level is increased, both the flexural and inclined tension cracking loads increase. The ultimate midspan deflection is comparable for all three cases, but there is a palpable improvement in the ultimate load with increase in prestress, caused primarily by the attendant increase in the inclined tension cracking load. Also, the "life" of the beam, in terms of the load carried beyond inclined cracking becomes proportionately shorter as the prestress level is raised.

The effects of both web thickness and prestress level are illustrated in Fig. 34b which shows load-deflection curves for four I-beams having nearly the same values for concrete strength and reinforcement ratio, p, but different values of web thickness and prestress level. It should be noted prior to any discussion that these beams have a rather high value of Q and are not typical of beams normally encountered in practice. However, their load-deflection curves emphasize strongly the differences in behavior caused by the variables considered. The additional load-carrying capacity contributed by the prestress at the expense of

some ductility is indicated clearly in the figure. This increase is wholly due to the increase in the inclined cracking load. The ratio of the load at ultimate to that at inclined tension cracking is about two for the beams with zero prestress, and is one for the beams with prestress. The increase in web thickness appears to have improved the load carrying capacity at both levels of prestress.

14. Measured Concrete Strains

(a) Measurements

Concrete is not an ideal material for the application of electric strain gages. Its porosity, heterogeneity, and water content are not conducive to accurate local measurements with such gages. However, hundreds of electrical strain gages have been used to measure concrete strains with reasonable success in Talbot Laboratory during the last fifteen years. In this particular investigation, one-inch electrical strain gages were used on the top surface of the beams to determine the concrete strains at crushing and to obtain an understanding of the development and distribution of concrete strains along the length of the span. Neither of these goals demands precision and short gage lengths are necessitated by the non-uniform distribution of strains over the length of the beam. Warwaruk (4), in tests of beams with aggregate similar to that used in these beams, found that the readings of the one-inch electric strain gages were corroborated by those of mechanical strain gages. For these reasons, the use of the one-inch electrical strain gages in these tests is believed to be justified.

The strain data from each gage were plotted against the measured midspan deflection to determine if the readings were consistent. However, there was no way of checking the magnitude of the readings, other than a general comparison of all the data. The values of the strains at crushing were obtained from extrapolations of the strain-deflection curves. For locations affected by the inclined

cracks, these curves could be idealized by three straight lines at different slopes. The part before flexural cracking had a high slope. The shortening of the depth to the neutral axis after flexural cracking resulted in a reduction in slope. Inclined cracking caused strain concentrations which raised the slope near the loadpoints, and redistributions of stress which lowered the slope near the reactions.

(b) Strain at First Crushing

It has been established that the crushing strain for concrete in flexure is practically independent of the concrete strength. Various investigators have assigned values ranging from 0.003 to 0.004 to this critical strain depending on the instrumentation and type of loading used in the tests. The values of the crushing strain measured in the course of this investigation are plotted against the concrete strength in Fig. 35. The data were obtained from the beams that failed in flexure or in shear-compression. Preliminary plots showed virtually no influence of geometry of cross-section, size of coarse aggregate, or type of cement. On the basis of the data in Fig. 35, which show no trend with the concrete strength, a constant value of 0.004 was adopted for the crushing strain. Warwaruk (4), from a study of his results and those of Gaston, Billet, Feldman and Allen, has come to similar conclusions.

From the scatter of the data, which may be partially attributed to experimental error, it is evident that for any given case the crushing strain may be 25 percent above or below any assumed average value. It should also be noted that the crushing strains considered here are those for concrete in flexure. Under different conditions of stressing, the apparent magnitude of the crushing strain and its significance may be quite different.

(c) Distribution of Concrete Strain on Top Surface of Beam

The distributions of concrete strains determined from electric strain gages on the top surface were extremely useful in interpreting the behavior of the beams. Such distributions at various stages of loading for beams B.12.07, B.12.14, and B.12.34 are presented on Fig. 36, 37, and 38, respectively. These beams have similar properties except for value of Q. Beam B.12.07 failed in flexure. Beams B.12.14 and B.12.34 failed in shear-compression. The plotted strain distributions for these beams are of interest from two points of view. They show typical strain distributions for shear-compression and flexural failures as well as the changes in these distributions as cracks developed under increasing load.

Comparison of the final distributions on Figs. 36 and 38 illustrate the difference between distributions for flexure and shear-compression failures. The strains are fairly uniformly distributed over the flexure span of beam B.12.07, which failed in flexure, but are not uniformly distributed over the flexure span of beam B.12.34, which failed in shear-compression. For B.12.34, there are concentrations of high strain at the top of the inclined cracks, while the strain at midspan is comparatively low. The final distribution on Fig. 37 represents an intermediate case for which the concentrations are not much higher than the strain at midspan, resulting in a shear-compression failure that is hard to distinguish from a flexural failure on the basis of strength or ductility.

The development of the strain distributions can be followed by comparing the distributions on Fig. 36 through 38. The first distribution on each figure refers to conditions before inclined cracking, as the crack patterns indicate. At this stage, the distributions are qualitatively similar for the three beams, and are all fairly uniform. The second set of distributions correspond to conditions after inclined cracking for beams B.12.14 and B.12.34. The second distribution

for B.12.07 is plotted for maximum load and at this stage the strains are still fairly uniform. On the other hand, strain concentrations are present in the distributions for B.12.14 and B.12.34, and these concentrations are more pronounced on the sides where the development of inclined cracking is more advanced. The strains on the left shear span of B.12.34 are less than they were prior to the initiation of inclined cracking. Further development of the strain distributions are shown on the bottom plot of each figure which represents the condition at failure by crushing of the concrete. For beam B.12.17, the strains at this stage have increased more or less uniformly over the flexure span. In beam B.12.14, the strains near the tops of the inclined cracks and at midspan have increased at a comparable rate, while in beam B.12.34, which has the highest Q-value of the three, the strains near the inclined cracks have increased at a faster rate than those at midspan, and the strains in the shear span have decreased. All beams failed by crushing of the concrete at locations indicated by the higher strains.

To recapitulate, it appears from the measured distributions of strains on the top surface of the beam that inclined cracking causes concentrations of strain resulting in crushing of the concrete at a location within or immediately adjacent to the flexure span although comparable strains are not developed throughout the flexure span. Such concentrations, of necessity do not exist prior to the development of inclined cracking, and if inclined cracking occurs at a load close to the flexural capacity, the concentrations and their effects cannot be drastic. However, if the cracking load is considerably less than the flexural capacity, the concentrations and their effects are of the utmost significance in determining the strength and behavior of the beam.

(d) Relation Between Critical Concrete and Steel Strains

Because of the basic assumptions involved in the interpretation of shear-compression failure as described in this report, it is interesting to study the

increase in concrete strains with increase in steel strain. Ideally, the concrete strain measured at the location of the failure should be compared with the steel strain measured at the same section. This could not be done, because, although measurements of the concrete strain at or immediately near the zones of crushing were available, the steel strains were measured only near midspan. However, since the steel strains should be relatively constant throughout the flexure span, it was deemed feasible to compare the critical concrete strains with the steel strain at midspan. This study was further justified by the facts that trends rather than exact values were sought and the steel strain gage was almost always located at a cracked section.

A representative plot of steel vs. concrete strains is shown on Fig. 39. The increases during test in measured concrete and steel strains are plotted as ordinates and abscissas, respectively. Curves A, B, and C are for the concrete strains at locations shown in the sketch of beam C.12.19 from which the data were taken.

Curves A and C are fairly similar in all respects. Before flexural cracking, the rate of increase of concrete strain with steel strain is high. After flexural cracking, the relation between concrete and steel strains changes, and remains constant up to the load corresponding to the development of inclined cracking, where there is a sudden change in the slope of the curve. Curve B which refers to concrete strain at midspan is not affected by inclined cracking.

In general, these curves indicate that the relation between concrete and steel strains are distinctly different before and after inclined cracking. However, if the inclined cracks were prevented or restrained, curves A and C would be expected to be similar to curve B.

15. Tensile Stresses and Their Effects

In order to satisfy equilibrium conditions, tensile stresses develop in a transversely loaded structural member acting essentially as a beam. These stresses are horizontal, that is, parallel to the longitudinal axis of the beam, at points where no shearing stresses exist. At points where there are shearing stresses, the maximum principal tensile stress is inclined with respect to the longitudinal axis of the beam. In members made of concrete, for which tensile and compressive strengths are normally in the ratio of 1 to 12, the tensile stresses are critical.

In order to make full use of the compressive strength of concrete, it has become common practice always to use horizontal steel reinforcement on the tension side of concrete beams. It has not been common practice, however, always to provide reinforcement against the inclined tensile stresses. Web reinforcement is frequently omitted, sometimes with and sometimes without good reasons.

The following discussion of the cracking of concrete under tension is confined to simply-supported bonded prestressed concrete beams without web reinforcement, loaded statically over moderate spans of constant or nearly constant shear. It is assumed that cracking of the concrete is a stress phenomenon, and its very probable time-dependence is ignored.

As the load on the beam is increased, a crack caused by the horizontal tensile stress is initiated at the bottom fiber in a region of maximum bending moment when the tensile stress exceeds the sum of the compressive prestress on that fiber and the modulus of rupture, this latter quantity being determined with the aid of the conventional flexure formula from plain concrete beams stressed more or less in the same manner. The crack is vertical.

An inclined-tension crack starts at a point in the shear span when the sum of a component of the compressive stress in a certain direction and the tensile strength of the concrete is exceeded by the tensile stress in that direction. The tensile strength of the concrete in the beam is not as easy to determine as the modulus of rupture. The inclined crack may be initiated either prior or subsequent to a vertical or nearly vertical crack at the same location and with almost any inclination, depending on the combination of shear, flexure, and prestressing stresses.

As the horizontal-tension crack moves perpendicularly towards the neutral axis of the beam, more and more of the necessary internal tensile reaction is supplied by the horizontal steel.

As long as beam action is maintained, the propagation of the inclined-tension crack is accompanied by an increase in the inclined tensile stresses which is only partially compensated by the horizontal reinforcement.

The penetration of the horizontal-tension crack is limited by the relative load-carrying capacities of the horizontal steel in tension and the concrete in compression. The crack extends almost to the neutral axis.

The propagation of the inclined-tension crack is never stopped, but only diverted by the relatively high compressive stresses in the compression zone of the beam. The crack may extend to above the neutral axis.

The horizontal-tension crack does not greatly disturb the linearity of the strain distribution over the depth of the cross-section. Beam-action is preserved at all stages of its development.

The inclined-tension crack distorts the strain distribution over the depth of the cross-section severely. After its full development, beam-action is replaced by arch-action, and the member may fail in a manner associated with the

latter. Following the formation of the inclined-tension crack, bond and horizontal shear stresses assume greater significance.

The behavior of all but a few of the beams without web reinforcement tested in the course of this investigation was significantly and detrimentally affected by inclined tension cracking. This is to be expected, since the premise behind the omission of web or inclined reinforcement is of the same nature as that behind the omission of longitudinal reinforcement. The difference is a matter of degree.

One of the primary objectives of this investigation was to study the behavior and establish the modes of failure of prestressed concrete beams with longitudinal reinforcement only. The observed development of inclined and horizontal tension cracks and their consequences are described qualitatively in the following sections.

16. Definition of Shear and Flexural Failures

In reinforced concrete literature it has almost always been tacitly assumed that there is a distinct difference between shear and flexural failures, and that the two types of failure can readily be distinguished on the basis of behavior. Although this is generally true, it is an equally valid fact that there is a transition range between shear and flexure failures. If its properties place a beam in this transition range, the manner of failure may not be much different whether it fails in shear or in flexure. For example, an increase in the value of Q with the other variables remaining constant will tend to induce shear failure beyond a critical value or range of values of Q. Unless the mechanism of failure changes drastically, it is reasonable to expect that a beam having a value of Q slightly over the critical value will fail in shear; however, neither its capacity

nor its behavior should be significantly different from those of a beam having a slightly lower value of Q.

Thus, the distinction made below with respect to shear and flexure failures does not necessarily distinguish the details of behavior. It is based on the initial cause of the failure. In the case of flexural failure, the ultimate cause of failure can also be easily incorporated in the definition. In the case of the shear failure, it is not convenient to present a definition that also includes the various ultimate causes of failure which are described in the following sections.

A beam is said to have failed in flexure if it fails by crushing of the concrete or fracture of the longitudinal reinforcement as a result of bending stresses.

A beam is said to have failed in shear if its failure is initiated by an inclined tension crack resulting from a combination of bending and shearing stresses.

The question of primary bond failure is ignored in this report. It is felt that a primary bond failure is mainly a result of poor proportioning and irrelevant to the general discussion of behavior. When it is considered that for the same beam, a shear failure is more violent than a flexural failure and results in lower carrying and energy-absorbing capacities, and also that, in prestressed concrete beams, the addition of a little web reinforcement may prevent a shear failure, it also becomes doubtful whether shear failures are "typical".

17. Flexural Failures

This series of tests was carried out to investigate shear strength; however, a few of the beams failed in flexure. Their behavior was typical of bonded prestressed concrete beams failing in flexure. All but one of these beams, in

which the longitudinal reinforcement fractured, failed by crushing of the concrete. At failure, the concrete strains were nearly uniform over the length of the flexure span and no critical inclined tension cracks had developed in the specimens with the low Q-values. Failure was gradual and gentle.

18. Shear Failures

(a) Development of Cracks

Up to the time of inclined tension cracking, the behavior of beams that failed in shear was not different from the behavior of beams that failed in flexure.

In all the specimens tested, the flexural crack or cracks at midspan were the first to form. Others soon followed in the flexure span, if the beam had one, at a spacing of about six inches. This spacing was somewhat wider for the post-tensioned and grouted beams. Except for the beams which had extremely high ratios of the prestressing force to the cross-sectional area, the cracks developed to their full height in the early stages of the test. In most of the beams, the cracks in the shear span were initiated by horizontal tension, and thus originated vertically. However, these cracks "bent over" in a very short distance.

The occurrence of flexural cracks decreased the stiffness of the beam; there was a definite reduction in the slope of the load-deflection curve, this reduction being less for beams with high values of Q than those with low values of Q. There was also an accompanying increase in the rates of increase of steel and top concrete strains with load.

Before the development of severe inclined tension cracking, the outer portion of the shear span over which the moment was less than the cracking moment remained uncracked. In fact, in the case of a flexural failure, this was true also at the time of failure. As long as this condition existed, the strains in

this part of the beam, which sometimes covered the greater portion of the shear span, were low and could be computed easily. This characteristic of the prestressed specimens is noteworthy because of the "elastic" boundary conditions it imposes on the cracked middle portion of the beam.

Except for a few extreme cases mentioned later, inclined tension cracks formed near the point of application of the load and developed towards it. However, neither their development nor their immediate effects were always identical.

In beams having zero prestress or low prestressing forces compared to the cross-section, the inclined tension crack originated from or immediately above a horizontal tension crack. Such a crack is shown in Fig. 40. This crack apparently originated from the vertical crack marked "2" and crossed the web rapidly up to the level marked "4". (The numbers on this photograph and on others mentioned later in this section refer to the number of the load increment.)

In beams having high ratios of the prestressing force to the cross-sectional area, the inclined crack originated independently of the vertical cracks and sometimes in an uncracked region of the beam. Figure 41 illustrates the inception of such a crack.

Often, there was more than one inclined tension crack. Sometimes, they developed simultaneously, and sometimes one formed and the others followed shortly afterwards. Examples of these are shown on Figs. 42 and 43.

In general, the slopes of the inclined tension cracks were affected by the ratio of the prestressing force to the cross-sectional area; the larger the ratio, the flatter the crack. The length of the shear span, however, appeared to have a more perceptible influence on the slope of the crack. The inclined cracks in the beams loaded at midspan were the longest measured along the length of the span, sometimes as long as twice the depth of the beam.

It should also be noted that in some instances the inclined tension crack formed five to ten minutes after loading was stopped to take readings. It is conceivable that if loading had not been interrupted, the beam might have carried a greater load before developing inclined cracks. Conversely, if loading had been carried out very slowly, the loads at inclined tension cracking might have been smaller than those measured in the tests.

A few beams with extremely high ratios of the prestressing force to the cross-sectional area developed an inclined crack which, because of its location and effects, demands special consideration. This crack, which was observed in four I-beams with the 1 3/4-in. webs, originated above the mid-height of the web and near the reaction, as it would in a restrained beam and because of similar conditions of stress distribution (Fig. 44). In this report, this type of crack is referred to as a secondary inclined tension crack. Its effects are described in the following paragraphs.

The phenomenon of inclined tension cracking is discussed quantitatively in Section 19.

(b) Observed Modes of Shear Failure

There was one general and consistent consequence of inclined tension cracks no matter what the circumstances were. They destroyed beam action partially or completely. Immediately following the development of inclined tension cracking, the top fiber concrete strains increased at sections near the upper end of the crack, and decreased at sections near the lower end. In beams with higher values of Q and prestress, and with thin webs, this transformation took place faster and with telling results once the inclined crack formed. The beams with low values of Q and prestress and with thicker webs lingered on longer after the

inclined tension crack; however, their behavior in this stage was far from being structurally reliable.

Even if the inclined tension crack formed suddenly and was followed equally suddenly, in terms of applied load, by collapse, the final cause of collapse was not observed to be the inclined crack itself, but other conditions which were created by the crack. Basically, shear failures may be subdivided into two categories: (1) failure by shear-compression, and (2) failure by distress in the web. The latter is more violent and certainly more erratic with its several possible failure mechanisms.

(1) The Shear-Compression Failure

This type of shear failure was considered to have occurred when the beam failed by crushing of the concrete at or near the top of an inclined tension crack which had, in most instances, penetrated into the flexure span. Figure 45 shows the state of a specimen after shear-compression failure.

At failure, the distribution of top concrete strains over the length of the span showed peaks at locations corresponding to the top of the inclined cracks, indicating severe concentrations of strain as shown in Fig. 38 and discussed in Section 14.

The violence of the failure depended on the value of Q. Beams with low values of Q which failed in shear compression failed relatively gently. Crushing in the concrete was observed well in advance of collapse. Measured midspan deflections in all beams, which might have been increased by distortions in the shear span, were comparable to those that would be developed for flexural failures.

(2) Failure by Distress in the Web

Under this heading are lumped various phenomena of failure observed chiefly in the I-beams almost immediately following the inception of an inclined crack. These phenomena are discussed below.

Separation of Tension Flange from the Web: In specimens with high values of Q, the inclined crack was followed by a single horizontal crack or by a series of short almost horizontal inclined cracks slightly above or at the level of the reinforcement. These cracks extended from the major inclined cracks toward the reaction. In the I-beams, these cracks developed along the junction of the bottom flange and the web as shown in Fig. 40. Figure 46 shows similar cracks at a more advanced stage of development.

These cracks, when fully developed, transformed a bonded beam into essentially an unbonded beam. Often, they exhibited a marked tendency to separate the reinforcement entirely from the compression flange, but this was prevented by the presence of prestressed external stirrups in the I-beams, and end-anchorages in the rectangular beams. For example, one rectangular beam failed practically as an unbonded beam because of such cracking (Fig. 47).

In general, if it were not for special conditions of the tests such as the transversely prestressed end-blocks and the end-anchorages, these cracks would themselves have been the direct cause of failure in the manner illustrated in Fig. 48 for an I-beam which did not have external stirrups on the end-block.

Crushing of the Web: The loss of shear flow between the tension and compression flanges due to horizontal and inclined cracks transformed the beams into tied arches. In the rectangular beams, this was not a major cause of distress and the compressive stresses were still highest at the top of the inclined cracks. In the I-beams, the thrust developed in the tied arch caused very high compressive stresses in the web. Moreover, because of their geometry and the fact that the steel was placed at a greater depth, the thrust in the I-beams acted with a considerable eccentricity at sections near the reaction. This was evidenced by tensile cracks in the top flange (Fig. 46). These cracks were followed immediately

by crushing of the web as illustrated by Fig. 49 which refers to the same beam shown in Fig. 46.

These failures were sudden and very destructive. Had it not been for the fact that the load dropped considerably with the appearance of the first inclined cracks, the failures might have been more "explosive" than they were.

Secondary Inclined Tension Cracking: Although this type of cracking, like inclined tension cracking, was not in itself the final cause of failure, it can be regarded as such since it transformed the simple beam into a complicated and unstable structure.

Secondary inclined tension cracking occurred only in beams with the 1 3/4-in. webs and extremely high prestressing forces. In two of the four beams in which this phenomenon was distinctly observed, the crack originated in an uncracked web as shown in Fig. 44. In two others, inclined tension cracks were already present in the same shear span. Simultaneously with or immediately following the major crack, a series of short inclined cracks formed at the junction of the web and the compression flange and soon separated the two. From this stage on, the loads apparently were being resisted by the web and the bottom flange acting like an inverted T-beam with some aid from the top flange, which was clamped down by the loading block on one side and by the external stirrup on the other. The failure of the specimen of Fig. 44 is shown on Fig. 50a. In this case distress was first observed in the web near the load-point following the occurrence of the vertical crack in the top flange. The separation of the bottom flange and crushing of the web near the reaction were secondary effects of a very violent failure. Another case in which an inclined tension crack followed the secondary inclined tension crack is shown in Fig. 50b. The intact condition of the other shear span indicates the suddenness of this type of failure and its sensitivity to incidental variations of beam strength.

V. STRENGTH OF PRESTRESSED CONCRETE BEAMS WITHOUT WEB REINFORCEMENT

19. Inclined Tension Cracking

The inclined tension crack marks a very significant stage in the loading history of a beam without web reinforcement. Therefore, its prediction is a question of prime importance to the understanding of the behavior of such beams.

The initiation and development of inclined cracks have been discussed in Sections 15 and 18 of this report. From this discussion it would appear that the definition of inclined tension cracking load would necessarily be somewhat flexible. Both the initiation and development of inclined cracks may be different in beams having different properties. However, no matter how the inclined crack forms and propagates, its overall effects on the behavior of the beam are essentially the same. The inclined crack becomes critical when it distorts severely the strain distribution over the depth of the beam, and/or when it triggers a chain of local failures which leads to total or partial loss of beam action. Therefore, in this report, the inclined tension cracking load has been defined as the load at which the inclined crack starts to affect the behavior of the beam. In most cases this is simultaneous with the formation of the crack. The fine points of this definition must be considered chiefly when the inclination of the crack is very steep, or when it develops very slowly.

If inclined tension cracking is regarded as a limiting stress phenomenon, a knowledge of the stress distribution at a section and of the tensile strength of concrete would make possible a generally applicable solution. In the case of an uncracked section, the stress distribution at a section can be estimated. The resolution of questions about the location of the critical stress with respect to

both the vertical and horizontal axes of the beam, its direction, and the tensile strength of the concrete in the same place and direction, will demand some judgment and knowledge based on observation. In the case of a cracked section, even the determination of the stress distribution at a section involves several assumptions about the behavior of the concrete which may never be accurate enough to justify such elaborations. Therefore, in this study the problem of inclined tension cracking has been approached on an empirical level.

For the beams tested, the dominant variables affecting inclined tension cracking were assumed to be the geometry of cross-section, the ratio of the shear span to the effective depth of the beam, the compressive stress exerted by the prestressing force, and the tensile strength of the concrete.

The load corresponding to inclined tension cracking was obtained from the results of the tests in accordance with the definition given above.

The average compressive stress exerted by the effective prestressing force was taken as a measure of the contribution of the prestress to the inclined tension cracking load. This was computed on the basis of the nominal gross cross-sectional area of each specimen.

Since no tests giving the tensile strength of the concrete directly were available, this quantity was assumed to be two-thirds of the modulus of rupture as determined from tests on plain concrete beams. The data and the derivation of empirical expressions for the modulus of rupture are described in Section 5 of this report. Accordingly then, the tensile strength for each beam was evaluated from the following expressions on the basis of the concrete strength indicated by test cylinders corresponding to the first batch that was placed in the beam. Since the first batch of concrete filled the form up to about three-quarters of the height, its strength was assumed to be critical for inclined tension cracking.

For concrete with regular coarse aggregate:

$$f_t = \frac{1000}{1 + \frac{6000}{f'_c}} \tag{4}$$

For concrete with small size coarse aggregate:

$$f_t = \frac{1000}{2 + \frac{6000}{f'_c}} \tag{5}$$

where f_t = assumed tensile strength, in psi

f'_c = compressive strength indicated by 6 by 12-in. test cylinders, in psi

The data on inclined tension cracking loads were expressed as functions of various factors expected to affect the stresses in the beams and compared with various parameters involving variables expected to contribute to the strength of the beam. The most consistent and simple relationship representing all the test data was found to be the one involving the parameters plotted in Fig. 51 and represented by the following empirical expression:

$$\frac{M_c}{f_t\, bd^2\sqrt{b'/b}} = 1 + \frac{F_{se}}{A_c f_t} \tag{6}$$

where M_c = moment at inclined tension cracking defined as the product of the applied shear at the inclined tension cracking load and the length of the shear span

f_t = assumed tensile strength of concrete

b = top flange width

b' = web thickness

d = effective depth

F_{se} = effective prestress force

A_c = gross area of cross-section

The measured and derived data on inclined tension cracking are listed in Table 4.

In order to show its derivation and limitations, the left-hand term of Eq. (6) may be expanded as follows:

$$\frac{M_c}{f_t\, bd^2\sqrt{b'/b}} = \left[\frac{V_c}{f_t\, bd}\right]\left[\frac{1}{\sqrt{b'/b}}\right]\left[\frac{a}{d}\right]$$

where V_c = applied shear at inclined tension cracking load

a = length of shear span

The first term in parentheses, $V_c/f_t bd$, is a measure of the effect of shear. The term, $\sqrt{b'/b}$, reflects the form factor, and the last term, a/d, represents the effect of bending moment. In the tests reported here, the shear was practically constant throughout the shear span since the dead load shear was relatively negligible. The width of the flange, b, was nominally six inches for all the beams. The effective depth, d, varied from 8 to 11 in., and the ratio b'/b from 0.3 to 1.0. The range of a/d was from 2.8 to 6.7.

The significance of the tensile strength, f_t, in Eq. (6) decreases with an increase in the prestressing force; at practical levels of prestress, inaccuracies in the estimate of the tensile strength are unimportant. However, when the mean compressive prestress, F_{se}/A_c, is comparable to or less than the tensile strength, a correct estimate of the latter becomes critical.

The test data indicated that the shear at inclined tension cracking decreases in inverse ratio with an increase in the shear span. It is not expected that this trend will be true as the shear span increases indefinitely. However, it should be valid for the usual proportions of prestressed concrete beams.

The range of eccentricity of the prestressing force in these tests varied from about 15 percent to about 45 percent of the overall depth of the beams. Since the value of the inclined tension cracking shear should depend to some degree on whether or not flexure cracks are present, it is expected that the eccentricity of the prestressing force should have some effect. However, studies of the data with reference to this point disclosed no consistent trends.

20. Secondary Inclined Tension Cracking

In all but a few of the beams tested, inclined tension cracks started near the load and in the lower portion of the cross-section, where the tensile stresses were higher. Because of the nature of its derivation, Eq. (6) refers only to such cracks.

In beams with high prestressing forces and thin webs, the principal tension stresses near the supports and in the upper portion of the cross-section where the bending stresses are small, were comparable to those near the load. Because of this condition, the inclined tension crack started near the support in some of the beams tested (Figure 44). The empirical expression presented should not be expected to predict this type of crack.

Although this phenomenon has been referred to as "Secondary Inclined Tension Cracking", on the basis of its effects on the behavior of the beam, its significance is by no means secondary. Its initiation has been observed to be followed by shear flow distress between the top flange and the web, leading to complete separation of these two elements.

Although secondary inclined tension cracking takes place in a virtually uncracked portion of the web, its analysis is complicated by sensitivity to several factors such as the strength of the concrete, the actual distribution of stresses, and planes of preference for the crack. Moreover, an empirical analysis is

unwarranted because of such special conditions of the tests as the size of the end-blocks and the presence of prestressed external stirrups on the end-block, and also because of the very limited data available. In the following paragraphs, this problem is discussed on the basis of some simplifying assumptions and primarily in reference to the test specimens.

There were only four beams which exhibited distinct secondary inclined tension cracking. These were C.22.62, C.22.73, C.12.50, and C.12.57. The Q-values for these beams were all high. The cracks formed at a distance of about 10 inches from the reaction. Studies of the principal tension stresses at this section indicated that the tensile stresses were greater above mid-height, and that they were comparable to the stresses that existed in the web near the load. Furthermore, the principal tensile stress at mid-height, at least for the cases considered, was very close in magnitude to the tensile stress existing above mid-height. This last condition is, of course, dependent on the length of the end-block. However, even without an end-block, it might hold true at sections located far enough from the supports.

In order to estimate the principal tension stresses to which the web concrete is subjected, the principal tension stresses at mid-height at the time of inclined tension cracking were computed for all prestressed I-beams with the thinner web. Computations were not performed for loads greater than the measured inclined tension cracking loads because, especially in cases where the prestressing force was high enough to make secondary cracking possible, beam action was not predominant beyond this stage.

The computed stresses are shown plotted against concrete strength on Fig. 52. The computed principal tensile stresses at mid-height corresponding to secondary inclined tension cracking are shown as solid circles on Fig. 52. The principle

tensile stress at mid-height should be constant throughout most of the shear span. However, in all but a few of the specimens for which the computations were made, flexural cracks were present in the shear span so that the computed values strictly refer to the region near the supports.

A comparison of the computed tensile stresses with concrete strengths indicates that, in general, the web was able to sustain a stress equal to the assumed tensile strength, f_t, which is represented by the curve on Fig. 52. In two cases, the computed tensile stresses at secondary inclined tension cracking were as low as the assumed tensile strength, in two other cases they were considerably higher.

If the tensile stress at mid-height is assumed to be critical for secondary inclined tension cracking, the likelihood of the types of cracks may be compared theoretically for the dimensions of the beams tested in this series. The solid line on Fig. 53 describes the relation between $M_c/f_t bd^2 \sqrt{b'/b}$ and $F_{se}/A_c f_t$ as indicated by the empirical expression (Eq. 6). The dotted curves indicate, in terms of the same parameters, the magnitude of the applied shear when the computed principal tension stress at mid-height reaches the assumed tensile strength, f_t, for a shear span of 36 inches. The curves refer to beams with 3-in. and 1 3/4-in. web thicknesses as indicated on the figure. In the computations for these curves it was assumed that the effective depth of the beam was 85 percent of the overall depth.

At face value, the curves on Fig. 53 indicate that the possibility of secondary inclined tension cracking in the beams with the 3-in. web is very remote, but that the beams with the thinner web may undergo such cracking at relatively high values of the parameter $F_{se}/A_c f_t$. It should also be noted that since the slopes of the dotted and solid curves are comparable, any error in estimating the critical tensile stress and the tensile strength will be magnified in its effects

on the possibility of secondary inclined tension cracking. In any case, it is seen that if the computed principal tension stress at mid-height exceeds a known or assumed value of the tensile strength of the concrete at the load indicated by Eq. (6), it would be on the safe side to reduce the estimated inclined tension cracking load in reference to the computed tensile stress. As stated earlier, such a reduction should be required only when the parameter $F_{se}/A_c f_t$ is extremely high. It is doubtful, however, whether such cases would be encountered in practical applications.

21. Analysis of Flexural Strength

The prevalent approach to the flexural strength of reinforced concrete members is based on a fundamental assumption about the state of strains at failure. Essentially, this approach requires that there be a fixed relation, depending on the properties of the cross-section, between the critical concrete and steel strains at the instant of failure. This condition by itself does not enable the prediction of the ultimate strength. However, all other assumptions including the value or values adopted for this strain compatibility factor are incidental to particular applications of this general concept, the more rigid the assumptions, the less the scope of application. The general success of this method is largely due to the insensitivity of the results for the practical ranges of most of the variables.

The critical concrete and steel strains are shown on Fig. 54a by heavy lines. The critical concrete strain is at the extreme compressive fiber in compression and the critical steel strain is assumed to be at the center of gravity of the reinforcement. The neutral axis is at a distance $k_u d$ from the extreme fiber in compression. If the beam is not extremely under-reinforced, failure will be due to crushing of the concrete. Assuming that the concrete crushes at a

limiting strain, ϵ_u, which is independent of other variables, the basic relation may be stated for ordinary non-prestressed reinforced concrete beams as

$$\epsilon_{su} = \epsilon_{sa} = F\epsilon_u \left[\frac{1 - k_u}{k_u}\right] \tag{7}$$

where F is a factor which is usually close to unity but which may be greater or less if the strains are not linearly distributed as usually assumed.

The basic principles of equilibrium may be used to solve this equation. However, the procedure requires some assumptions about the relation between stress and strain. For a particular type of reinforcing steel, a fairly consistent empirical relation can be obtained between stress and strain experimentally. Thus, the stress in the steel can be readily and reliably obtained, if the strain is known. For the concrete, the stress-strain relationship is not as consistent or reliable. The problem of describing the variation of stresses in the compression zone may be approached in several ways and at various levels. A pragmatical solution is to assume an average concrete stress in the beam at failure, f_{cu}, which can be experimentally determined in terms of an index value such as the cylinder strength.

If the tensile strength of the concrete is ignored, the following condition is obtained from the basic principles of equilibrium (Fig. 5-4b):

$$T = C$$

$$pbd\, f_{su} = bk_u d\, f_{cu}$$

$$k_u = \frac{p\, f_{su}}{f_{cu}} \tag{8}$$

Equation (7) solved simultaneously with Eq. (8) together with the known or assumed stress-strain relationship for the steel will yield the value for the ultimate steel stress (5). With the help of a further assumption fixing the

location of the compressive force at a distance $k_2 k_u d$ from the top of the beam, the ultimate moment can be obtained by simply taking moments about this point:

$$M_u = A_s f_{su} d (1 - k_2 k_u) \tag{9}$$

Thus, the flexural strength of a reinforced concrete beam can be stated in terms of its cross-sectional properties if the strain compatibility factor, F, the limiting concrete strain at crushing, ϵ_u, the stress-strain relationship for the reinforcement, the average concrete stress at failure, f_{cu}, and the location of the compressive force are known or assumed. Unfortunately, these all must be determined empirically. Fortunately, the effects on the flexural strength of possible inaccuracies in the assumptions are small for practical ranges of the variables involved.

Equation (7) for the steel strain at failure may be modified to apply to beams with prestressed reinforcement. This is accomplished by adding on the right-hand side of Eq. (7) the terms for the effective prestrain in the steel, and the effective compressive strain in the concrete at the level of the critical steel strain. This condition is also illustrated in Fig. 54a. The modified equation is:

$$\epsilon_{su} = \epsilon_{sa} + \epsilon_{ce} + \epsilon_{se} \tag{10}$$

or

$$\epsilon_{su} = F\epsilon_u \left[\frac{1 - k_u}{k_u}\right] + \epsilon_{ce} + \epsilon_{se} \tag{11}$$

The implications of this equation for steel strain at failure for a particular case are shown graphically on Fig. 55. The curve on this figure describes a typical stress-strain relationship for high tensile strength single wire. The prestrain, ϵ_{se}, and the compressive strain at the level of the critical strain, ϵ_{ce}, are marked on the figure, and the corresponding points on the stress-strain curve are marked A and B, respectively. The increase in steel strain above the sum of ϵ_{se} and ϵ_{ce} is, in accordance with the relations presented.

$$\epsilon_{sa} = F\epsilon_u \left[\frac{1 - k_u}{k_u}\right] \tag{7}$$

A reasonable relative value for this strain is also shown on the figure and the point C on the stress-strain curve marks the ultimate stress attained for this hypothetical case.

As the moment is increased, the steel stress starts from point A and goes up to point C. In the way in which this phenomenon has been interpreted symbolically, it is implied that the compatibility factor is constant, although this may not be true. However, as far as the conditions at ultimate are concerned, this is unimportant. It is significant only if the development of strains are studied at different stages of loading. For example, in fully-bonded members the strain distribution is linear, that is, F is equal to unity, up to the time of flexural cracking. Beyond flexural cracking, the compatibility factor may be greater or less than unity depending upon the nature of bonding and the Q-value. Moreover, this change occurs not at once but gradually, so that the effective value of the compatibility factor at ultimate is actually an average.

When it is considered that for moderately reinforced beams the ultimate moment is almost directly dependent on the steel stress (Eq. 9), it is seen that for the case considered on Fig. 55, there will be little change in the ultimate moment for considerable variations of the factors F and k_u. Thus, inaccuracies in the assumptions for F, ϵ_u, and f_{cu} would be unimportant for this case. The flexural strength becomes quite sensitive to changes in these quantities only when the prestress level is low, the Q-value is high, and/or the compatibility factor is very small. That is, if the steel strain at ultimate is equal to or less than the "yield" strain, the accuracy of the assumptions is critical; if it is greater than the "yield" strain, the accuracy of the assumptions is unimportant. The "yield" strain can be loosely defined here as the strain at which the slope of the stress-strain curve is reduced considerably.

The flexibility of this type of analysis is in the choice or derivation of the compatibility factor to suit different conditions. In the following

paragraphs, the derivation of such a compatibility factor for the analysis of shear-compression failures in prestressed concrete beams is presented.

22. Analysis of Shear-Compression Failures

The observed behavior of beams failing in shear-compression has been described in Section 18. Since the conditions at ultimate for a shear-compression failure were observed to be essentially similar to those for a flexural failure, the analysis of the strength of beams failing in shear-compression has been carried out in a manner similar to the analysis of flexural strength.

Basically, it is assumed that there is a fixed relation, modified by the position of the neutral axis, between critical concrete and steel strains at failure. However, this relation cannot be expressed by a single compatibility factor since the beam undergoes two distinctly different stages of behavior. The first stage refers to the behavior of the beam before inclined tension cracking when the compatibility factor is, in most cases, unity or very close to unity. The second stage refers to the behavior of the beam after inclined tension cracking, when the compatibility factor is considerably less than unity.

Referring to Fig. 56, the steel strain at inclined tension cracking for a prestressed beam may be expressed as

$$\epsilon_{sc} = F_1 \epsilon_{cc} \left[\frac{1 - k_c}{k_c}\right] + \epsilon_{ce} + \epsilon_{se} \qquad (12)$$

The steel strain at ultimate, then, becomes

$$\epsilon_{su} = \epsilon_{sc} + F_2 (\epsilon_u - \epsilon_{cc}) \left[\frac{1 - k_u}{k_u}\right] \qquad (13)$$

or

$$\epsilon_{su} = F_1 \epsilon_{cc} \left[\frac{1 - k_c}{k_c}\right] + F_2 (\epsilon_u - \epsilon_{cc}) \left[\frac{1 - k_u}{k_u}\right] + \epsilon_{ce} + \epsilon_{se} \qquad (14)$$

Equation (14), along with Eq. (8), can be solved to yield a steel stress, and consequently the strength of the beam, if F_1, F_2, k_c, k_u, f_{cu}, ϵ_{cc}, and ϵ_u are

assumed or known. Since it is very difficult to derive all these quantities from tests, and since it is equally complicated to solve the equations presented, Eq. (14) has been simplified on the basis of the following interpretation of the behavior of the beam.

At the beginning of loading, after tranfer of prestress, the steel is strained an amount corresponding to the effective prestress. The concrete strain at the extreme fiber may be slightly in tension or compression depending upon the relative eccentricity of the prestressing force. As the bending moment on the beam is increased, the steel and concrete strains increase and, up to the time of cracking, the strains are substantially linear over the depth of the cross-section, that is, F = 1. If flexural cracks occur first, the compatibility factor remains reasonably close to unity during further increase in moment. The critical strains at a stage immediately preceding inclined tension cracking are shown ideally in Fig. 56a. When the inclined tension crack as defined in Section 19 forms, the compatibility factor is drastically reduced. This is indicated by the strain measurements shown on Fig. 39 and is attributed to the concentration of the deformation required for a certain angle-change over a very small distance on the compression side of the beam, while for the reinforcement this deformation is distributed over a distance at least equal to the horizontal projection of the inclined tension crack at the level of the steel. The top of the inclined tension crack penetrates into the compression zone, and it is assumed that the strain distribution in the compression zone pivots about a point "x" as shown on Fig. 56b. Depending on the properties of the beam and loading, compressive stresses can exist below the top of the inclined tension crack. A further increase of compressive strains or stresses below the top of the inclined tension crack after its development is conceivable. Moreover, the so-called pivot-point "x" need not necessarily be fixed, and it may translate

towards the compression side. Thus, it appears very difficult to establish a neutra axis, or rather a pivot-point, for the stage of loading between inclined tension cracking and the ultimate. Because of this difficulty in measuring the depth to the neutral axis, the determination of the average concrete strength from tests of beams failing in shear-compression is practically impossible. These problems have been handled with some simplifying assumptions which are discussed below along with other assumptions.

Assumptions

1. The critical concrete strain occurs at the extreme fiber in compression parallel to the longitudinal axis of the beam.

There is little reason to doubt that the strains in intact concrete under bending are linear, in which case the maximum strain occurs at the extreme fiber. It is unlikely that the presence of shearing stress will change this condition. However, the principal strain will not be parallel to the longitudinal axis when shearing stresses exist. In the majority of the observed shear-compression failures, crushing took place in the flexure span where the effect of shear, if any, should be negligible. Moreover, the scatter in the measured values of the ultimate concrete strain hardly justifies accuracy about the orientation of the critical strain.

2. Concrete crushes at a limiting local strain of 0.004.

Values ranging from 0.002 to 0.007 have been measured for the crushing strain of concrete over various gage lengths by various investigators. Those measured in the course of this investigation for beams failing in flexure and shear-compression are shown in Fig. 35. The value 0.004 was chosen as a reasonable representation of the data. All strain data were obtained from gages on the concrete which were nominally one-inch long. It is conceivable that if it were possible to

measure strain at the locations of maximum concentration over a shorter gage length, higher strains might have been observed.

3. The strain compatibility factor is unity before inclined tension cracking.

Strains have been observed to vary linearly over the depth of reinforced concrete beams up to the time of flexural cracking. In beams which do not have extremely low values of Q, the strain compatibility factor decreases after flexural cracking. The rate of this reduction should be fairly low at the early stages of loading following flexural cracking. Therefore, the error is unimportant in cases where the load difference between flexural and inclined tension cracking is small compared to the ultimate load. In cases where there is a large difference, usually the properties of the beam are such that the ultimate steel strain falls in the inelastic range, and the error caused by assuming a slightly higher value of the compatibility factor becomes unimportant. This is certainly the case for flexural failures.

4. After inclined tension cracking, the strain compatibility factor is less than unity.

The increase in the slopes of the measured concrete versus steel strain curves on Fig. 39 at strains corresponding to inclined tension cracking indicate that the strain compatibility factor is greatly reduced at such cracking. Since the value of the compatibility factor is expected to change during inclined tension cracking and in the interval between inclined tension cracking and failure, an effective average value based on the depth of the neutral axis at failure is used in the analysis.

5. The inclined tension cracking load is given by the empirical expression:

$$\frac{M_c}{f_t\, bd^2\sqrt{b'/b}} = 1 + \frac{F_{se}}{A_c f_t} \qquad (6)$$

This expression is derived and discussed in Section 19 and is based directly on the results of the tests described in this report. Although the trends it registers for the critical variables appear reasonable, its application in cases definitely different than those covered in the tests is questionable. However, this is not a limitation of the analysis. An expression for inclined tension cracking with a wider scope should work just as well, since the compatibility factor was derived using the observed cracking load.

6. The average concrete stress in the beam at failure is given by the empirical expression:

$$f_{cu} = \frac{f'_c}{2}\left[\frac{f'_c + 6000 \text{ psi}}{f'_c + 1500 \text{ psi}}\right] \qquad (15)$$

This relationship between the 6 by 12-in. cylinder strength and the average effective strength of the concrete in the beam was derived by Billet and Appleton (6) from their tests of prestressed concrete beams failing in flexure. It appears impossible to derive such a relation from tests of beams failing in shear-compression unless elaborate instrumentation is provided. In general the use of the above expression results in a computed neutral axis below the top of the inclined tension crack. Since compression below the top of the inclined tension crack is admissible, the assumption is not unreasonable. In cases where the width of the cross-section is not constant over the depth of the compressive stress block, the value of f_{cu} may be weighted to suit. At practical ranges of the variables, such refinement should be unnecessary.

7. The stress-strain relationship for the steel is known.

The stress-strain relationship for the reinforcing steel is assumed to be known throughout its entire range. In most cases, the determination of the

stress-strain curve up to a strain of two or three percent is sufficient. If steel having a flat-top stress-strain relationship is used, only the co-ordinates of the yield point need be known.

8. The depth of the neutral axis at inclined tension cracking load is the same as that at ultimate.

This assumption affects the evaluation of the steel stress, f_{sc}, and the concrete strain, ϵ_{cc}, at inclined tension cracking. When the steel stress at inclined tension cracking is comparable to the ultimate steel stress, the error due to this assumption is negligible. When the steel stress at inclined tension cracking is small compared to the ultimate steel stress, the magnitude of the former may be underestimated. However, the error should not be greater than what could be expected from normal variations of the actual length of the internal lever arm. In such cases the error in the estimate of the concrete strain, ϵ_{cc}, is unimportant because this quantity itself is very small compared to the crushing strain. Moreover, the assumption greatly simplifies the analysis, and this advantage outweighs the inaccuracies that it might introduce in the case of beams of ordinary proportions with extremely high values of Q or very low values of prestress.

9. The resultant of the compressive force acts at a distance $0.42\ k_u d$ from the top of the beam, where $k_u d$ is the depth to the neutral axis.

For beams failing in flexure, unless extremely high compressive strains are developed in the concrete, the range of this ratio should be between 0.5 and 0.333 corresponding to rectangular and triangular distributions of stress, respectively. An average value of 0.42 was adopted by Billet and Appleton (6), who also showed that the flexural strength is relatively insensitive to variations in this ratio for low and moderate values of the parameter Q. The shape of the compressive stress block for a shear-compression failure is not expected to be the same

as that for a flexural failure, especially when and if the inclined crack penetrates the compression zone. The development of strains and consequently of the stresses above and below the top of the crack may not be compatible. However, the center of compression should still lie somewhere close to the level indicated by $k_2 = 0.42$. Therefore, this value has been adopted, although values somewhat lower or even higher should be acceptable. When the width of the cross-section is not constant over the depth of the compressive stress block, k_2 may be weighted to suit.

10. Concrete does not carry tension.

Concrete does carry some tension. However, at conditions corresponding to ultimate, the depth of the tensile stress block is about three percent of the compressive stress block, and its contribution to the moment carrying capacity is negligible.

11. The conditions of equilibrium are valid.

Derivations

Figure 57 shows the critical steel and concrete strains at inclined tension cracking and at ultimate in accordance with the assumptions stated. Thus, the increase in strain beyond inclined tension cracking becomes

$$\epsilon'_{sa} = F\left(\epsilon_u - \epsilon'_{sc} \cdot \frac{k_u}{1 - k_u}\right) \cdot \frac{1 - k_u}{k_u} \qquad (16)$$

The total steel strain at failure can then be written as:

$$\epsilon_{su} = \epsilon_{sc} + F\ \epsilon_u \left(\frac{1 - k_u}{k_u}\right) - \epsilon'_{sc} \qquad (17)$$

This form is much simpler than Eq. (14). Substituting for k_u from Eq. (8) and rearranging, the following equation is obtained:

$$\epsilon_{su} = \epsilon_{sc} + F\ \epsilon_u \cdot \frac{f_{cu}}{pf_{su}} - (\epsilon_u + \epsilon'_{sc}) \qquad (18)$$

The value of the steel stress at inclined tension cracking can be computed from the cracking load given by Eq. (6)

$$f_{sc} = \frac{M'_c}{A_s\, d\, (1 - 0.42\, k_u)} \tag{19}$$

The ultimate stress can be determined by a trial-and-error procedure from Eqs. (18) and (19) provided that the stress-strain curve for the steel, the ultimate concrete strain, the value of the compatibility factor F are known or assumed.

The assumed location of the centroid of the compressive force is shown on Fig. 57. Taking moments about this centroid, the ultimate moment corresponding to a shear-compression failure is obtained as:

$$M_u = A_s f_{su} d\, (1 - 0.42\, k_u) \tag{20}$$

This equation for ultimate moment is the same as that for failure in flexure. It can also be rewritten as

$$\frac{M_u}{f_{cu}\, bd^2} = \frac{pf_{su}}{f_{cu}} \left(1 - 0.42\, \frac{pf_{su}}{f_{cu}}\right) \tag{21}$$

for studying the effects of variables and for general applications.

The implications of this analysis can best be illustrated by following the development of steel strains with reference to the stress-strain curve on Fig. 55.

On this curve the points A and B correspond to the strains ϵ_{se}, and $\epsilon_{se} + \epsilon_{ce}$, respectively. Point C is the ultimate steel strain for a flexural failure.

For a qualitative discussion, it is assumed that two identical beams are loaded to failure, one with prestressed external stirrups to avoid inclined cracks and the other without.

As the load is increased, the steel stress in the beam with stirrups will increase from A to C on the stress-strain curve. This beam will attain its full flexural capacity.

The response of the beam without stirrups will be similar to that of the beam with stirrups up to a steel strain, ϵ_{sc}, corresponding to inclined tension cracking marked by point D on the stress-strain curve. Beyond this point, the compatibility factor will be reduced to about a tenth of its original value. Consequently, the total increase in steel strain after inclined tension cracking, ϵ'_{sa}, will be very small and the ultimate steel strain for this beam will end up at some point such as E which is considerably short of point C.

Since the moment-carrying capacity is almost directly dependent on the steel stress, the ultimate load for the beam without stirrups will be less than the ultimate load for the other beam as indicated by the ordinates of points E and C.

If the stress at inclined tension cracking had been higher, say at D', then the ultimate stress would be still to the right of it, as shown by E'. In a case like this, although the failure would be in shear-compression, the ultimate moment would be almost as high as that for a flexural failure. In discussing the flexural analysis, the insensitivity of the computed moment to inaccuracies in the assumptions when the steel strain was in the inelastic range was brought out. This is also true for the shear-compression analysis. On the other hand, if the ultimate strain falls on the elastic part of the stress-strain curve, and this happens more often in shear-compression than in flexure, the result is very sensitive to the assumptions made.

The shear-compression analysis will automatically differentiate between shear and flexural failures. If the cracking load is greater or comparable to the

flexural capacity, there is no need to get a solution for a shear-compression failure which will converge to the flexural capacity if attempted.

To show the effect of the compatibility factor on moment carrying capacity, three sets of curves are presented on Figs. 58 through 60. All of the computations were made for a concrete cylinder strength of 4,000 psi, Lot VIII reinforcement, and an effective prestress of 120,000 psi. The effective depth was taken as 85 percent of the overall height. The tensile strength of the concrete was computed from Eq. (5).

The curves on Figs. 58, 59, and 60 have been computed for the rectangular beam, the I-beam with the 3-in. web, and the I-beam with the 1 3/4-in. web, respectively. On each figure, the upper solid curve marked M_f describes the flexural strength. The solid straight line below indicates the moment at inclined tension cracking. The broken lines refer to shear-compression failures for the indicated values of the compatibility factor F.

According to these curves, the rate of increase of moment with increase in F is high up to about F = 0.1. Beyond this value of F, the rate is reduced considerably. Above an F value of 0.3, there is hardly any increase at all in the moment.

A comparison of the three curves indicates that the relative amount of longitudinal steel at which shear-compression failures become likely decreases with a decrease in web thickness. Also, at values of the reinforcement ratio, p, slightly greater than these critical values, there is very little difference in strength for either mode of failure. It should also be noted here that, considering the possible scatter, each of the curves should be represented as a band covering a "thickness" of at least $\pm$ 10 percent of the ordinate. The intersection of the boundaries of the bands for the curves corresponding to cracking and flexural

strength would cover a wide range in the abscissa values, but not as much in ordinates. Consequently, it is difficult to predict the modes of failures for beams in this range, but the ultimate to capacities can be estimated within reasonable limits.

23. Web Distress

In Section 18, three types of failure initiated by inclined tension cracking and generally classified as web distress failures were described. One of these, secondary inclined tension cracking, has already been discussed in Section 20. In the following paragraphs, the other two types of web distress phenomena, separation of the web from the tension flange and crushing of the web, will be discussed with reference to beam and loading characteristics.

Before going any further, it should be brought out here that this discussion is attempted only to describe these three types of failure in more detail than was done earlier in the report. Otherwise, on the basis of all evidence available, they neither lend themselves to, nor are worthy of detailed analysis. However, the mechanism of failure involved in these phenomena brings out fully the fact that lack of an adequate reinforcing scheme in a concrete beam, prestressed or not, may result in a "beam" that resists the applied loads in a somewhat unorthodox manner.

(1) Separation of the Tension Flange from the Web. Figure 61 is an idealized representation of the conditions in the shear span of a simply-supported bonded prestressed concrete I-beam after the development of inclined tension cracking. Although this type of failure is possible in rectangular beams, it is more likely in beams with webs thinner than the flange; therefore an I-beam has been chosen for this discussion. The I-beam is reinforced in the longitudinal direction only, and all of the reinforcement is in the bottom flange.

The internal conditions after the development of the inclined tension crack may be interpreted in several ways. One of these is an overall consideration of the equilibrium of internal forces and compatibility of attendant deformations; another is an evaluation of the stresses in the beam created by some rather severe conditions of shear flow. Although these are different statements of the same fundamental phenomenon, one has the advantage of presenting a simple physical picture, while the other is more convenient for analysis. They are described briefly and in the same order in the following paragraphs.

For a general investigation of the problem at hand, it is justifiable to assume that the steel stress remains constant over the horizontal projection of the inclined tension crack. As mentioned before, this condition transforms the beam partially into a tied arch. Therefore, at least for a length equal to the horizontal projection of the inclined crack, the centroid of the compressive force should lie along a line as shown by the broken line on Fig. 61. Equilibrium conditions on a plane AB, perpendicular to the thrust-line and passing through the intersection of the inclined crack with the reinforcement, demand that there be compressive stresses all along plane AB. The reinforcement thus tends to "pull-out" from a concrete block that is entirely in compression. "Pull-out" may occur by loss of bond, by splitting of the concrete, and, in the case of beams with thin webs, by "tearing" of the entire tension flange from the web. In other words, if steel-to-concrete bond is not lost, before the beam can redevelop beam-action, very high shearing distortions of the concrete are required at the junction of the web and the flange to be compatible with tensile strains at the level of the steel.

The same phenomenon can be investigated by tracing the history of shear flow before and after inclined tension cracking between the two flanges of the beam. For convenience, this may be done with reference to the simplified diagrams of steel stress distribution shown on Fig. 61. It is assumed that the prestress is fully developed in the end-block. The broken curve represents the assumed

distribution of steel stress before inclined cracking, the solid line immediately after inclined cracking.

According to the assumption previously made the steel stress remains constant to point C. Beyond this point, in the direction of the reaction, the steel stress should decrease at as fast a rate as the developed bond between the steel and the concrete will allow. Unless the difference between the stress levels at C before and after inclined cracking or the area of the steel is very low, it is reasonable to expect that the maximum possible bond strength will be developed. This stress is the maximum slope of the steel stress curve beyond point C.

The change in the tensile force must "flow" to the compression flange. This requires that for the restoration of beam action, not only must there be adequate bond between the concrete and the steel, but the concrete section itself must be able to carry the shear flow from the tension to the compression flange. In the I-beams, for example, the "bond" between the web and the flange, must be as good as the bond between the steel and the concrete. The condition can be roughly formulated to state that the product of the shearing strength of the concrete and the width of the web must be equal to the product of the total peripheral area of the steel and the maximum bond strength.

At present there are several difficulties that prevent a full analysis of this problem, over and above the fact that such an analysis would be of little practical value. As discussed earlier in this report, the steel stress may not remain constant over the horizontal projection of the inclined crack. Just how much it varies depends on the nature, arrangement, and amount of the longitudinal reinforcement, geometrical properties of the beam, length of the shear span, and other such incidental factors as the crack pattern. The maximum bond stress that can be developed between the rusted wires and the concrete under the conditions

involved cannot be accurately estimated. The separation of the web from the flange is an integrated result of a series of inclined cracks evidently formed under a combination of shear and compressive stresses at a level where it would be very laborious to determine the existing stresses even if concrete were a homogeneous material.

Thus, it appears that it is quite difficult to predict the exact load or conditions for separation of the web from the bottom flange. A reasonable but conservative rule would be to expect this phenomenon whenever the thickness of the web is less than the sum of the perimeters for the bars. However, this is a very approximate statement and ignores most of the variables which can affect the results critically.

If the beam is provided with an adequately reinforced end-block, separation of the bottom flange does not lead to failure directly, but final failure takes place by crushing of the concrete in the flange -- a shear-compression failure -- or in the web. The former mode has been described in Section 22. The latter is discussed below.

(2) Failure by Crushing of the Web. Essentially, this mode of failure is a result of arch-action in the beam. Thus, it necessitates a complete or nearly complete loss of shear flow within the beam for a considerable portion of the shear span. The actual cause of this loss is unimportant. It can result from a series of inclined cracks, a single flat inclined crack, or separation of the tension flange from the web following inclined tension cracking. For the sake of simplicity and continuity of discussion, web crushing following separation of the tension flange from the web will be discussed here. However, the discussion is applicable, with a few reservations which will be mentioned later, to web crushing following the other two mentioned causes.

Figure 61c represents ideally the beam shown in Fig. 61a after separation of the web from the tension flange up to the end-block.

If the total loss of shear flow is assumed in the cracked region, the variation in the level of the compressive thrust along the length of the beam is shown by the broken line on the figure. The web and the top flange may now be regarded as a plain concrete column loaded eccentrically. In the case of rectangular beams, this condition is not very severe. In the case of beams with webs thinner than the flange, the stresses in the web may become critical. This is due to both the reduction in area and eccentricity as compared to a rectangular section.

Inspection of the stresses at various sections along the thrust line indicates that, ideally at least, the worst conditions occur at a plane DE perpendicular to the thrust-line and passing through the intersection of the edges of the end-block with the top flange. Experimental evidence has corroborated this assumption within reasonable limits (Fig. 49). Computing the stresses on this plain concrete column directly is somewhat involved. On the other hand, by constructing an interaction curve for the plain concrete column, the maximum thrust and its sensitivity to the critical variables can be studied.

The interaction curve on Fig. 62a was constructed for the idealized cross-section shown on Fig. 62b for a concrete strength of 4000 psi. The shape of the stress-strain curve assumed for concrete is shown on Fig. 62c. The tensile strength of the concrete was ignored. This curve should ostensibly indicate the ultimate strength of a plain concrete column having the properties described, under combinations of axial thrust, plotted vertically, and bending moment plotted horizontally. The maximum ordinate refers to the axial capacity. Since the tensile strength of concrete has been neglected, the bending moment capacity is zero when there is no thrust.

In order to simplify the history of loading, it is assumed that the web and the tension flange were separated from the beginning of loading. Then, the thrust has constant eccentricity with respect to the geometrical centroid of the cross-section considered at all stages of loading. On the interaction diagram, this corresponds to a straight line emanating from the origin and having a slope equal to the eccentricity. The value of the ordinate for the interaction point of the straight line and the interaction curve is the maximum thrust that can be developed.

Two straight lines passing through the origin and corresponding to eccentricities of four and five inches are drawn on Fig. 62a. The actual eccentricity of the thrust line may easily vary between four and five inches depending on the extent of separation between the flanges and the web and on the actual shape and condition of the point between the end-block and the web. This variation in eccentricity corresponds to 100 percent variation in thrust which is a measure of the transverse load. Moreover, if there is a further increase in eccentricity, the thrust is reduced to a negligible value at a very fast rate. This would be true even if the tensile strength of the concrete were recognized in constructing the interaction curve.

From the foregoing particular and very much simplified analysis of web crushing, it appears that the load corresponding to this mode of failure is very sensitive to the variables, and therfore virtually impossible to determine. Moreover, to repeat what has already been often stated in this report, the precise determination of this load is not important.

VI. COMPARISON OF MEASURED AND COMPUTED QUANTITIES

24. Evaluation of the Effective Strain Compatibility Factor

One of the assumptions in the procedure for the analysis of shear-compression failures relates to the effective strain compatibility factor, F, defined in Section 22. Since it is very difficult to predict the exact shape and extent of the inclined tension crack and the consequent local strain disturbances in the concrete, this factor could not be computed directly on the basis of the properties of the beam and loading. An elaborate and costly arrangement of strain gages on each specimen might have made it possible to evaluate F almost directly from test results. However, this was impractical. Therefore, values for F were obtained indirectly from load measurements made during the tests.

The derivation of the compatibility factor was based on the idealized condition of strain and stress shown on Fig. 57. Thus, Eq. (17) can be rewritten for this purpose as follows:

$$F = \frac{\epsilon_{su} - \epsilon_{sc}}{\epsilon_u \left(\frac{1}{k_u} - 1\right) - \epsilon'_{sc}} \tag{22}$$

All the quantities on the right-hand side of the figure were derived or assumed in accordance with the assumptions enumerated in Section 22. The limiting concrete strain was assumed to be 0.004. The data pertinent to this assumption are shown on Fig. 35 and discussed in Section 14. The ratio k_u was derived from the measured ultimate moment, the concrete strength in the top flange, the amount of longitudinal steel, and the geometrical properties of the cross-section, with the assumption that the average stress in the concrete was given by the following expression:

$$f_{cu} = \frac{f'_c}{2}\left[\frac{f'_c + 6000 \text{ psi}}{f'_c + 1500 \text{ psi}}\right] \qquad (15)$$

The total steel strain at ultimate, ϵ_{su}, was obtained from the ultimate steel steel stress with the help of the stress-strain curve for the steel. The steel stress was computed from the measured ultimate moment, the amount of longitudinal steel, and the lever arm, $d\ (1 - 0.42k_u)$.

The steel strain at inclined tension cracking was similarly obtained from the corresponding steel stress. The value of the steel stress at inclined tension cracking was determined from the total moment at the load point corresponding to the load at inclined cracking. In accordance with assumption 8 in Section 22, the internal moment arm was assumed to be equal to that at ultimate. Although this is an approximation, the error involved at practical levels of the variables is not great. Furthermore, an "accurate" evaluation of the steel stress at inclined tension cracking involves more labor and assumptions than would be warranted by the bases and the results of the analysis. The term ϵ'_{sc} was obtained by deducting the sum of ϵ_{se} and ϵ_{ce} from ϵ_{sc}.

The values of the strain compatibility factor so derived are tabulated in Table 5. Preliminary studies indicated that the compatibility factor was a function of the ratio, k_u. Figure 63 compares F with k_u. Although the majority of the plotted data indicates a definite trend, the scatter is considerable. However, when the extreme sensitivity of the compatibility factor to the ultimate load at low values of the ratio k_u is considered, the scatter of the data is understandable. In the inelastic range, a very large amount of strain is required to change the stress perceptibly.

The concave upward trend of the data imply a variation of F with k_u which could be represented by an equation having the form

$$F = C \cdot \frac{k_u}{1 - k_u}$$

where C is a constant. This form also suggests a constant increase in steel strain over the strain at inclined cracking no matter what the other variables are, such that the trend shown on Fig. 63 might have been forced by the manner in which the data were derived. However, further studies did not corroborate this implication.

Therefore, for sake of simplicity, the following equation was selected to represent the data

$$F = 2.5\, k_u^2 \tag{23}$$

with a limiting value of 0.3. Despite some computed values of F above 0.3, the curves on Figs. 58-60 indicate that limiting F to a maximum value of 0.3 does not greatly curtail the ultimate strength, at least at practical levels of prestress.

25. Comparison of Measured and Computed Ultimate Strengths of Beams Failing in Shear-Compression.

The computation of the strength of a beam failing in shear-compression requires a lengthy trial and error procedure. However, the number of trials may be reduced to as few as one with some experience.

For a given specimen, it is best to compute first the flexural strength and the load at inclined tension cracking. The former is accomplished by the use of the following equations, and the properties of the beam:

$$\epsilon_{su} = F\epsilon_u \left[\frac{1 - k_u}{k_u}\right] + \epsilon_{se} + \epsilon_{ce} \tag{11}$$

$$k_u = \frac{pf_{su}}{f_{cu}} \tag{8}$$

Although it may not be safe and correct in every possible instance, F may be taken as unity for flexural failures, especially for pretensioned beams. If an expression can be written for the steel stress in terms of the strain, the two equations can be combined to yield an equation with a single unknown. For example, this can easily be done if the steel stress remains in the elastic range. However, such an expression is not convenient in most cases, and the two equations have to be solved by a simple trial and error procedure. The most convenient method is: (1) select a reasonable value for f_{su}, (2) evaluate k_u from Eq. (8), (3) determine ϵ_{su} from Eq. (11), and (4), check if ϵ_{su} and f_{su} are compatible. If ϵ_{su} and f_{su} are not compatible, then the whole preocedure is repeated using the value of f_{su} obtained in the last trial, or an intermediate value between the steel stresses assumed and that obtained in the last trial.

Once the steel stress is determined, the moment can be computed from Eq. (9), with $k_2 = 0.42$ as shown below:

$$M_u = A_s f_{su} d (1 - 0.42 k_u) \qquad (20)$$

At present, only an empirical equation based on the results of the tests reported here is available to determine the cracking load. Equation (6) presented in Section 19, by the nature of its derivation, yields values for the applied load only. Since the total steel stress at the loading point is critical in shear-compression failures, the dead-load moment at this point must be added to the moment indicated by Eq. (6).

If the cracking moment is greater than or equal to the flexural strength, no analysis for shear-compression is required. In fact, in view of the possible scatter in either quantity, especially the cracking moment, no such analysis is warranted if the flexural strength turns out to be only a little greater than the cracking moment.

The steps to be followed in the rest of the operation to compute the shear-compression strength are listed below.

(1) Assume f_{su}

(2) Determine k_u from Eq. 8

(3) Determine f_{sc} from Eqs. (6) and (19)

(4) Determine ϵ_{sc} from the stress-strain curve for steel

(5) Determine F from Eq. (23) or the limit 0.3

(6) Evaluate ϵ_{su} from Eq. (17) or (18)

(7) Check if ϵ_{su} is compatible with f_{su}

This operation is repeated until the assumed value of the ultimate steel stress in step (1) agrees with the value of the ultimate steel strain in step (7). Then, the moment corresponding to shear compression is computed from Eq. (20).

The sensitivity of the results of the shear-compression analysis to the variables involved has been discussed earlier in this report. The overall accuracy of the analysis cannot be expected to be better than that of the prediction of the inclined cracking load. The shear-compression capacity lies somewhere between the inclined cracking load and the flexural capacity. As the inclined cracking load approaches the flexural capacity, due to variations in the critical parameters, the precision of the shear-compression analysis should by necessity improve. And as the difference between the inclined cracking load and the flexural capacity increases, say, due to decrease in prestress, there develops more "room" for deviation.

Table 6 lists moments computed on the basis of the shear-compression analysis, those measured in the tests, and the ratios of the latter to the former, in columns (4), (5), and (8), respectively, for 74 beams. Computations were not

carried out for beams that failed by web distress and for cases in which the analysis indicated flexural failures.

The ratios of the measured to computed moment average 1.01 with a mean deviation of 0.065. The average for the beams in the high, medium, and low prestress groups are 1.02, 0.97, and 1.04, with mean deviations of 0.049, 0.060, and 0.098, respectively. The mean deviation for the ratios of measured to computed inclined tension cracking moment is 0.074, with this quantity increasing to 0.13 for the low prestress group only.

26. Prediction of Mode of Failure

In accordance with the adopted definitions, a shear failure is predicted when the computed cracking load is less than the flexural capacity. The modes of failure indicated by comparison of columns (3) and (4) are listed in column (10) of Table 6, the symbols S and F denoting shear and flexural failures, respectively. The actual modes of failure are shown similarly in column (9). Flexural failures are predicted for seven beams, only five of which failed in flexure. The other two, beams B.12.10 and B.12.12 failed in shear. On the other hand, four specimens, for which shear failures were predicted, failed in flexure.

As mentioned before, both the computed inclined cracking load and the flexural capacity are not to be regarded as precise quantities. Thus, when the two are within five or even ten percent of each other, the mode of failure cannot be predicted with certainty. In such cases, it is safer to assume a shear failure. For example, although flexural and balanced failures are indicated for beams B.12.10 and B.12.12, respectively, they should be treated as shear failures. However, even if the computed quantities are interpreted literally, the results cannot be far off, since in this range the values of shear-compression and flexural capacities are comparable. The ratios of test moment to computed moment for the six beams

average 1.00 with a mean deviation of 0.055, despite the incorrect prediction of the modes of failure.

27. Flexural Failures

Column (9) in Table 6 indicates that nine beams failed in flexure. The comparison of the results of these tests with capacities computed on the basis of the flexure analysis shows a reasonable agreement. The average is 0.99, and the mean deviation 0.026. Evidently, the assumption of unity for the strain compatibility factor in flexural failures in this range is satisfactory. The reasons for this are discussed in Section 17.

28. Comparison of Ultimate Capacity with Load at Inclined Tension Cracking

The ratios of the measured ultimate load to the computed cracking load are plotted on Fig. 64 against the parameter $F_{se}/A_c f_t$. Different symbols are used for the data pertaining to beams with different prestress levels and web thicknesses. The choice of the parameter $F_{se}/A_c f_t$ is incidental; the ratios plotted are not functions of this parameter alone.

If the results of the specimens with zero or nearly zero prestress are ignored, it is seen that all but two of the computed ratios are less than 1.4. Moreover, the vast majority of the points fall below 1.2.

The tests have covered a fairly wide range of the critical variables. Thus, the results plotted on Fig. 64 should be sufficient to show that simply-supported prestressed concrete beams with longitudinal reinforcement only develop relatively little strength beyond inclined tension cracking. This is also evident from a comparison of the expressions for flexural strength and for inclined tension cracking load. At practical levels of the variables, the flexural strength is not very sensitive to variations in the prestress level; but the inclined tension cracking load is almost directly dependent on it. As the prestress

is increased, the difference between the two quantities is reduced, so that even if the beam develops its flexural capacity, and it should not, the increase beyond cracking is not great (Figs. 58-60). If there is little or no prestress, the difference between flexural strength and the inclined tension cracking load is considerable, especially in relation to the magnitude of the cracking load. This is reflected in Fig. 64. Also, because of the sudden and drastic redistribution of stress that marks web distress, the ratio of ultimate load to inclined tension cracking load approaches unity with an increase in Q or decrease in the web thickness.

29. General Discussion of Measured and Computed Strengths

The main issue of this investigation was an understanding of the useful ultimate strength of prestressed concrete beams with longitudinal reinforcement only. The ultimate strength and the useful ultimate strength of a structural unit are not necessarily the same. The latter may be a fraction of the former depending on the intended function and the inherent behavior of the unit. Insofar as the short-time static strength of such beams is concerned, the results discussed in the preceding sections indicate that the ratio of the useful ultimate to the ultimate may vary over some range.

If the computed inclined tension cracking load for a beam exceeds its flexural strength, the latter can be assumed as the useful ultimate strength. In this case, which calls for an extremely low ratio of longitudinal reinforcement, p, the ultimate strength and the useful ultimate strength are the same. Theoretically, no web reinforcement is needed. It was brought out in the earlier sections that even if the computed cracking load were not accurate and indicated the mode of failure incorrectly, shear and flexural failures were comparable in almost all respects in this transition range so that the computed strength would be reasonably accurate.

If the flexural strength of a beam exceeds its inclined tension cracking load, a shear failure is to be expected. If the beam fails in shear-compression, its strength can be predicted, and the computed strength represents some increase beyond the inclined cracking load. If it fails by web distress, the strength may or may not be greater than the inclined cracking load. In rectangular beams with end-anchorages, a shear-compression failure may be expected to follow inclined cracking. In sections having webs thinner than their compression flanges, failure may be by shear-compression or web distress. Differentiating between these two modes of shear failure is difficult, especially since the latter is critically affected by several local and special conditions.

Despite the fact that shear-compression failures, when they occur, can be satisfactorily though laboriously analyzed, it seems reasonable to limit the useful ultimate strength of prestressed concrete beams with longitudinal reinforcement only to the load at inclined tension cracking if positive precautions to prevent web distress are not taken. The limitation is not drastic at practical levels of prestress as indicated by the data on Fig. 64, and it is strongly supported by the unstable behavior of the prestressed test beams beyond inclined cracking.

30. Nominal Shear Stresses at Ultimate

Ever since the standardization of reinforced concrete design, the nominal shear stress, $v = V/bjd$, has been used as a measure of inclined tension. This approach has also been recommended for the ultimate strength design of prestressed concrete beams. Although such a study was not warranted by any aspect of the tests, the nominal shear stresses corresponding to ultimate load were computed to check the possibility of using the nominal shear stress in ultimate strength estimates. The computed nominal shear stresses are shown in Table 7. The ratios of the computed nominal shear stresses to concrete strength for all beams failing in

shear are plotted against values of Q on Fig. 65. The choice of the parameter Q for the abscissas was arbitrary. The nominal shear stresses were based on $v = V/bjd$ for the rectangular beams and $v = V/b'jd$ for the I-beams. The value for "j" was assumed to be 0.9. Dead load shear was included.

It appears from the calculated values that the nominal shear stress cannot be used generally as an index value for ultimate strength. This is true even if only the stresses for beams with high prestresses are considered. The ultimate nominal shear stresses increase with increase in values of Q, which reflects partially the increase in prestressing force for the same prestress level. They also increase with a decrease in web thickness. A comparison of the tabulated stresses also indicates that they decrease with increase in shear span. Thus, for the data presented here at least, it would be impossible to estimate the ultimate strength on the basis of the nominal shear stress alone and still be safe and economical in every case.

VII. SUMMARY

31. Outline of Investigation

The primary object of this investigation was to obtain a better understanding of the behavior of prestressed concrete beams without web reinforcement. Tests of 43 rectangular beams and 56 I-beams are described in this report. The concrete strength, f'_c, varied from 1750 to 8560 psi, and the reinforcement ratio, p, from 0.0010 to 0.0096. The range of prestress was from zero to 140,000 psi. Beams were tested with shear spans ranging from 2 ft to 4 ft 6 in. All beams had overall cross-sectional dimensions of 6 by 12 in. The I-beams had web thicknesses of 1 3/4 in. or 3 in.

Each beam was loaded to failure within four to six hours. Records of load, deflection, concrete strains at the top, steel strain, and crack pattern were obtained throughout all stages of loading.

Results of the tests indicated that web reinforcement would be a very desirable element in prestressed concrete beams as it is in reinforced concrete beams. Studies of the data resulted in an empirical expression for the inclined tension cracking load and a hypothesis for shear-compression failures.

32. Behavior of Test Beams

Of the 99 beams tested, 90 failed in shear and 9 in flexure. The beams exhibited distinctly different characteristics of behavior only after the formation of inclined tension cracks. Up to this level of loading, the response of the beams to load was essentially similar.

The few beams which did not develop critical inclined cracks failed in flexure by crushing of the concrete or fracture of the steel. Those that did develop inclined cracks failed in shear as a result of redistributions of stress

caused by these cracks. Shear failures were classified into two categories: (1) shear-compression, and (2) web distress. Shear-compression failures were similar to flexural compressive failures, except that the concrete crushed at the upper end of the inclined crack where there was a very high strain concentration. This mode of shear failure was observed in both rectangular and I-beams. Web distress represented three different mechanisms of destruction of the web: (1) Secondary inclined tension cracks formed near the supports and above mid-height of the beam and separated the compression flange from the web, leading to a violent failure. (2) Inclined cracks near the loading points extended horizontally toward the supports tending to separate the web from the bottom flange entirely. (3) The web crushed under high compressive stresses due to arch action created by the loss of shear flow between the steel and the compression flange. Web distress prevailed in I-beams with thin webs and high prestress forces.

In general, shear failures were violent and caused complete destruction. Web distress was more violent in its symptoms than shear compression. The behavior of the beams after the development of inclined cracks was unstable.

33. Analysis of Test Results

An empirical expression, Eq. (6), for the inclined tension cracking load was derived from the data. The average ratio of measured to predicted inclined cracking loads for all the test beams was 1.00 and the mean deviation was 0.074. On the basis of the observed relations between concrete and steel strains at different stages of loading and the nature of the failure, an analysis for strength in shear-compression was presented which is similar to the analysis for strength in flexure except for the use of different strain compatibility factors before and after inclined tension cracking. The average ratio of measured to predicted loads for all the beams failing in shear-compression was 1.01 and the mean deviation was 0.065.

In general, it was concluded that the useful ultimate strength of prestressed concrete beams without web reinforcement should be limited to the inclined cracking load unless positive measures are taken to prevent web distress.

VIII. BIBLIOGRAPHY

1. Zwoyer, E. M., "Shear Strength of Simply-Supported Prestressed Concrete Beams," Ph.D. Thesis, University of Illinois, June 1953. Issued as a part of the Second Progress Report of the Investigation of Prestressed Concrete for Highway Bridges, Civil Engineering Studies, Structural Research Series No. 53, June 1953.

2. Zwoyer, E. M. and Siess, C. P., "The Ultimate Strength in Shear of Simply-Supported Prestressed Concrete Beams Without Web Reinforcement," Journal of the American Concrete Institute, V. 26, No. 2, October 1954.

3. Billet, D. F., "Study of Prestressed Concrete Beams Failing in Flexure," M. S. Thesis, University of Illinois, June 1953. Issued as a part of the Second Progress Report of the Investigation of Prestressed Concrete for Highway Bridges, Civil Engineering Studies, Structural Research Series No. 54, June 1953.

4. Warwaruk, J., "Strength in Flexure of Bonded and Unbonded Prestressed Concrete Beams," M. S. Thesis, University of Illinois, August 1957.

5. Siess, C. P., "Strength of Prestressed Concrete Members," Symposium on the Strength of Concrete Structures, Session B, Paper No. 3, Cement and Concrete Association, London, May 1956.

6. Billet, D. F. and Appleton, J. H., "Flexural Strength of Prestressed Concrete Beams," Journal of the American Concrete Institute, V. 25, No. 10, June 1954.

TABLE 1

PROPERTIES OF BEAMS

Mark	Concrete Strength f'_c psi	Flange Width b in.	Web Thickness b' in.	Effective Depth d in.	Area of Steel A_s sq. in.	Longit. Reinf. p %	Effective Prestress f_{se} ksi	Wire Lot	Shear Span a in.	Method of Prestressing
A.11.43	6220	6.0	--	8.24	0.440	0.889	116	I	54	Post*
A.11.51	2900	6.0	--	8.44	.249	.491	114	II	54	Post
A.11.53	4360	6.0	--	8.02	.373	.776	124.5	II	54	Post
A.11.96	2900	6.0	--	8.41	.467	.924	116	II	54	Post
A.12.23	5650	6.1	--	9.33	.249	.437	114.1	II	36	Post
A.12.31	5800	6.0	--	8.64	.311	.600	114	II	36	Pre**
A.12.34	7990	6.0	--	8.2	.440	.893	110	I	36	Post
A.12.36	3440	6.1	--	9.19	.232	.413	113.9	III	36	Post
A.12.42	6260	6.0	--	8.3	.440	.883	103.4	I	36	Post
A.12.46	4660	6.0	--	8.2	.352	.715	131.4	I	36	Post
A.12.48	4840	6.0	--	8.2	.381	.774	140	I	36	Post
A.12.53	3400	6.0	--	8.6	.311	.603	108.3	II	36	Pre
A.12.56	3790	6.0	--	8.59	.362	.703	120.5	VIII	36	Pre
A.12.60	3350	6.0	--	8.81	.352	.665	136	I	36	Post
A.12.69	2950	6.1	--	8.12	.342	.695	116	II	36	Post
A.12.73	3550	6.0	--	8.44	.440	.868	104.3	I	36	Post
A.12.81	2600	6.0	--	8.66	.362	.703	119.9	VIII	36	Pre
A.14.39	3350	6.0	--	8.35	.218	.435	117	II	24***	Post
A.14.44	3350	6.0	--	8.5	.249	.488	118	II	24***	Post
A.14.55	3320	6.0	--	8.53	.311	.608	117	II	24***	Post
A.14.68	2440	6.0	--	8.42	.280	.554	117.9	II	24***	Post

* Post-Tensioned
** Pretensioned
*** Total Span = 7 ft

TABLE 1 (Continued)

Mark	Concrete Strength f'_c psi	Flange Width b in.	Web Thickness b' in.	Effective Depth d in.	Area of Steel A_s sq. in.	Longit. Reinf. p %	Effective Prestress f_{se} ksi	Wire Lot	Shear Span a in.	Method of Prestressing
A.21.29	3350	6.0	--	8.45	0.156	0.307	61.1	II	54	Post
A.21.39	3130	6.0	--	8.95	.218	.405	58.9	II	54	Post
A.21.51	5630	6.0	--	8.12	.467	.958	59.1	II	54	Post
A.22.20	5350	6.0	--	8.45	.176	.347	61.2	I	36	Post
A.22.24	3470	6.0	--	8.8	.147	.277	58.9	I	36	Post
A.22.26	3665	6.0	--	9.28	.176	.316	50.0	I	36	Post
A.22.27	3850	6.0	--	8.38	.176	.350	60.0	I	36	Post
A.22.28	3480	6.1	--	8.75	.175	.327	49.3	I	36	Post
A.22.31	3530	6.0	--	8.06	.176	.364	89.4	I	36	Post
A.22.34	4150	6.0	--	8.31	.234	.470	59.0	I	36	Post
A.22.36	2890	6.0	--	8.35	.176	.351	88.0	I	36	Post
A.22.39	2580	6.0	--	8.8	.176	.333	36.1	I	36	Post
A.22.40	5790	6.0	--	8.20	.381	.774	72.0	I	36	Post
A.22.49	4760	6.0	--	8.20	.381	.774	56.8	I	36	Post
A.32.08	4180	6.0	--	9.24	.058	.104	0	I	36	Pre
A.32.11	4410	6.1	--	8.94	.087	.161	0	I	36	Pre
A.32.17	3810	6.0	--	8.85	.116	.218	0	I	36	Pre
A.32.19	4990	6.1	--	9.03	.175	.314	0	I	36	Pre
A.32.22	4290	6.0	--	9.38	.176	.312	24.0	I	36	Post
A.32.27	2800	6.0	--	9.16	.176	.320	10.0	I	36	Post
A.32.37	6120	6.0	--	8.20	.381	.758	5.0	I	36	Post
A.32.49	4760	6.0	--	8.20	.381	.774	34.0	I	36	Post
B.11.07	8260	6.05	3.02	11.07	.121	.180	121.6	VIII	54	Pre
B.11.20	4525	5.92	2.95	10.21	.178	.295	123.5	VII	54	Pre
B.11.29	4190	5.95	2.95	10.0	.239	.401	124	IX	54	Pre
B.11.40	4500	5.95	2.95	10.0	.359	.603	117	IX	54	Pre

TABLE 1 (Continued)

Mark	Concrete Strength f'_c psi	Flange Width b in.	Web Thickness b' in.	Effective Depth d in.	Area of Steel A_s sq. in.	Longit. Reinf. p %	Effective Prestress f_{se} ksi	Wire Lot	Shear Span a in.	Method of Prestressing
B.12.07	8400	6.02	3.0	11.05	.121	.181	125	VIII	36	Pre
B.12.10	5600	6.0	3.06	11.11	.121	.181	123	VIII	36	Pre
B.12.12	4570	6.0	3.0	11.13	.121	.181	125	VIII	36	Pre
B.12.14	3850	6.0	3.0	11.14	.121	.181	123	VIII	36	Pre
B.12.19	2890	6.0	2.98	11.09	.121	.181	122.2	VIII	36	Pre
B.12.26	4460	6.14	3.03	10.06	.233	.377	110	VI	36	Pre
B.12.29	4180	6.0	3.0	9.76	.238	.406	121.7	VII	36	Pre
B.12.34	4825	6.19	3.08	10.18	.349	.544	107.4	VI	36	Pre
B.12.35	3210	6.3	3.08	9.99	.238	.378	121	VII	36	Pre
B.12.50	2950	6.0	2.96	10.2	.299	.489	116	IX	36	Pre
B.12.61	2980	6.0	3.0	9.9	.359	.604	114.5	IX	36	Pre
B.13.07	8560	6.02	2.96	11.03	.121	.184	127	VIII	28	Pre
B.13.16	5540	6.0	3.0	10.38	.179	.287	125.5	IX	28	Pre
B.13.26	4600	6.0	2.94	10.03	.239	.397	124	IX	28	Pre
B.13.41	4320	6.0	2.9	10.04	.359	.596	118.5	IX	28	Pre
B.21.26	4470	6.0	2.96	10.21	.238	.393	62.3	VII	54	Pre
B.22.09	6320	6.0	2.96	11.07	.119	.179	63.5	VII	36	Pre
B.22.23	5120	6.05	3.0	10.03	.238	.391	55.3	VII	36	Pre
B.22.30	2770	6.15	3.11	10.15	.175	.280	56.7	VI	36	Pre
B.22.41	2710	6.25	3.16	10.02	.233	.372	51.2	VI	36	Pre
B.22.65	1750	6.2	3.12	9.95	.233	.377	59.9	VI	36	Pre
B.22.68	2670	6.0	3.0	9.9	.359	.604	59.0	IX	36	Pre
B.31.15	5820	5.98	2.95	10.21	.178	.292	0	VII	54	Pre
B.32.11	5220	6.0	2.98	10.40	.119	.190	0	VII	36	Pre
B.32.19	4330	6.16	3.12	10.21	.175	.278	0	VI	36	Pre
B.32.31	2720	6.19	3.1	10.20	.175	.277	0	VI	36	Pre
B.32.34	2510	6.26	3.2	10.11	.178	.282	0	VII	36	Pre

TABLE 1 (Continued)

Mark	Concrete Strength f'_c psi	Flange Width b in.	Web Thickness b' in.	Effective Depth d in.	Area of Steel A_s sq. in.	Longit. Reinf. p %	Effective Prestress f_{se} ksi	Wire Lot	Shear Span a in.	Method of Prestressing
B.32.41	3275	6.0	2.96	10.59	.299	.444	0	IX	36	Pre
B.32.54	3200	6.0	2.78	10.38	.358	.576	0	IX	36	Pre
C.12.09	6460	6.0	1.75	11.04	.121	.182	126	VIII	36	Pre
C.12.18	5310	6.0	1.75	9.69	.187	.321	113.7	II	36	Pre
C.12.19	6040	6.0	1.79	10.11	.233	.384	111.1	VI	36	Pre
C.12.32	3620	6.17	1.86	9.86	.233	.383	103	I	36	Pre
C.12.33	5470	6.11	1.88	10.08	.373	.606	115.4	II	36	Pre
C.12.40	2390	6.1	1.75	9.69	.187	.316	115.5	II	36	Pre
C.12.44	2890	6.2	1.75	9.5	.249	.422	101.1	II	36	Pre
C.12.50	3020	6.0	1.80	10.0	.299	.498	116.7	IX	36	Pre
C.12.57	3100	6.1	1.83	9.91	.359	.594	117	IX	36	Pre
C.22.29	2490	6.19	1.84	10.40	.116	.181	60	I	36	Pre
C.22.31	2700	6.0	1.77	10.88	.181	.277	62	VIII	36	Pre
C.22.36	3300	6.07	1.86	10.23	.241	.392	60	VIII	36	Pre
C.22.39	2150	6.15	1.85	10.18	.175	.279	54.5	I	36	Pre
C.22.40	4620	6.2	1.75	9.85	.373	.611	88.8	II	36	Pre
C.22.46	3160	6.05	1.79	10.11	.299	.489	57.7	IX	36	Pre
C.22.62	2060	6.1	1.89	9.0	.233	.424	54.3	I	36	Pre
C.22.73	2910	6.0	1.75	9.91	.419	.704	55.3	IX	36	Pre
C.32.11	7310	6.14	1.77	11.06	.179	.264	0	IX	36	Pre
C.32.22	3870	6.08	1.82	10.0	.175	.287	0	I	36	Pre
C.32.37	3060	6.14	1.83	10.01	.233	.377	0	I	36	Pre
C.32.42	2690	6.14	1.88	10.10	.233	.375	0	I	36	Pre
C.32.50	3230	6.1	1.84	10.68	.356	.547	0	VII	36	Pre
C.32.80	3000	6.0	1.81	10.0	.478	.797	0	IX	36	Pre

TABLE 2

PROPERTIES OF CONCRETE MIXES

Mark	Cement:Sand:Gravel by weight	Water/Cement by weight		Slump in.		Compressive Strength f'_c psi		Modulus of Rupture f_r psi		Age at Test days	Cement Type	Coarse Aggregate Type
Batch	1 and 2	1	2	1	2	1	2	1	2			
A.11.43	1:2.6:3.9	.61	.59	1 1/2	1 1/2	5870	6220	704	---	39	I	R*
A.11.51	1:4.9:5.4	.95	.92	3	1 1/2	2960	2900	512	---	32	I	R
A.11.53	1:3.8:5.3	.89	.86	1 1/2	2	4150	4360	596	---	39	I	R
A.11.96	1:3.9:5.5	.93	.90	2	2 1/2	2770	2900	460	---	32	I	R
A.12.23	1:2.9:4.2	.60	.60	1/2	1 1/2	6260	5650	805	---	87	I	R
A.12.31	1:2.8:4.6	.66	.66	1/2	1/2	4730	5800	514	---	9	III	P**
A.12.34	1:1.6:2.9	.44	.44	3 1/2	5 1/2	7367	7990	835	---	68	I	R
A.12.36	1:4.0:5.6	.87	.87	2	6 1/2	4180	3440	---	615	120	I	R
A.12.42	1:2.7:4.2	.71	.69	2	1/2	6279	6260	773	---	65	I	R
A.12.46	1:3.0:4.3	.69	.64	2	3	4360	4660	596	---	35	I	R
A.12.48	1:3.0:4.2	.70	.65	3	2 1/2	5190	4840	606	---	35	I	R
A.12.53	1:3.1:5.2	.84	.82	0	3/4	3020	3400	342	---	8	III	P
A.12.56	1:3.2:3.5	.83	.83	6	7 1/2	4360	3790	533	384	8	III	P
A.12.60	1:4.0:5.5	.97	.92	1	2 1/2	3440	3350	542	---	32	I	R
A.12.69	1:3.9:5.6	.95	.90	4 1/2	7	3470	2950	450	475	44	I	R
A.12.73	1:3.9:5.5	.93	.93	5	7	3350	3550	580	---	30	I	R
A.12.81	1:3.7:3.9	1.00	1.00	8	8	2930	2600	410	370	9	III	P
A.14.39	1:4.1:5.5	.88	.85	6	2	3440	3350	509	---	42	I	R
A.14.44	1:4.0:5.5	.84	.84	2	2	2795	3350	377	---	27	I	R
A.14.55	1:4.0:5.6	.85	.88	1 1/2	1 1/2	3660	3320	434	---	29	I	R
A.14.68	1:4.1:5.6	.88	.87	1 1/2	1 1/2	2130	2440	366	---	34	I	R
A.21.29	1:3.9:5.4	.97	.97	2	6	3525	3350	485	---	36	I	R
A.21.39	1:3.9:5.4	.92	.91	2 1/2	1 1/2	2655	3130	519	---	34	I	R
A.21.51	1:2.7:3.9	.64	.61	5	4	5770	5630	642	---	39	I	R

* R = Regular-size coarse aggregate

** P = Small-size coarse aggregate

TABLE 2 (Continued)

Mark	Cement:Sand:Gravel by weight	Water/Cement by weight		Slump in.		Compressive Strength f'_c psi		Modulus of Rupture f_r psi		Age at Test days	Cement Type	Coarse Aggregate Type
Batch	1 and 2	1	2	1	2	1	2	1	2			
A.22.20	1:3.7:5.3	.86	.80	1/2	1/2	4200	5350	566	---	37	I	R
A.22.24	1:4.0:5.5	.98	.95	4 1/2	5	2905	3470	451	---	28	I	R
A.22.26	1:4.0:5.4	1.00	.96	3 1/2	1	3660	3665	670	---	41	I	R
A.22.27	1:3.9:5.3	.86	.83	3	1	3350	3850	521	---	40	I	R
A.22.28	1:3.9:5.5	.84	.84	3	6	3480	3770	480	450	36	I	R
A.22.31	1:4.0:5.5	.86	.79	5 1/2	5 1/2	3370	3530	500	---	42	I	R
A.22.34	1:3.9:5.3	.90	.86	5	5	3525	4150	575	---	38	I	R
A.22.36	1:4.0:5.5	.84	.84	6	6	3940	2890	538	---	32	I	R
A.22.39	1:3.9:5.5	.91	.91	6 1/2	6	2880	2580	412	---	27	I	R
A.22.40	1:2.9:4.1	.69	.69	2	2 1/2	5440	5790	748	---	31	I	R
A.22.49	1:2.9:4.1	.68	.68	1 1/2	5	4910	4760	670	---	28	I	R
A.32.08	1:3.4:5.2	.74	.70	2	1 1/2	4000	4180	480	---	22	I	R
A.32.11	1:3.4:5.2	.85	.86	1 1/2	1	4430	4410	600	---	24	I	R
A.32.17	1:3.5:5.1	.70	.71	1	2	4120	3810	490	---	21	I	R
A.32.19	1:2.8:4.3	.66	.63	2 1/2	2	4810	4990	550	---	19	I	R
A.32.22	1:4.0:5.5	.87	.90	1 1/2	2	3510	4290	682	---	70	I	R
A.32.27	1:4.0:5.6	.82	.82	2 1/2	2	3620	2800	641	---	40	I	R
A.32.37	1:2.7:4.0	.64	.64	1/2	1/2	5770	6120	722	---	32	I	R
A.32.49	1:3.0:4.2	.67	.67	2	6	4460	4760	660	---	32	I	R
B.11.07	1:2.3:2.7	.53	.53	1/2	1/2	8375	8260	585	660	15	III	P
B.11.20	1:3.3:3.4	.70	.70	3 1/2	3 1/2	4650	4525	510	480	6	III	P
B.11.29	1:3.3:3.6	.81	.81	6	6	4180	4190	450	390	7	III	P
B.11.40	1:3.3:3.6	.78	.78	3	3	4220	4500	540	520	6	III	P
B.12.07	1:2.3:2.7	.53	.53	1/2	1/2	8540	8400	580	540	15	III	P
B.12.10	1:3.0:3.3	.67	.67	1 1/2	1 1/2	5360	5600	450	460	7	III	P
B.12.12	1:3.2:3.5	.75	.75	6	6 1/2	4380	4570	420	410	11	III	P
B.12.14	1:3.4:3.6	.81	.81	7 1/2	7 1/2	3810	3850	390	400	9	III	P

TABLE 2 (Continued)

Mark	Cement:Sand:Gravel by weight	Water/Cement by weight		Slump in.		Compressive Strength f'_c psi		Modulus of Rupture f_r psi		Age at Test days	Cement Type	Coarse Aggregate Type
Batch	1 and 2	1	2	1	2	1	2	1	2			
B.12.19	1:3.8:3.8	.99	.99	8	8	2400	2420	510	500	9	III	P
B.12.26	1:3.6:3.7	.71	.69	2	2	4460	4420	---	300	9	III	P
B.12.29	1:3.7:3.6	.72	.74	1	2	4400	4180	430	420	8	III	P
B.12.34	1:2.6:2.9	.72	.69	8	8	5140	4825	380	480	8	III	P
B.12.35	1:4.6:4.5	.91	.91	3	3	3240	3210	400	360	13	III	P
B.12.50	1:4.2:4.5	.96	.96	3	3	2880	2950	350	350	9	III	P
B.12.61	1:4.3:4.4	.92	.92	3	4 1/2	3060	2980	290	300	9	III	P
B.13.07	1:2.3:2.7	.53	.53	1 1/2	1 1/2	8200	8560	540	590	15	III	P
B.13.16	1:3.4:3.5	.70	.70	1	1 1/2	5060	5540	570	580	7	III	P
B.13.26	1:3.3:3.6	.77	.77	2	2	4730	4600	500	460	8	III	P
B.13.41	1:3.3:3.6	.78	.78	2	2 1/2	4440	4325	560	490	6	III	P
B.21.26	1:3.3:3.4	.75	.75	4	4	4320	4470	510	520	7	III	P
B.22.09	1:2.3:2.7	.54	.54	1/2	1/2	6200	6320	660	575	10	III	P
B.22.23	1:3.3:3.5	.70	.70	2	2 1/2	5160	5120	390	390	14	III	P
B.22.30	1:4.4:4.4	.95	.95	3	4	3290	2770	500	---	7	III	P
B.22.41	1:4.6:4.6	.93	.95	1	6	2750	2710	300	---	10	III	P
B.22.65	1:4.7:4.7	1.10	1.10	6	6 1/2	1770	1750	220	---	10	III	P
B.22.68	1:4.2:4.5	.97	.94	1 1/2	3 1/2	3000	2670	290	260	9	III	P
B.31.15	1:3.0:3.3	.61	.61	2	2	5650	5820	450	510	9	III	P
B.32.11	1:2.3:2.7	.58	.58	2 1/2	3	5000	5220	425	460	7	III	P
B.32.19	1:3.3:3.5	.74	.74	4	5	4580	4330	320	---	12	III	P
B.32.31	1:4.7:4.7	.94	.94	3	6	2620	2720	250	250	8	III	P
B.32.34	1:4.7:4.7	1.08	1.08	6 1/2	6 1/2	2360	2510	300	275	13	III	P
B.32.41	1:3.7:4.3	.85	.85	3	5	3220	3275	340	325	16	III	P
B.32.54	1:4.1:4.5	.95	.95	2 1/2	6 1/2	2460	2910	380	330	10	III	P

TABLE 2 (Continued)

Mark	Cement:Sand:Gravel by weight	Water/Cement by weight		Slump in.		Compressive Strength f'_c psi		Modulus of Rupture f_r psi		Age at Test days	Cement Type	Coarse Aggregate Type
Batch	1 and 2	1	2	1	2	1	2	1	2			
C.12.09	1:3.2:3.3	.67	.67	1	2	6220	6460	460	475	7	III	P
C.12.18	1:2.2:3.8	.68	.67	2	2	4383	5310	460	---	7	III	P
C.12.19	1:2.7:3.0	.67	.65	5	3 1/2	5890	6040	400	---	12	III	P
C.12.32	1:4.0:4.0	.84	.83	2	1 1/2	1880	3620	---	---	7	III	P
C.12.33	1:2.7:3.0	.64	.61	2 1/2	2 1/2	5390	5470	480	---	7	III	P
C.12.40	1:3.6:5.6	.92	.88	6	1/2	2890	2390	340	---	7	III	P
C.12.44	1:3.2:5.1	.71	.77	2	1/2	3985	2890	470	---	9	III	P
C.12.50	1:4.3:4.5	.82	.82	1 1/2	3	3100	3020	370	400	6	III	P
C.12.57	1:4.2:4.5	.88	.90	1	1 1/2	3100	3100	430	340	7	III	P
C.22.29	1:4.4:4.5	1.05	1.04	1 1/2	3 1/2	2270	2490	---	330	7	III	P
C.22.31	1:4.4:4.4	1.04	1.04	2	4 1/2	3650	2700	370	280	14	III	P
C.22.36	1:4.3:4.2	.96	.96	1	1	3600	3300	350	380	9	III	P
C.22.39	1:5.0:5.0	1.07	.97	1	1/2	1030	2310	---	170	8	III	P
C.22.40	1:2.8:4.7	.70	.68	1/2	1	4540	4620	460	---	9	III	P
C.22.46	1:4.0:4.5	.99	.95	3	5	3440	3160	370	380	11	III	P
C.22.62	1:4.0:4.0	.91	.94	7	8	2510	2135	240	---	6	III	P
C.22.73	1:4.1:4.5	.95	.95	2 1/2	6 1/2	2460	2910	380	350	10	III	P
C.32.11	1:2.2:2.7	.60	.60	1 1/2	1 1/2	6870	7310	500	---	23	III	P
C.32.22	1:4.0:4.0	.85	.82	1 1/2	1 1/2	3920	3870	---	470	8	III	P
C.32.37	1:4.5:4.6	.92	.92	1	1 1/2	3630	3060	---	---	6	III	P
C.32.42	1:4.5:4.5	1.07	1.02	5 1/2	7 1/2	2610	2690	350	---	13	III	P
C.32.50	1:4.0:4.0	.91	.91	3	4 1/2	2820	3230	350	375	16	III	P
C.32.80	1:4.1:4.5	.91	.91	3	6	3250	3000	380	430	12	III	P

TABLE 3

PROPERTIES OF REINFORCEMENT

Lot	Manufacturer	Heat Analysis C %	Mn %	P %	S %	Si %	Diameter in.	0.2% Offset Stress ksi	Ultimate Strength f'_s ksi
I	AS and W*	.80	.70	----	----	----	.193	208	240
II	Roebling**	---	---	----	----	----	.199	218	248
III	Roebling	---	---	----	----	----	.192	206	246
VI	AS and W	.82	.73	.010	.034	0.20	.193	212	250
VII	AS and W	.86	.87	.010	.025	0.18	.195	236	265
VIII	AS and W	.83	.75	.010	.035	0.20	.196	213.5	255
IX	As and W	.82	.83	.010	.027	0.27	.195	199	251

* American Steel and Wire Division of the U. S. Steel Corporation.

** John A. Roebling's Sons Corporation.

TABLE 4

MEASURED AND COMPUTED VALUES OF INCLINED TENSION CRACKING LOAD

Mark	Tensile Strength f'_t psi	Effective Prestress Force F_{se} kips	$\frac{F_{se}}{A_c f'_t}$	Cracking Load P_c kips	$\frac{M_c}{f_t\, bd^2\sqrt{b'/b}}$ Meas.	Comp.	$\frac{\text{Meas.}}{\text{Comp.}}$
A.11.43	493	51.0	1.44	19	2.58	2.44	1.06
A.11.51	332	28.4	1.19	13	2.49	2.19	1.14
A.11.53	410	46.5	1.58	17	2.88	2.58	1.12
A.11.96	317	54.1	2.37	17	3.40	3.37	1.01
A.12.23	510	28.4	0.77	23	1.61	1.77	0.91
A.12.31	306	35.5	1.61	20	2.63	2.61	1.01
A.12.34	550	48.3	1.22	28	2.28	2.22	1.03
A.12.36	410	26.4	0.90	20.8	1.77	1.90	0.93
A.12.42	510	45.4	1.24	27	2.29	2.24	1.02
A.12.46	420	46.2	1.53	23	2.46	2.53	0.97
A.12.48	462	53.3	1.61	--	----	2.61	----
A.12.53	250	33.7	1.87	18	2.94	2.87	1.02
A.12.56	296	43.6	2.05	22	3.02	3.05	0.99
A.12.60	367	47.8	1.81	27	2.85	2.81	1.02
A.12.69	368	39.7	1.50	21	2.55	2.50	1.02
A.12.73	360	45.8	1.77	23	2.71	2.77	0.98
A.12.81	247	43.4	2.44	21.5	3.46	3.44	1.01
A.14.39	367	25.5	0.96	28	2.21	1.96	1.13
A.14.44	318	29.4	1.28	27.5	2.32	2.28	1.02
A.14.55	380	36.4	1.33	33	2.37	2.33	1.02
A.14.68	262	33.0	1.75	29	3.06	2.75	1.11
A.21.29	370	9.8	0.37	7	1.19	1.37	0.87
A.21.39	308	12.8	0.58	8	1.46	1.58	0.92
A.21.51	490	27.6	0.78	14	1.97	1.78	1.11

TABLE 4 (Continued)

Mark	Tensile Strength f_t psi	Effective Prestress Force F_{se} kips	$\frac{F_{se}}{A_c f_t}$	Cracking Load P_c kips	$\frac{M_c}{f_t\, bd^2\sqrt{b'/b}}$ Meas.	Comp.	Meas./Comp.
A.22.20	410	10.8	0.37	12	1.24	1.37	0.91
A.22.24	327	8.6	0.37	10	1.43	1.37	1.04
A.22.26	380	8.8	0.32	14	1.29	1.32	0.98
A.22.27	358	10.6	0.41	12	1.44	1.41	1.02
A.22.28	386	8.6	0.31	11	1.10	1.31	0.84
A.22.31	360	15.7	0.61	11.3	1.47	1.61	0.91
A.22.34	370	13.8	0.52	13	1.51	1.52	0.99
A.22.36	397	15.5	0.54	12	1.41	1.54	0.92
A.22.39	326	6.4	0.27	10	1.19	1.27	0.94
A.22.40	475	27.4	0.80	21	1.98	1.80	1.10
A.22.49	450	21.6	0.67	16	1.59	1.67	0.95
A.32.08	400	0	0	(6.4)	(.56)	1.0	----
A.32.11	424	0	0	(9.18)	(.80)	1.0	----
A.32.17	407	0	0	(11.47)	(1.07)	1.0	----
A.32.19	445	0	0	8.3	0.73	1.0	0.73
A.32.22	370	4.22	0.16	12	1.09	1.16	0.94
A.32.27	375	1.76	0.07	12	1.13	1.07	1.05
A.32.37	490	1.9	0.05	10.6	0.95	1.05	0.90
A.32.49	427	11.6	0.38	12.6	1.32	1.38	0.96
B.11.07	368	14.7	0.75	(12.55)	(1.75)	1.75	----
B.11.20	304	22.0	1.35	12	2.44	2.35	1.04
B.11.29	291	29.6	1.91	13.5	2.97	2.91	1.02
B.11.40	292	42.0	2.70	17.8	3.92	3.70	1.06
B.12.07	370	15.1	0.76	(18.2)	(1.70)	1.76	----

( ) No inclined tension cracking.

TABLE 4 (Continued)

Mark	Tensile Strength f_t psi	Effective Prestress Force F_{se} kips	$\frac{F_{se}}{A_c f_t}$	Cracking Load P_c kips	$\frac{M_c}{f_t\ bd^2\sqrt{b'/b}}$ Meas.	Comp.	$\frac{\text{Meas.}}{\text{Comp.}}$
B.12.10	320	14.9	0.87	14	1.50	1.87	0.80
B.12.12	297	15.1	0.95	14.9	1.82	1.95	0.93
B.12.14	280	14.9	1.00	14.13	1.73	2.00	0.86
B.12.19	247	14.8	1.12	14.3	2.00	2.12	0.94
B.12.26	299	25.6	1.60	18.34	2.65	2.60	1.02
B.12.29	297	29.0	1.83	19.6	2.94	2.83	1.04
B.12.34	316	37.5	2.22	25.1	3.15	3.22	0.98
B.12.35	260	28.8	2.07	18.0	2.80	3.07	0.91
B.12.50	245	34.7	2.65	22.86	3.83	3.65	0.95
B.12.61	253	41.1	3.04	23.86	4.09	4.04	1.01
B.13.07	367	15.4	0.78	(23.48)	(1.75)	1.78	----
B.13.16	319	22.4	1.34	24.7	2.37	2.34	1.01
B.13.26	306	29.6	1.81	26.4	2.83	2.81	1.01
B.13.41	299	42.5	2.66	30.1	3.29	3.66	0.90
B.21.26	295	14.8	0.94	8.56	1.83	1.94	0.94
B.22.09	337	7.56	0.42	12.7	1.30	1.42	0.92
B.22.23	316	13.2	0.78	12.8	1.70	1.78	0.96
B.22.30	261	9.92	0.71	11.0	1.69	1.71	0.99
B.22.41	272	11.9	0.82	12.0	1.79	1.82	0.98
B.22.65	185	14.0	1.42	10.8	2.42	2.42	1.00
B.22.68	250	21.2	1.59	15.7	2.71	2.59	1.05
B.31.15	327	0	0	8.26	1.55	1.0	1.55

TABLE 4 (Continued)

Mark	Tensile Strength f_t psi	Effective Prestress Force F_{se} kips	$\frac{F_{se}}{A_c f_t}$	Cracking Load P_c kips	$\frac{M_c}{f_t\, bd^2 \sqrt{b'/b}}$ Meas.	Comp.	$\frac{\text{Meas.}}{\text{Comp.}}$
B.32.11	313	0	0	6	0.75	1.0	0.75
B.32.19	302	0	0	6	0.79	1.0	0.79
B.32.31	233	0	0	6.95	1.18	1.0	1.18
B.32.34	220	0	0	6	1.08	1.0	1.08
B.32.41	259	0	0	7	1.02	1.0	1.02
B.32.54	237	0	0	6	1.00	1.0	1.00
C.12.09	337	15.2	0.95	14.5	1.96	1.95	1.00
C.12.18	292	21.3	1.53	14.5	2.94	2.53	1.16
C.12.19	331	25.9	1.64	17.0	2.80	2.64	1.06
C.12.32	193	24.0	2.61	13.5	3.88	3.61	1.07
C.12.33	321	43.0	2.81	24.5	4.10	3.81	1.08
C.12.40	245	21.6	1.85	10.2	2.42	2.85	0.85
C.12.44	285	25.2	1.86	12.85	2.65	2.86	0.93
C.12.50	254	34.9	2.89	18.1	3.96	3.89	1.02
C.12.57	254	42.0	3.47	21.0	4.60	4.47	1.03
C.22.29	215	7.0	0.68	7.5	1.73	1.68	1.03
C.22.31	275	11.2	0.85	11.5	1.96	1.85	1.06
C.22.36	273	14.5	1.12	10.6	2.04	2.12	0.96
C.22.39	125	9.5	1.60	7.2	2.90	2.60	1.11
C.22.40	301	33.1	2.31	18	3.32	3.31	1.00
C.22.46	267	17.3	1.36	12	2.43	2.36	1.03
C.22.62	228	12.7	1.17	8.5	2.51	2.17	1.16
C.22.73	225	23.2	2.16	13.33	3.34	3.16	1.06

TABLE 4 (Continued)

Mark	Tensile Strength f_t psi	Effective Prestress Force F_{se} kips	$\frac{F_{se}}{A_c f_t}$	Cracking Load P_c kips	Meas.	$\frac{M_c}{f_t bd^2 \sqrt{b'/b}}$ Comp.	$\frac{\text{Meas.}}{\text{Comp.}}$
C.32.11	348	0	0	8	1.02	1.0	1.02
C.32.22	283	0	0	6.1	1.18	1.0	1.18
C.32.37	273	0	0	5.7	1.12	1.0	1.12
C.32.42	233	0	0	4	0.92	1.0	0.92
C.32.50	242	0	0	5.5	1.09	1.0	1.09
C.32.80	260	0	0	5.0	1.07	1.0	1.07

TABLE 5

DERIVED VALUES OF THE STRAIN COMPATIBILITY FACTOR

Mark	Ultimate Moment kip-in.	Inclined Cracking Moment kip-in.	Derived k_u	Steel Stress At Inclined Cracking ksi	Steel Stress At Ultimate ksi	Compatibility Factor F
A.11.51	383	360	.359	202	215	0.32
A.11.53	512	469	.418	190	208	0.78
A.11.96	516	469	.534	154	169	0.23
A.12.23	492	368	.222	175	234	1.17
A.12.31	486	404	.260	169	203	0.13
A.12.36	396	383	.262	202	203	0.14
A.12.42	567	494	.130	143	164	0.05
A.12.46	511	422	.372	173	210	0.74
A.12.53	443	332	.361	147	195	0.39
A.12.56	483	404	.367	154	184	0.19
A.12.69	451	386	.475	174	203	0.78
A.12.73	513	422	.437	139	169	0.29
A.12.81	423	395	.440	155	166	0.10
A.14.39	354	342	.300	215	222	0.49
A.14.44	390	336	.322	184	213	0.35
A.14.55	441	402	.374	180	197	0.29
A.14.68	365	354	.393	178	185	0.16
A.21.29	225	198	.175	162	184	0.09
A.21.39	302	225	.224	127	171	0.15
A.21.51	472	387	.296	117	142	0.12
A.22.20	269	224	.152	161	193	0.08
A.22.24	261	188	.183	158	219	0.88
A.22.27	258	224	.187	165	190	0.05
A.22.28	240	206	.166	145	168	0.05
A.22.31	277	212	.236	166	216	1.00
A.22.34	256	242	.179	135	142	0.01

TABLE 5 (Continued)

Mark	Ultimate Moment kip-in.	Inclined Cracking Moment kip-in.	Derived k_u	Steel Stress At Inclined Cracking ksi	Steel Stress At Ultimate ksi	Compatibility Factor F
A.22.36	273	242	.249	184	207	0.35
A.22.39	201	188	.171	131	140	0.06
A.22.40	483	386	.291	141	176	0.17
A.22.49	421	296	.291	108	154	0.19
A.32.19	212	157	.103	103	139	0.04
A.32.22	261	224	.137	144	168	0.08
A.32.27	233	224	.132	147	153	0.01
A.32.37	323	199	.174	69	112	0.08
A.32.49	384	235	.262	85	132	0.19
B.11.20	377	331	.166	196	223	0.98
B.12.10	290	258	.088	199	224	0.16
B.12.12	293	274	.104	213	228	0.30
B.12.14	308	261	.123	204	240	1.05
B.12.26	426	354	.192	164	197	0.12
B.12.29	458	358	.237	171	219	0.19
B.12.35	416	330	.234	154	194	0.18
B.13.16	374	351	.136	200	214	0.57
B.13.26	409	375	.183	169	185	0.03
B.21.26	339	238	.152	106	151	0.06
B.22.09	260	234	.075	186	204	0.02
B.22.23	341	236	.138	105	152	0.07
B.22.30	276	204	.164	124	167	0.08
B.22.41	319	222	.197	104	149	0.10
B.22.68	346	288	.234	90	108	0.05

TABLE 5 (Continued)

Mark	Ultimate Moment kip-in.	Inclined Cracking Moment kip-in.	Derived k_u	Steel Stress At Inclined Cracking ksi	Steel Stress At Ultimate ksi	Compatibility Factor F
B.31.15	245	230	.086	131	140	0.01
B.32.11	187	114	.068	95	155	0.04
B.32.19	195	114	.083	66	114	0.04
B.32.31	143	131	.082	76	83	0.01
B.32.34	180	114	.111	67	105	0.04
B.32.41	294	132	.133	44	98	0.07
B.32.54	266	132	.134	36	76	0.05
C.12.09	305	268	.085	208	237	0.49
C.12.18	331	267	.117	157	195	0.06
C.12.19	408	311	.148	141	185	0.08
C.22.29	170	140	.102	121	149	0.03
C.22.31	228	212	.121	114	122	0.01
C.32.11	185	149	.046	77	96	0.01
C.32.22	192	115	.092	68	115	0.04
C.32.37	172	108	.096	48	77	0.03
C.32.42	152	77	.090	34	67	0.03
C.32.50	196	99	.094	27	54	0.02
C.32.80	196	95	.115	21	43	0.02

TABLE 6

COMPUTED AND MEASURED CAPACITIES

Mark	Computed Total Bending Moments: Inclined Tension Cracking M'_c k-in.	Ultimate for Flexure M_f k-in.	Ultimate for Shear-Comp. M_s k-in.	Measured Ultimate Moment M_t k-in.	$\frac{M_t}{M'_c}$	$\frac{M_t}{M_f}$	$\frac{M_t}{M_s}$	Obs. Failure Mode	Predicted Failure Mode
(1)	(2)	(3)	(4)	(5)	(6)	(7)	(8)	(9)	(10)
A.11.43	499	643	610	665	1.33	1.03	1.09	S	S
A.11.51	320	395	371	383	1.20	0.97	1.03	S	S
A.11.53	417	535	503	512	1.23	0.96	1.02	S	S
A.11.96	462	556	530	516	1.12	0.93	0.98	S	S
A.12.23	488	490	489	492	1.00	1.00	1.00	S	S
A.12.31	366	538	453	486	1.33	0.90	1.07	S	S
A.12.34	501	667	626	602	1.20	0.90	0.96*	S	S
A.12.36	410	430	422	396	0.97	0.92	0.94	S	S
A.12.42	480	650	611	567	1.18	0.87	0.93	S	S
A.12.46	437	518	498	511	1.17	0.99	1.02	S	S
A.12.48	495	553	537	547	1.10	0.99	1.02	F	S
A.12.53	327	492	425	443	1.35	0.90	1.04	S	S
A.12.56	408	550	495	483	1.18	0.88	0.98	S	S
A.12.60	488	533	518	494	1.01	0.93	0.95	F	S
A.12.69	378	461	423	451	1.19	0.98	1.07	S	S
A.12.73	434	584	537	513	1.18	0.88	0.96	S	S
A.12.81	391	500	464	423	1.08	0.85	0.92	S	S
A.14.39	305	360	344	354	1.16	0.98	1.03	S	S
A.14.44	319	414	371	390	1.22	0.94	1.05	S	S
A.14.55	391	486	441	441	1.13	0.91	1.00	S	S
A.14.68	311	413	362	365	1.17	0.88	1.01	S	S
A.21.29	226	277	248	225	1.00	0.81	0.91	S	S
A.21.39	243	388	309	302	1.24	0.78	0.98	S	S
A.21.51	354	627	515	472	1.33	0.75	0.92	S	S

* Failed as an unbonded beam after development of inclined cracks.

TABLE 6 (Continued)

Mark	Computed Total Bending Moments: Inclined Tension Cracking M'_c k-in.	Computed Total Bending Moments: Ultimate for Flexure M_f k-in.	Computed Total Bending Moments: Ultimate for Shear-Comp. M_s k-in.	Measured Ultimate Moment M_t k-in.	$\frac{M_t}{M'_c}$	$\frac{M_t}{M_f}$	$\frac{M_t}{M_s}$	Obs. Failure Mode	Predicted Failure Mode
(1)	(2)	(3)	(4)	(5)	(6)	(7)	(8)	(9)	(10)
A.22.20	249	305	273	269	1.08	0.88	0.99	S	S
A.22.24	216	263	240	261	1.21	0.99	1.09	S	S
A.22.26	267	325	300	321	1.20	0.99	1.07	F	S
A.22.27	221	290	261	258	1.17	0.89	0.99	S	S
A.22.28	244	304	271	240	0.98	0.79	0.89	S	S
A.22.31	234	279	257	276	1.18	0.99	1.07	S	S
A.22.34	241	369	321	256	1.06	0.69	0.80	S	S
A.22.36	264	282	272	273	1.03	0.97	1.00	S	S
A.22.39	175	262	227	201	1.15	0.77	0.89	S	S
A.22.40	353	560	492	483	1.37	0.86	0.98	S	S
A.22.49	311	537	441	421	1.35	0.78	0.96	S	S
A.32.08	213	125	---	123	----	0.98	----	F	F
A.32.11	215	176	---	173	----	0.98	----	F	F
A.32.17	199	218	212	214	1.07	0.98	1.06	F	S
A.32.19	226	324	257	212	0.94	0.65	0.83	S	S
A.32.22	235	333	277	261	1.11	0.78	0.94	S	S
A.32.27	210	322	253	233	1.11	0.72	0.92	S	S
A.32.37	219	558	340	323	1.47	0.58	0.95	S	S
A.32.49	246	525	375	384	1.56	0.73	1.02	S	S
B.11.07	344	325	---	341	----	1.05	----	F	F
B.11.20	319	421	373	377	1.18	0.90	1.01	S	S
B.11.29	363	459	---	469	1.29	1.02	----	S	S
B.11.40	460	644**	---	567	1.23	0.88	----	S	S

** Computed depth of neutral axis greater than thickness of flange.

TABLE 6 (Continued)

Mark	Computed Total Bending Moments: Inclined Tension Cracking M'_c k-in.	Computed Total Bending Moments: Ultimate for Flexure M_f k-in.	Computed Total Bending Moments: Ultimate for Shear-Comp. M_s k-in.	Measured Ultimate Moment M_t k-in.	$\frac{M_t}{M'_c}$	$\frac{M_t}{M_f}$	$\frac{M_t}{M_s}$	Obs. Failure Mode	Predicted Failure Mode
(1)	(2)	(3)	(4)	(5)	(6)	(7)	(8)	(9)	(10)
B.12.07	345	328	---	334	----	1.02	----	F	F
B.12.10	320	316	---	290	----	0.92	----	S	F
B.12.12	310	310	---	293	----	0.95	----	S	F
B.12.14	300	307	301	308	1.03	1.00	1.02	S	S
B.12.19	279	296	282	314	1.12	1.06	1.11	S	S
B.12.26	347	477	412	426	1.23	0.89	1.03	S	S
B.12.29	346	504	424	458	1.32	0.91	1.08	S	S
B.12.34	463	687	576	523	1.13	0.76	0.91	S	S
B.12.35	361	524	427	416	1.15	0.79	0.97	S	S
B.12.50	401	537**	---	418	1.04	0.78	----	S	S
B.12.61	432	598**	---	436	1.01	0.73	----	S	S
B.13.07	329	330	---	334	----	1.01	----	F	F
B.13.16	341	389	353	374	1.10	0.96	1.06	S	S
B.13.26	372	462	418	409	1.10	0.89	0.98	S	S
B.13.41	479	643**	---	453	0.95	0.71	----	S	S
B.21.26	255	545	339	339	1.33	0.62	1.00	S	S
B.22.09	255	326	270	260	1.02	0.80	0.96	S	S
B.22.23	249	536	338	341	1.37	0.64	1.01	S	S
B.22.30	206	360	265	276	1.34	0.77	1.04	S	S
B.22.41	226	450	320	319	1.41	0.71	1.00	S	S
B.22.65	201	411**	---	202	1.00	0.49	----	S	S
B.22.68	276	568**	433	346	1.25	0.61	0.80	S	S
B.31.15	153	426	192	245	1.60	0.58	1.28	S	S

TABLE 6 (Continued)

Mark	Computed Total Bending Moments: Inclined Tension Cracking M'_c k-in.	Computed Total Bending Moments: Ultimate for Flexure M_f k-in.	Computed Total Bending Moments: Ultimate for Shear-Comp. M_s k-in.	Measured Ultimate Moment M_t k-in.	$\frac{M_t}{M'_c}$	$\frac{M_t}{M_f}$	$\frac{M_t}{M_s}$	Obs. Failure Mode	Predicted Failure Mode
(1)	(2)	(3)	(4)	(5)	(6)	(7)	(8)	(9)	(10)
B.32.11	150	350	154	187	1.25	0.53	1.21	S	S
B.32.19	143	378	203	195	1.35	0.52	0.96	S	S
B.32.31	112	360	157	143	1.28	0.40	0.91	S	S
B.32.34	106	389	161	180	1.70	0.46	1.12	S	S
B.32.41	130	571	273	294	2.26	0.52	1.08	S	S
B.32.54	115	577**	261	266	2.31	0.46	1.02	S	S
C.12.09	265	317	279	305	1.15	0.97	1.09	S	S
C.12.18	230	399	292	331	1.44	0.83	1.13	S	S
C.12.19	295	498	379	408	1.38	0.82	1.08	S	S
C.12.32	231	446	---	288	1.25	0.65	----	S	S
C.12.33	415	743**	---	465	1.12	0.63	----	S	S
C.12.40	221	366	---	223	1.01	0.61	----	S	S
C.12.44	252	463**	---	236	0.94	0.51	----	S	S
C.12.50	325	527**	---	331	1.02	0.63	----	S	S
C.12.57	373	606**	---	455	1.22	0.75	----	S	S
C.22.29	136	253	170	172	1.26	0.68	1.01	S	S
C.22.31	201	402	251	228	1.13	0.57	0.91	S	S
C.22.36	204	487	---	201	0.99	0.41	----	S	S
C.22.39	117	343	---	135	1.15	0.39	----	S	S
C.22.40	329	706**	---	329	1.00	0.47	----	S	S
C.22.46	216	535**	---	235	1.09	0.44	----	S	S
C.22.62	138	366	---	190	1.38	0.52	----	S	S
C.22.73	232	638**	---	245	1.06	0.38	----	S	S

TABLE 6 (Continued)

Mark	Computed Total Bending Moments: Inclined Tension Cracking M'_c k-in.	Computed Total Bending Moments: Ultimate for Flexure M_f k-in.	Computed Total Bending Moments: Ultimate for Shear-Comp. M_s k-in.	Measured Ultimate Moment M_t k-in.	$\frac{M_t}{M'_c}$	$\frac{M_t}{M_f}$	$\frac{M_t}{M_s}$	Obs. Failure Mode	Predicted Failure Mode
(1)	(2)	(3)	(4)	(5)	(6)	(7)	(8)	(9)	(10)
C.32.11	150	426	175	185	1.23	0.43	1.06	S	S
C.32.22	98	353	137	192	1.96	0.54	1.40	S	S
C.32.37	96	436	162	172	1.79	0.40	1.06	S	S
C.32.42	84	436	148	152	1.81	0.35	1.03	S	S
C.32.50	96	655**	197	196	2.04	0.30	1.00	S	S
C.32.80	90	650**	204	196	2.18	0.30	0.96	S	S

TABLE 7

NOMINAL SHEAR STRESSES AT ULTIMATE

Mark	Ultimate Load kips	Nominal Shear Stress v psi	v/f'_c
A.11.43	24.3	280	.048
A.11.51	13.85	153	.052
A.11.53	18.62	223	.054
A.11.96	18.79	214	.077
A.12.23	26.88	269	.043
A.12.31	26.55	292	.062
A.12.34	32.99	381	.052
A.12.36	21.52	220	.052
A.12.42	31.03	354	.056
A.12.46	27.93	323	.074
A.12.48	29.95	346	.067*
A.12.53	24.16	267	.088
A.12.56	26.39	292	.067
A.12.60	27.00	291	.085*
A.12.69	24.61	286	.082
A.12.73	28.04	315	.094
A.12.81	23.06	255	.087
A.14.39	28.95	329	.095
A.14.44	31.98	356	.127
A.14.55	36.25	407	.110
A.14.68	29.87	336	.158
A.21.29	8.0	95	.027
A.21.39	10.86	120	.045
A.21.51	17.15	204	.035
A.22.20	14.47	166	.040
A.22.24	14.04	155	.053
A.22.26	17.37	180	.049*
A.22.27	13.86	161	.048
A.22.28	12.88	141	.037
A.22.31	14.91	179	.053
A.22.34	13.75	161	.046
A.22.36	14.7	171	.043
A.22.39	10.7	120	.042
A.22.40	26.39	306	.056
A.22.49	22.93	267	.054
A.32.08	6.4	70	.018*
A.32.11	9.18	102	.023*

* Flexure Failure.

TABLE 7 (Continued)

Mark	Ultimate Load kips	Nominal Shear Stress v psi	v/f'_c
A.32.17	11.47	126	.031*
A.32.19	11.34	120	.025
A.32.22	14.04	145	.041
A.32.27	12.48	133	.037
A.32.37	17.51	202	.035
A.32.49	20.90	243	.055
B.11.07	12.55	217	.026*
B.11.20	13.70	262	.056
B.11.29	17.14	332	.079
B.11.40	20.70	400	.095
B.12.07	18.20	313	.037*
B.12.10	15.74	265	.049
B.12.12	16.85	290	.066
B.12.14	16.74	286	.075
B.12.19	17.18	297	.101
B.12.26	23.30	434	.097
B.12.29	25.10	485	.110
B.12.34	28.75	518	.101
B.12.35	22.78	420	.130
B.12.50	22.86	430	.149
B.12.61	23.86	455	.149
B.13.07	23.48	407	.050*
B.13.16	26.40	480	.095
B.13.26	28.85	554	.117
B.13.41	31.63	615	.139
B.21.26	12.30	239	.055
B.22.09	14.09	248	.040
B.22.23	18.60	352	.068
B.22.30	15.00	273	.083
B.22.41	17.40	314	.113
B.22.65	10.90	204	.115
B.22.68	18.87	362	.121
B.31.15	8.80	172	.030
B.32.11	10.90	204	.041
B.32.19	10.50	192	.042
B.32.31	7.6	142	.054
B.32.34	9.67	175	.074
B.32.41	16.00	293	.091
B.32.54	14.45	269	.099

TABLE 7 (Continued)

Mark	Ultimate Load kips	Nominal Shear Stress v psi	v/f'_c
C.12.09	16.63	490	.079
C.12.18	18.09	608	.139
C.12.19	22.34	698	.119
C.12.32	16.30	507	.270
C.12.33	25.50	762	.141
C.12.40	12.1	411	.142
C.12.44	12.85	444	.111
C.12.80	18.10	572	.185
C.12.57	26.0	810	.261
C.22.29	9.25	282	.124
C.22.31	12.40	371	.102
C.22.36	10.90	331	.092
C.22.39	7.22	226	.226
C.22.40	17.99	594	.131
C.22.46	12.77	406	.118
C.22.62	10.25	350	.139
C.22.73	13.33	442	.179
C.32.11	10.0	297	.043
C.32.22	10.35	330	.084
C.32.37	9.28	294	.081
C.32.42	8.15	251	.096
C.32.50	10.60	312	.111
C.32.80	10.58	338	.104

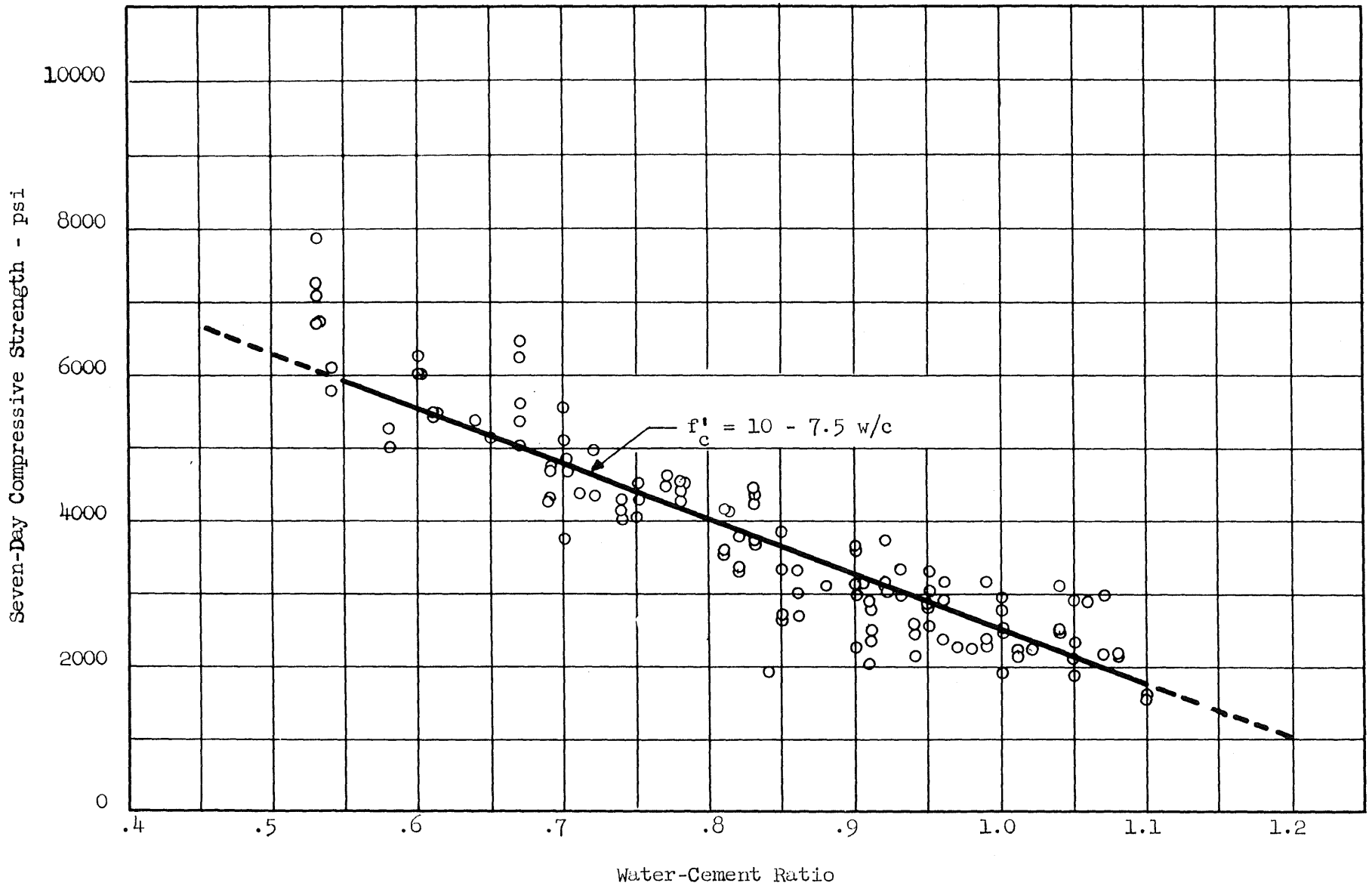

FIG.1 COMPARISON OF SEVEN-DAY COMPRESSIVE STRENGTH OF CONCRETE WITH WATER-CEMENT RATIO TYPE III PORTLAND CEMENT

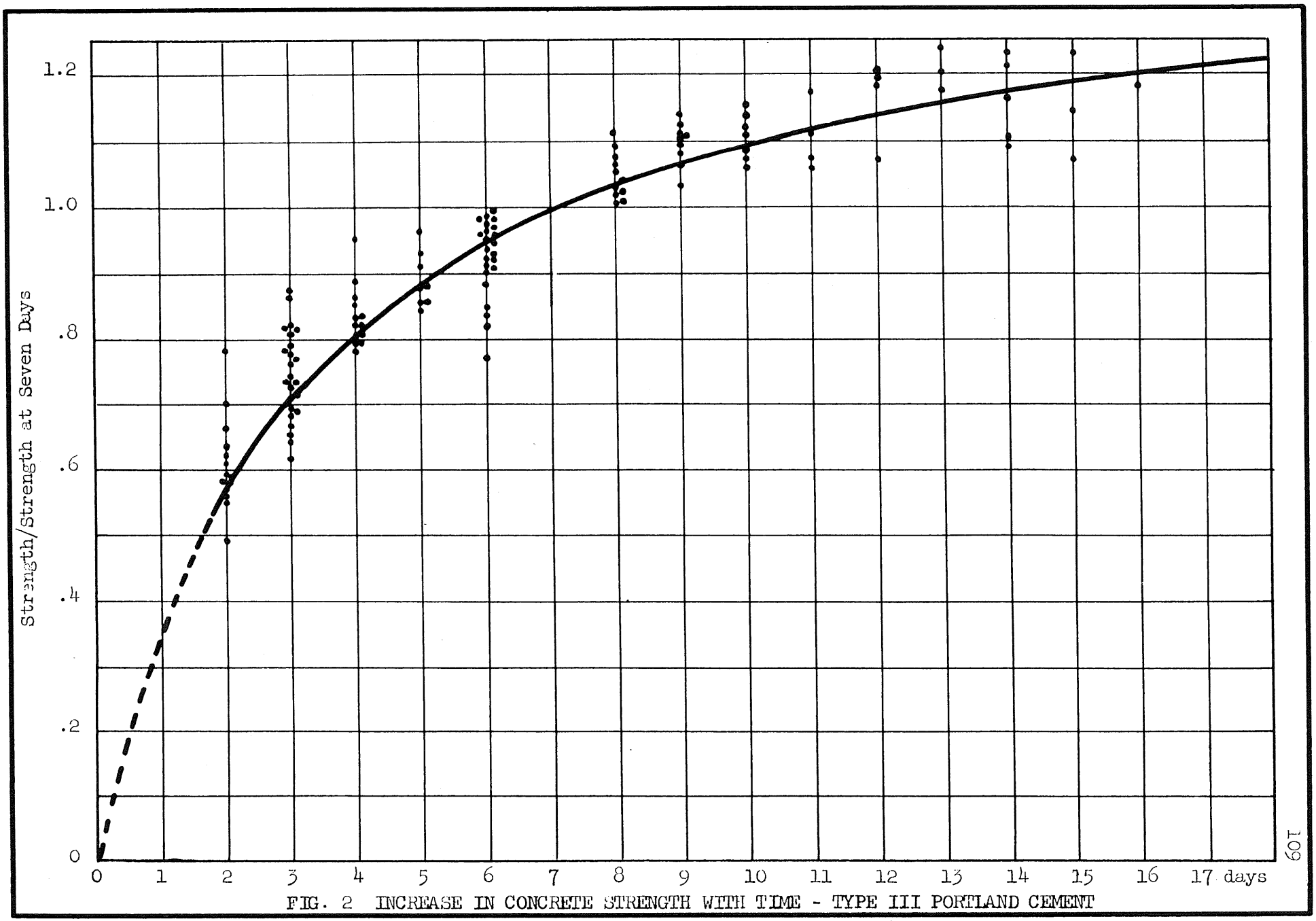

FIG. 2 INCREASE IN CONCRETE STRENGTH WITH TIME - TYPE III PORTLAND CEMENT

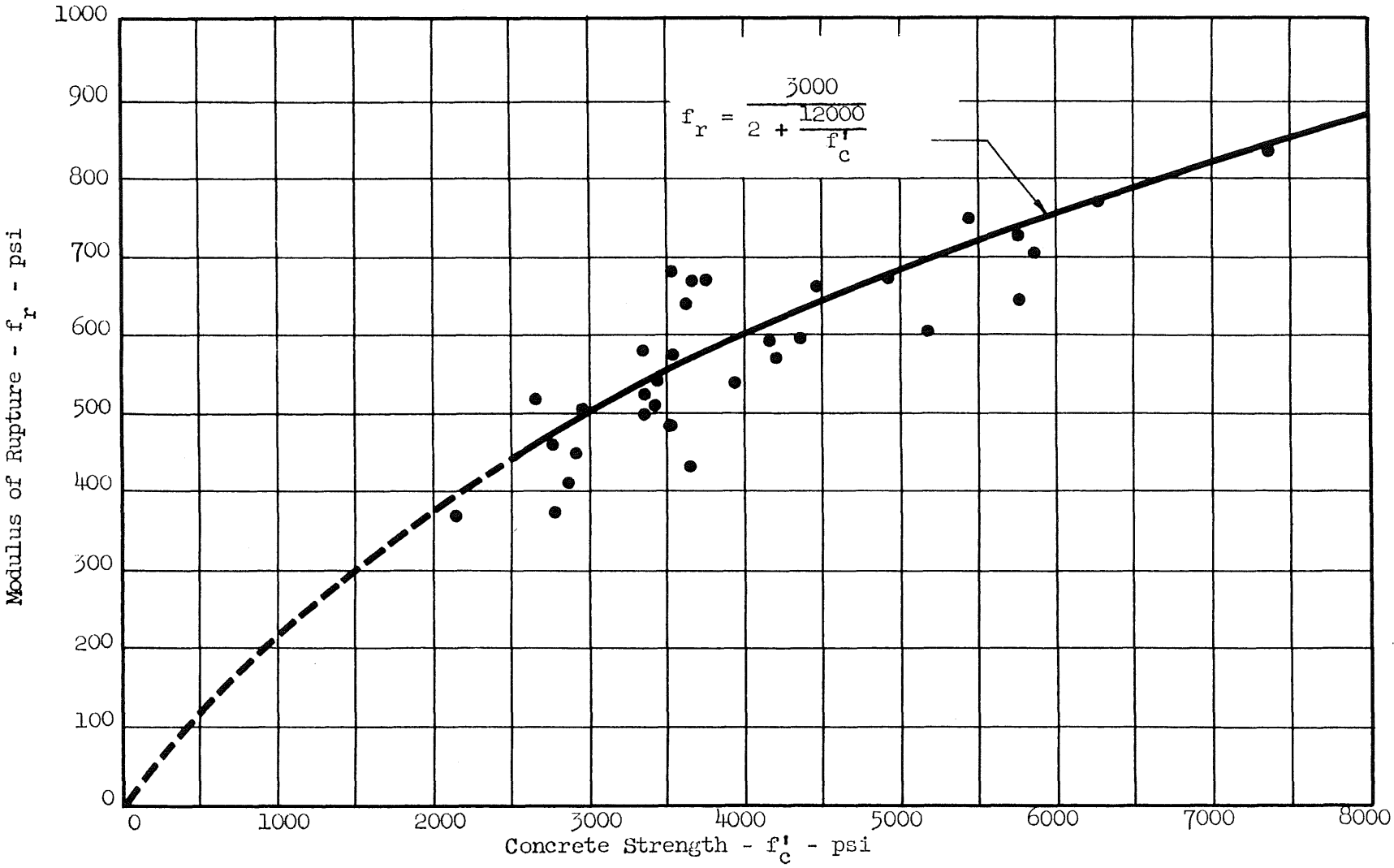

FIG. 3 COMPARISON OF MODULUS OF RUPTURE WITH CONCRETE STRENGTH
MAXIMUM SIZE OF COARSE AGGREGATE: 1 1/2 IN.

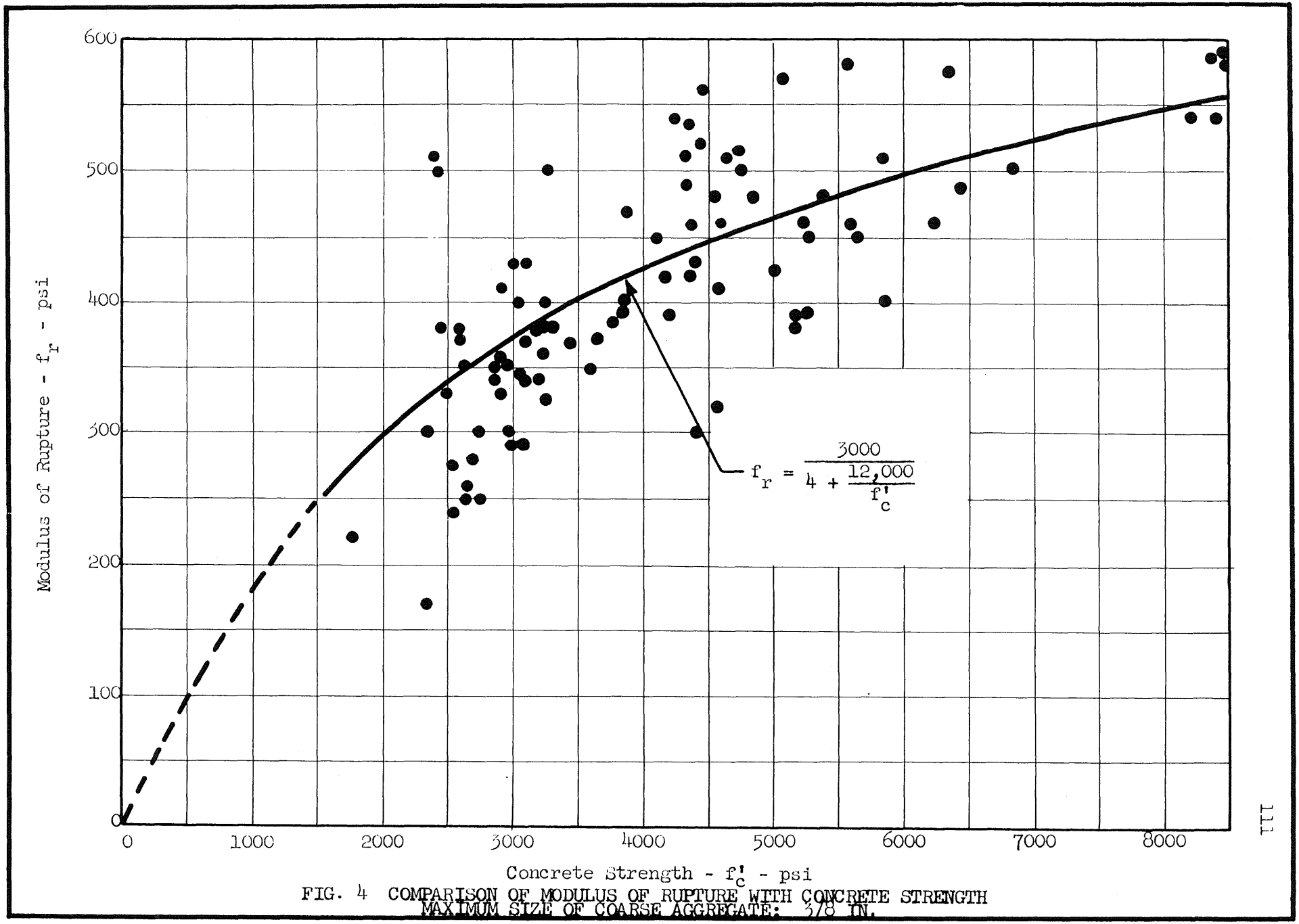

FIG. 4 COMPARISON OF MODULUS OF RUPTURE WITH CONCRETE STRENGTH
MAXIMUM SIZE OF COARSE AGGREGATE: 3/8 IN.

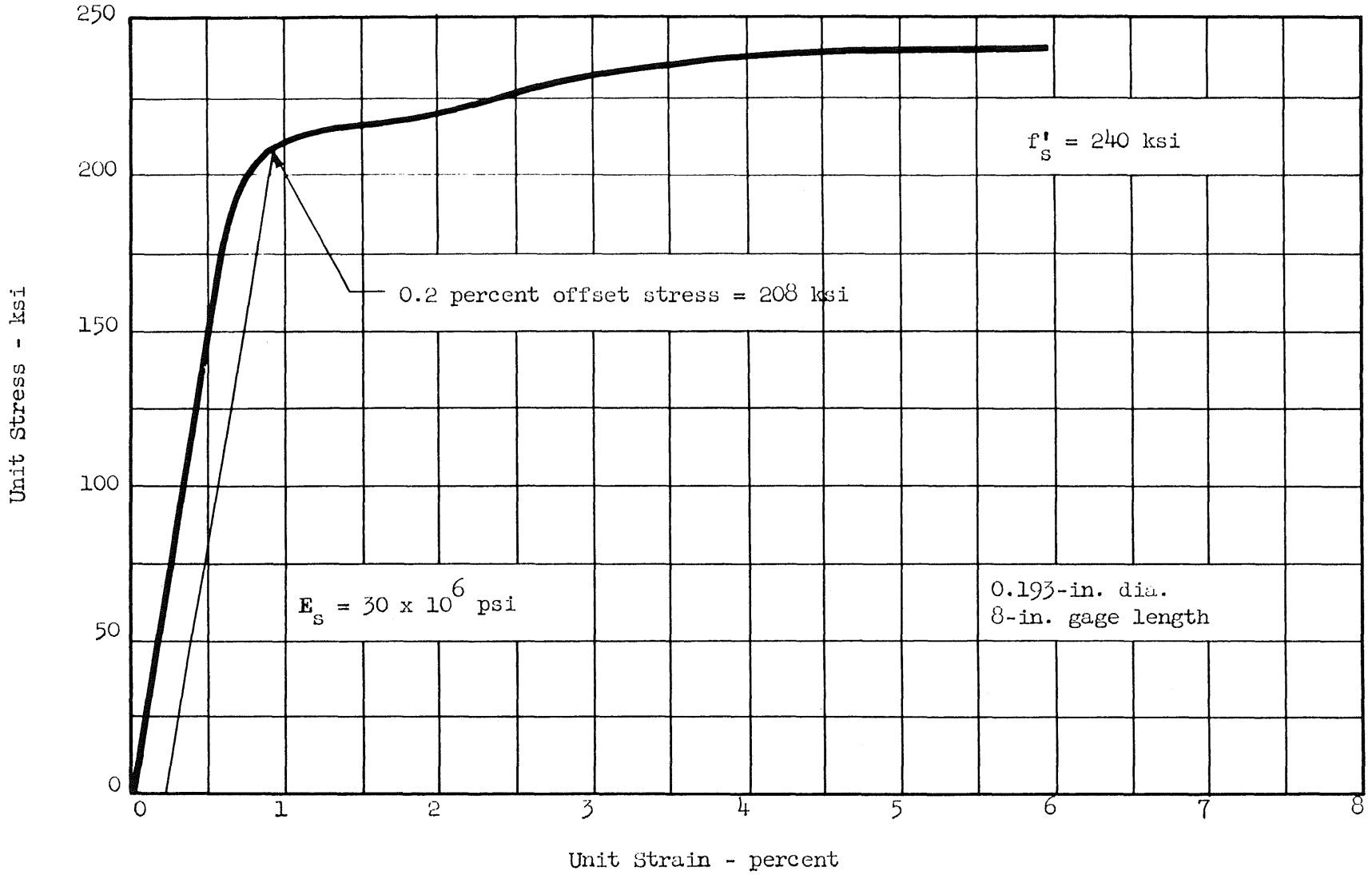

FIG. 5 STRESS-STRAIN RELATIONSHIP FOR REINFORCING WIRE FROM LOT I

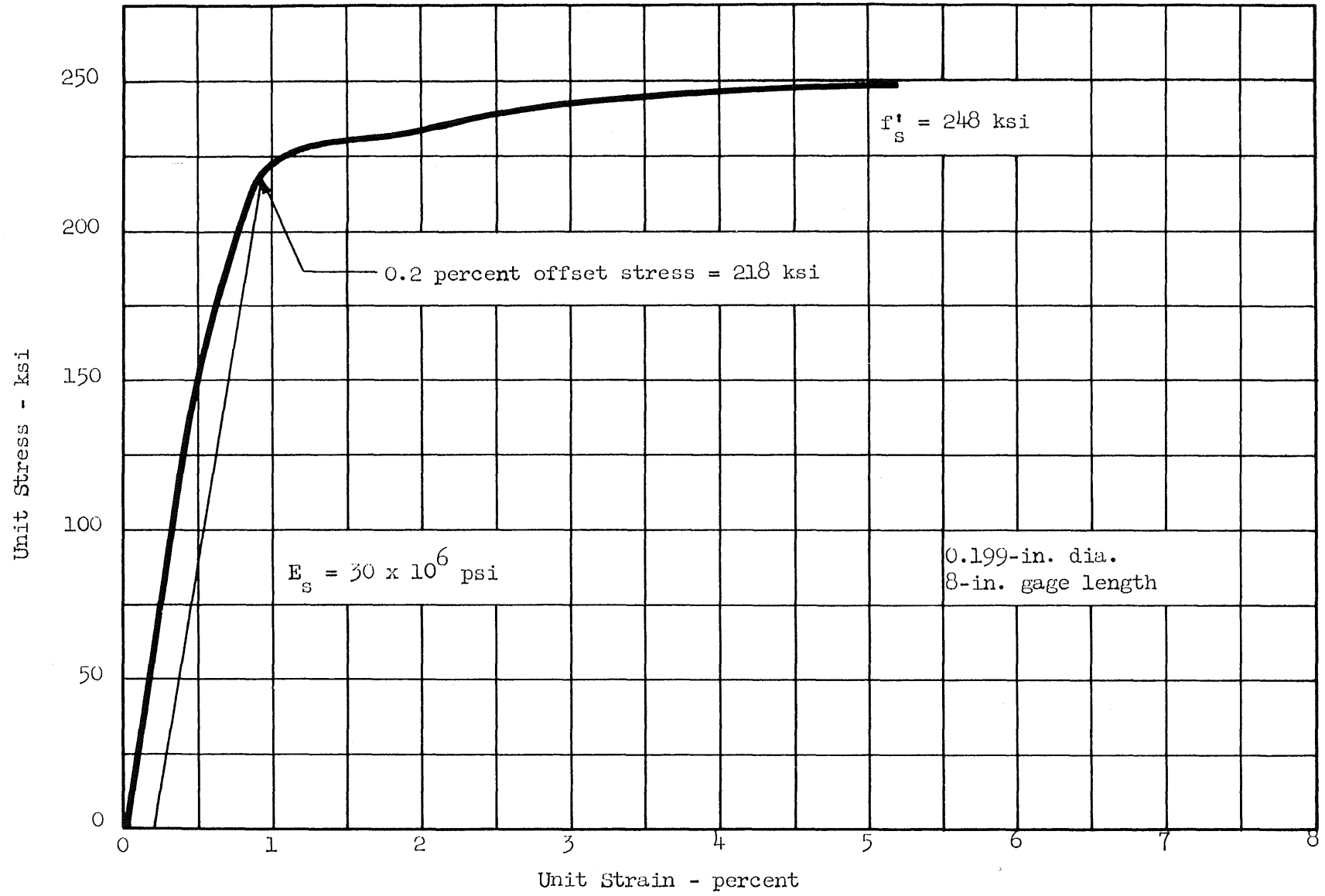

FIG. 6a STRESS-STRAIN RELATIONSHIP FOR REINFORCING WIRE FROM LOT II

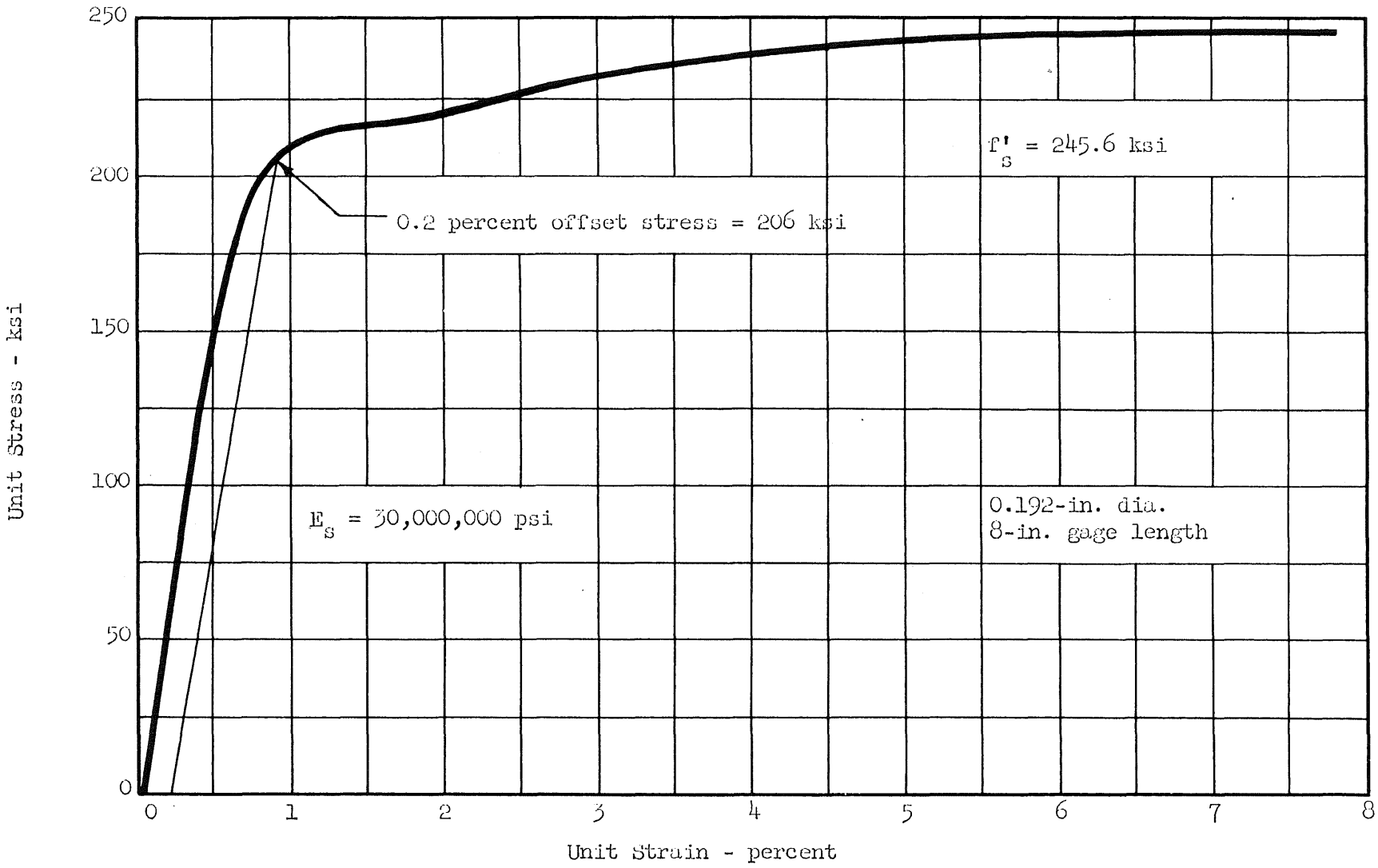

FIG. 6b STRESS-STRAIN RELATIONSHIP FOR REINFORCING WIRE FROM LOT III

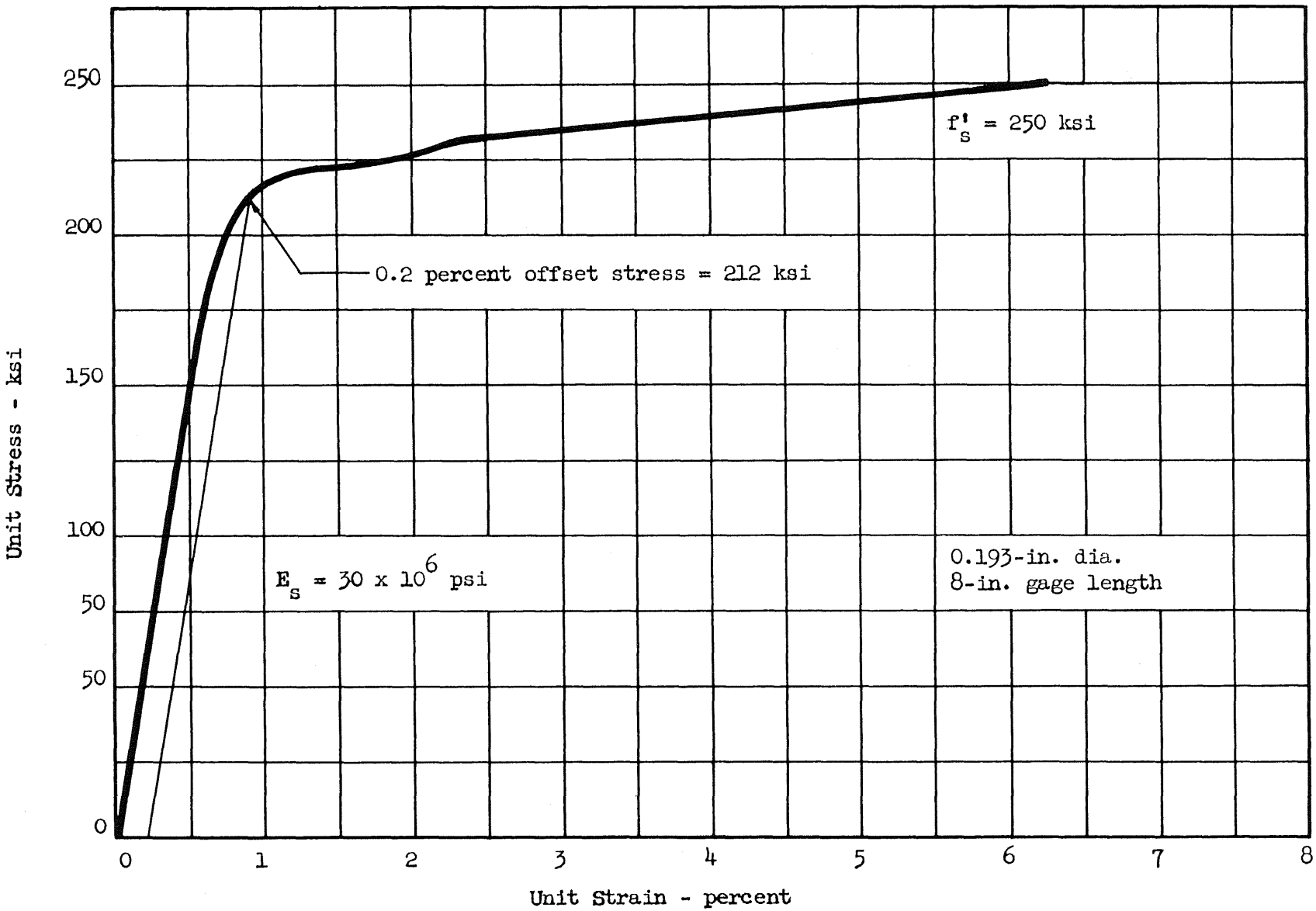

FIG. 7 STRESS-STRAIN RELATIONSHIP FOR REINFORCING WIRE FROM LOT VI

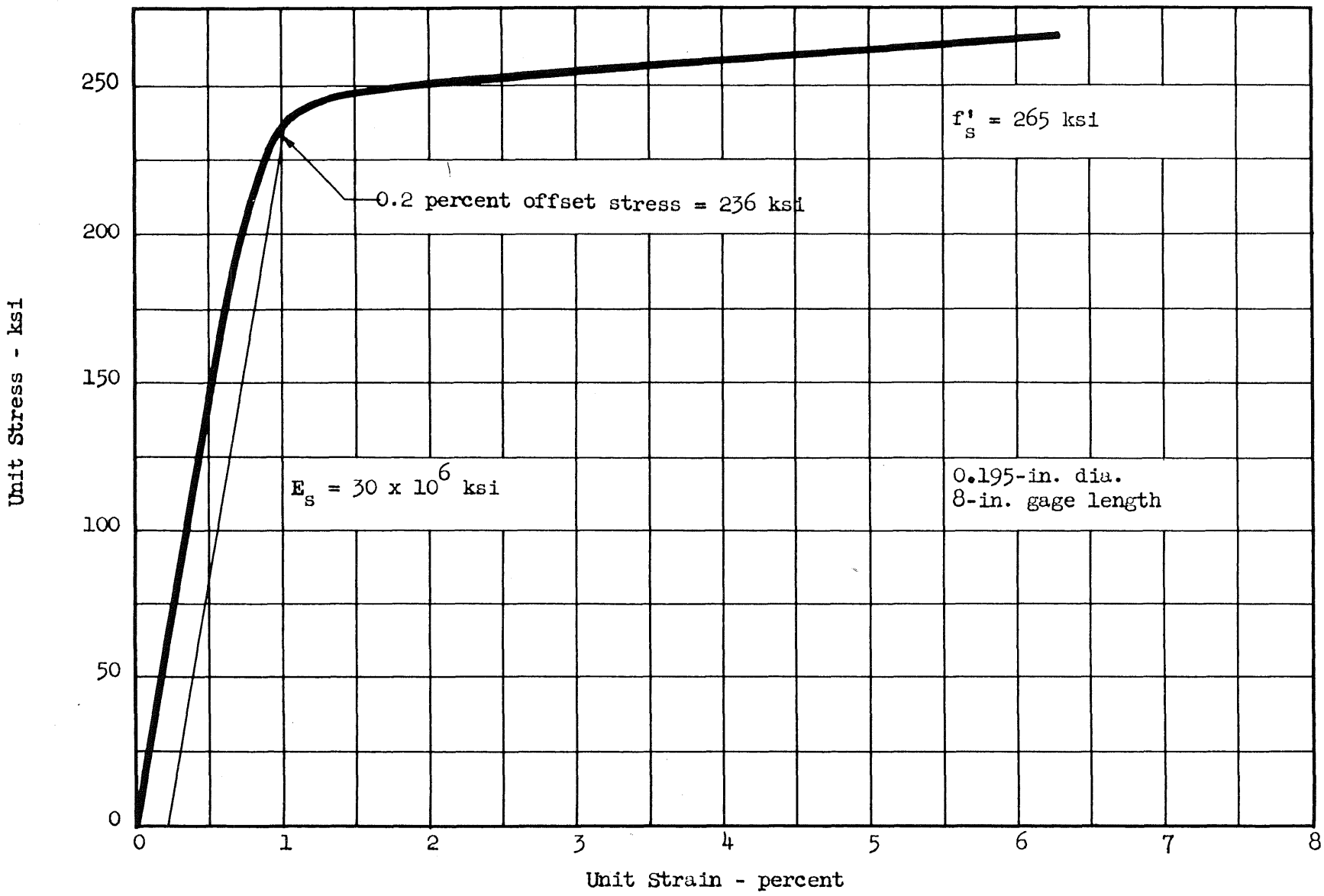

FIG. 8 STRESS-STRAIN RELATIONSHIP FOR REINFORCING WIRE FROM LOT VII

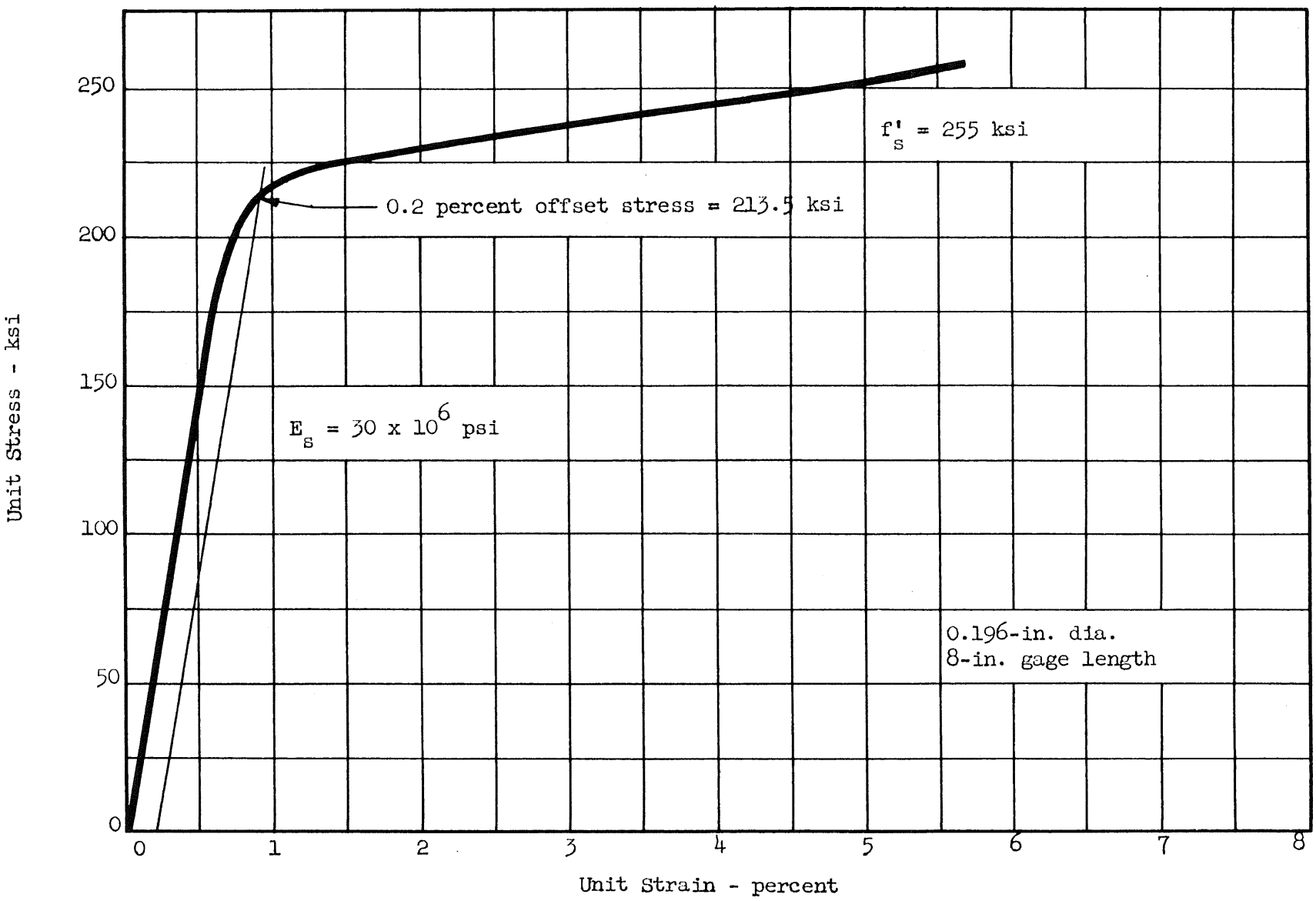

FIG. 9 STRESS-STRAIN RELATIONSHIP FOR REINFORCING WIRE FROM LOT VIII

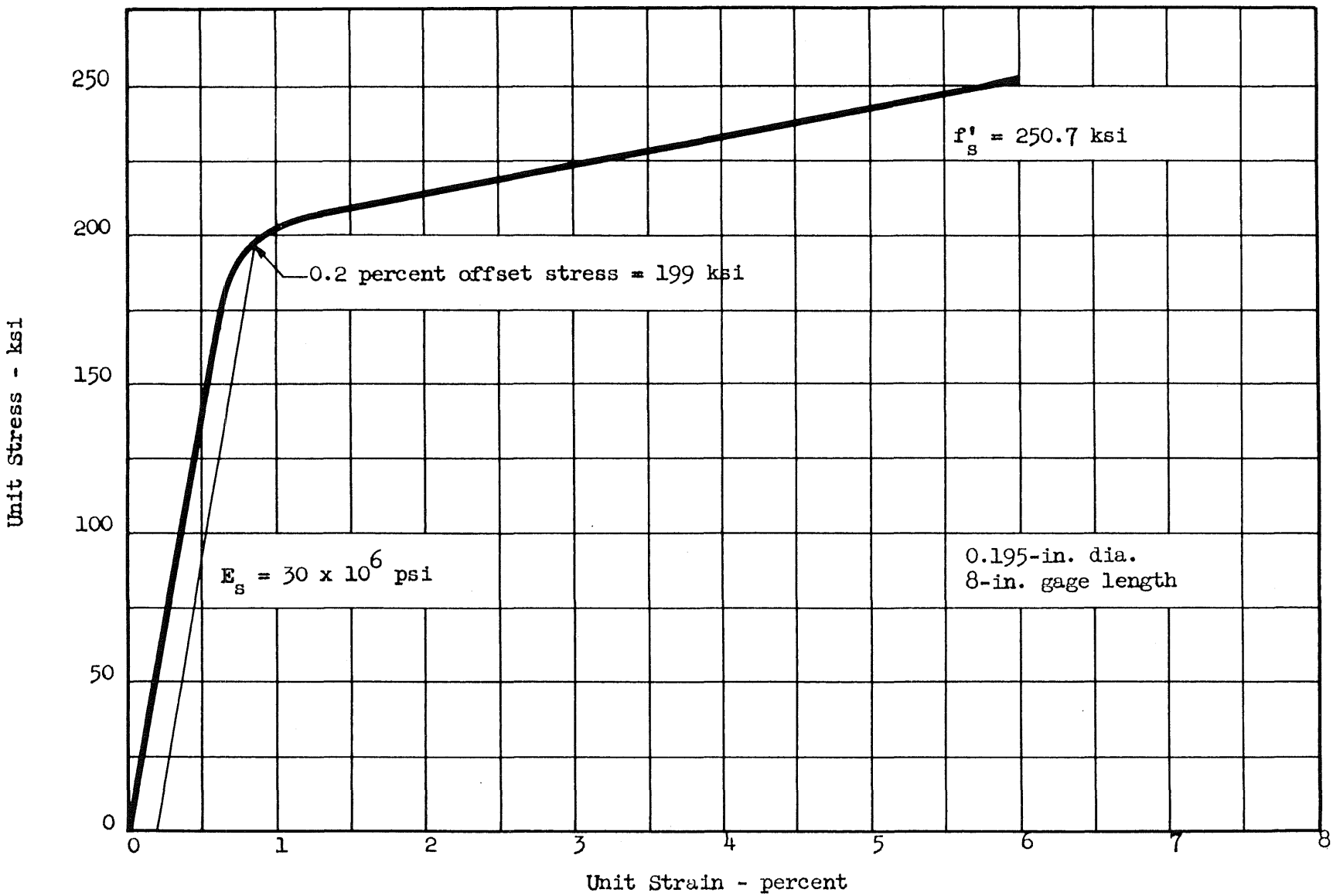

FIG. 10 STRESS-STRAIN RELATIONSHIP FOR REINFORCING WIRE FROM LOT IX

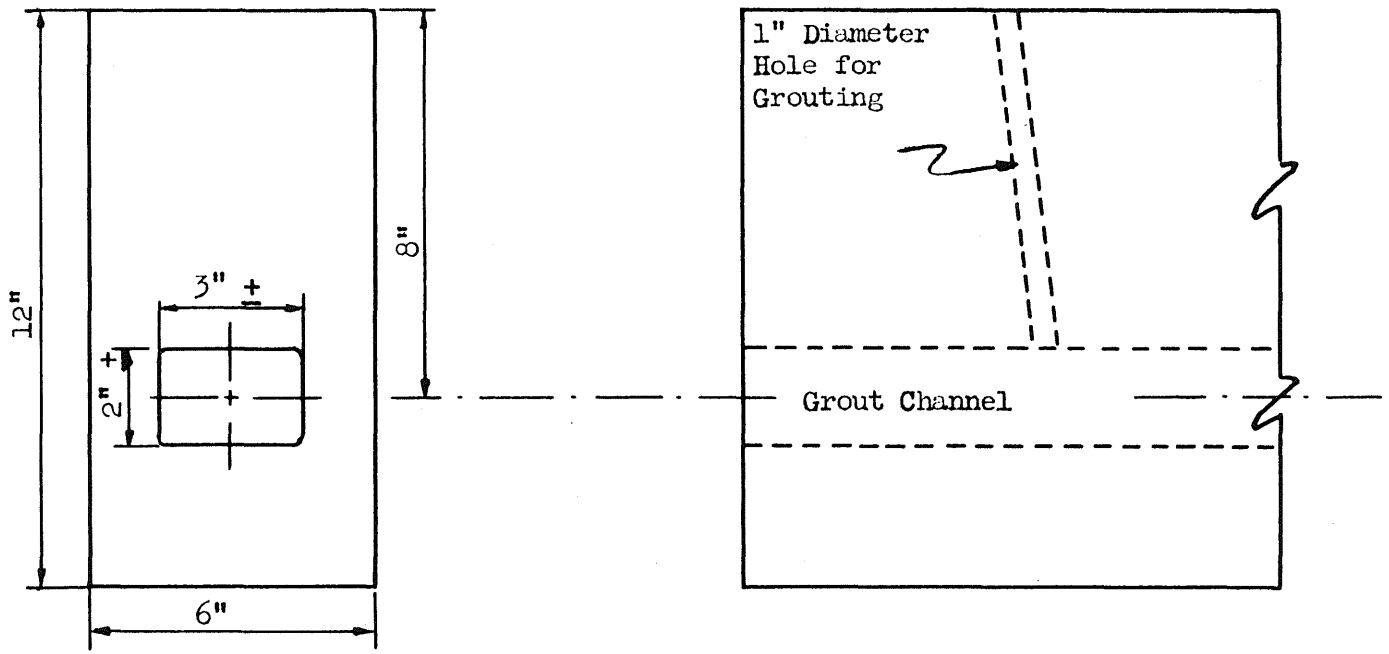

FIG. 11 DETAILS OF GROUT CHANNEL

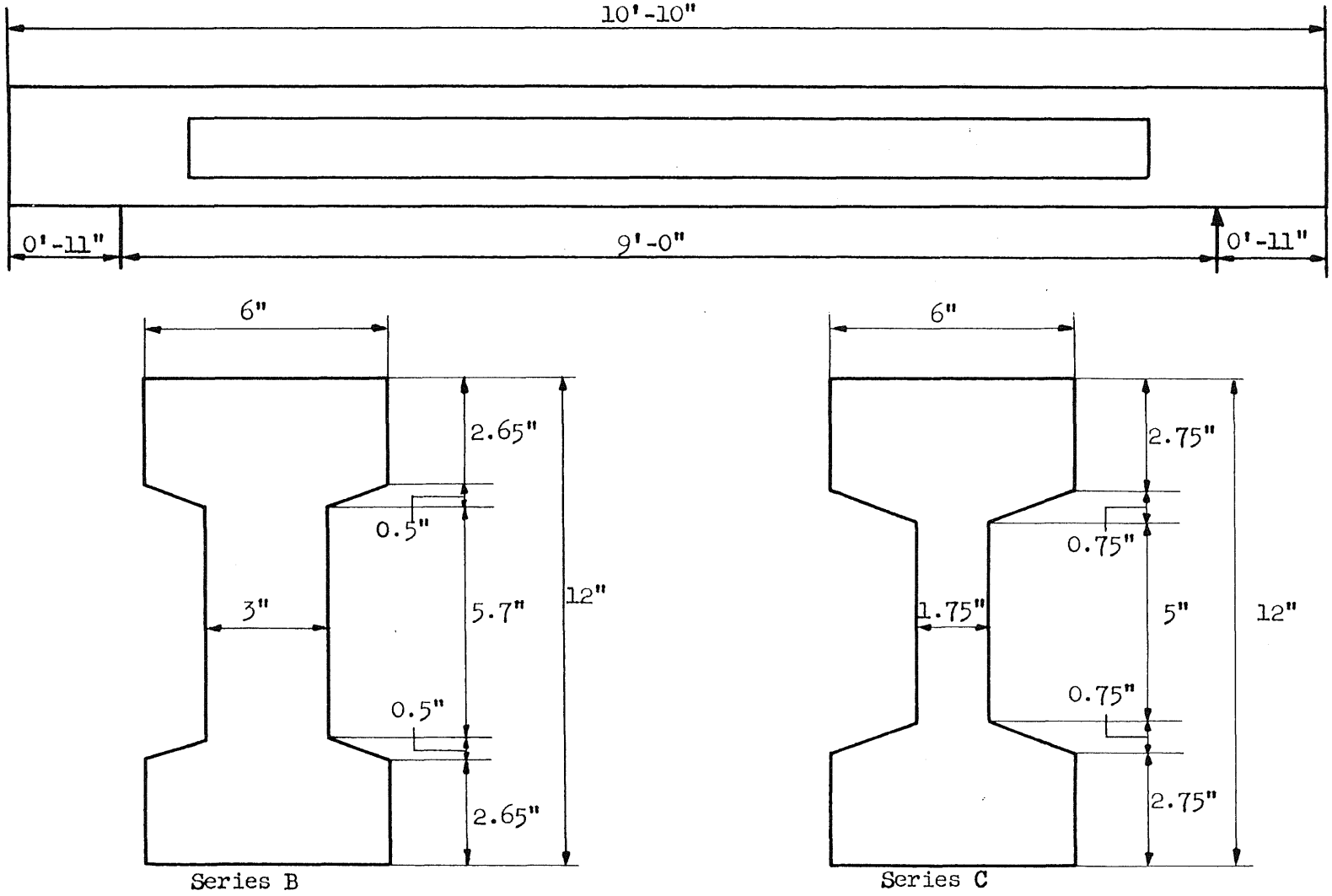

FIG. 12 NOMINAL DIMENSIONS OF I-BEAMS

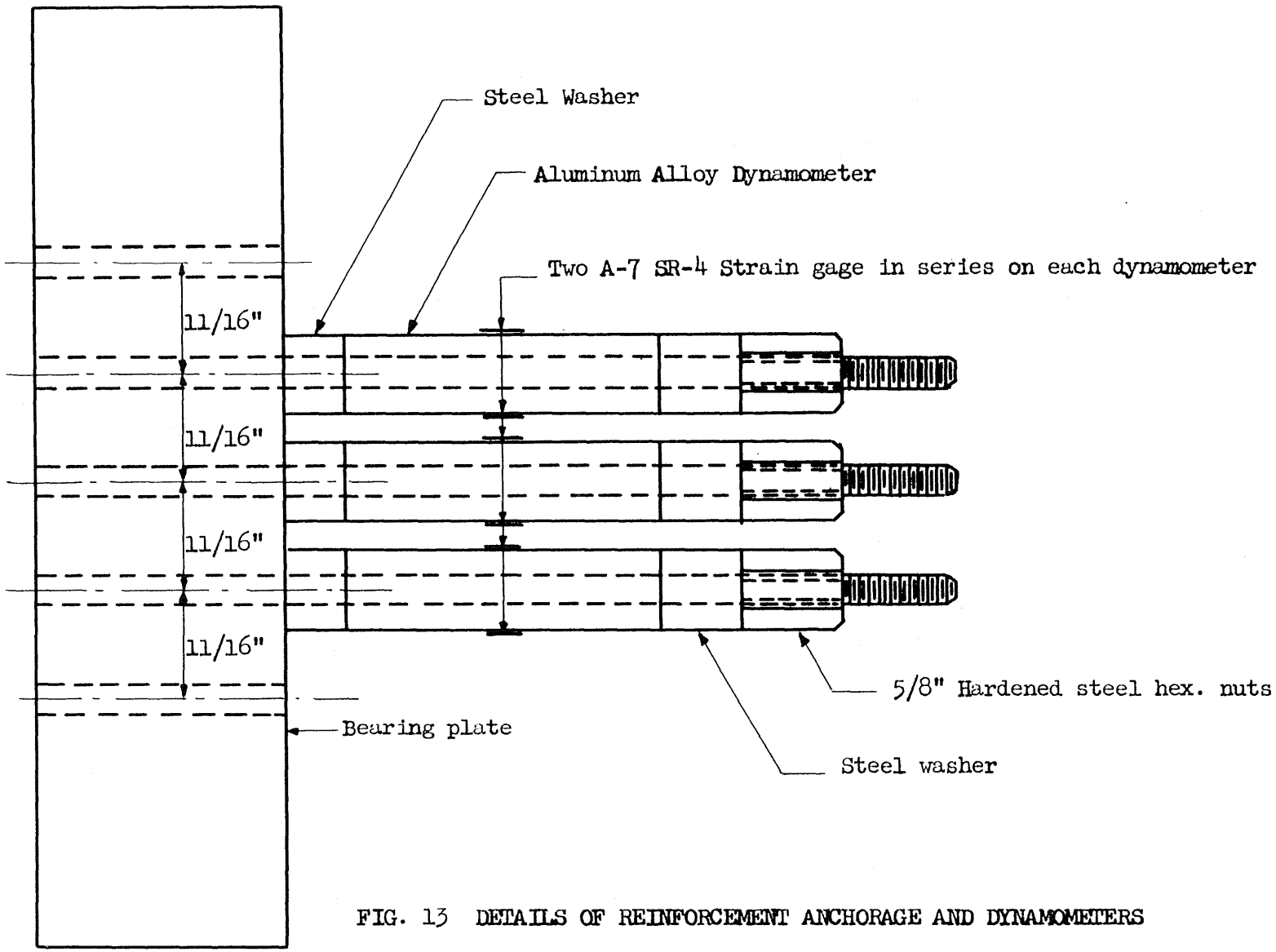

FIG. 13 DETAILS OF REINFORCEMENT ANCHORAGE AND DYNAMOMETERS

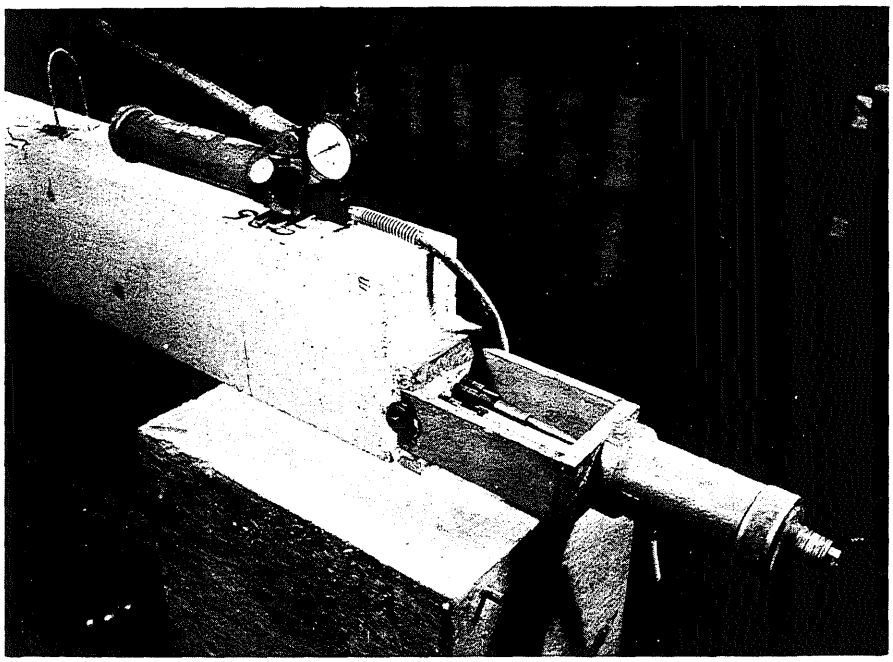

FIG. 14 POST-TENSIONING APPARATUS

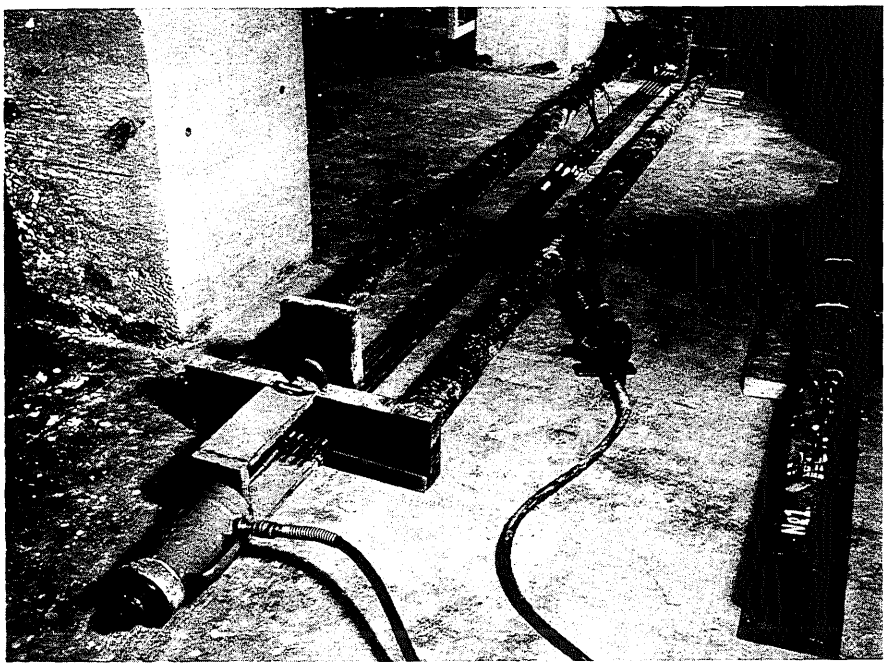

FIG. 15 PRETENSIONING FRAME

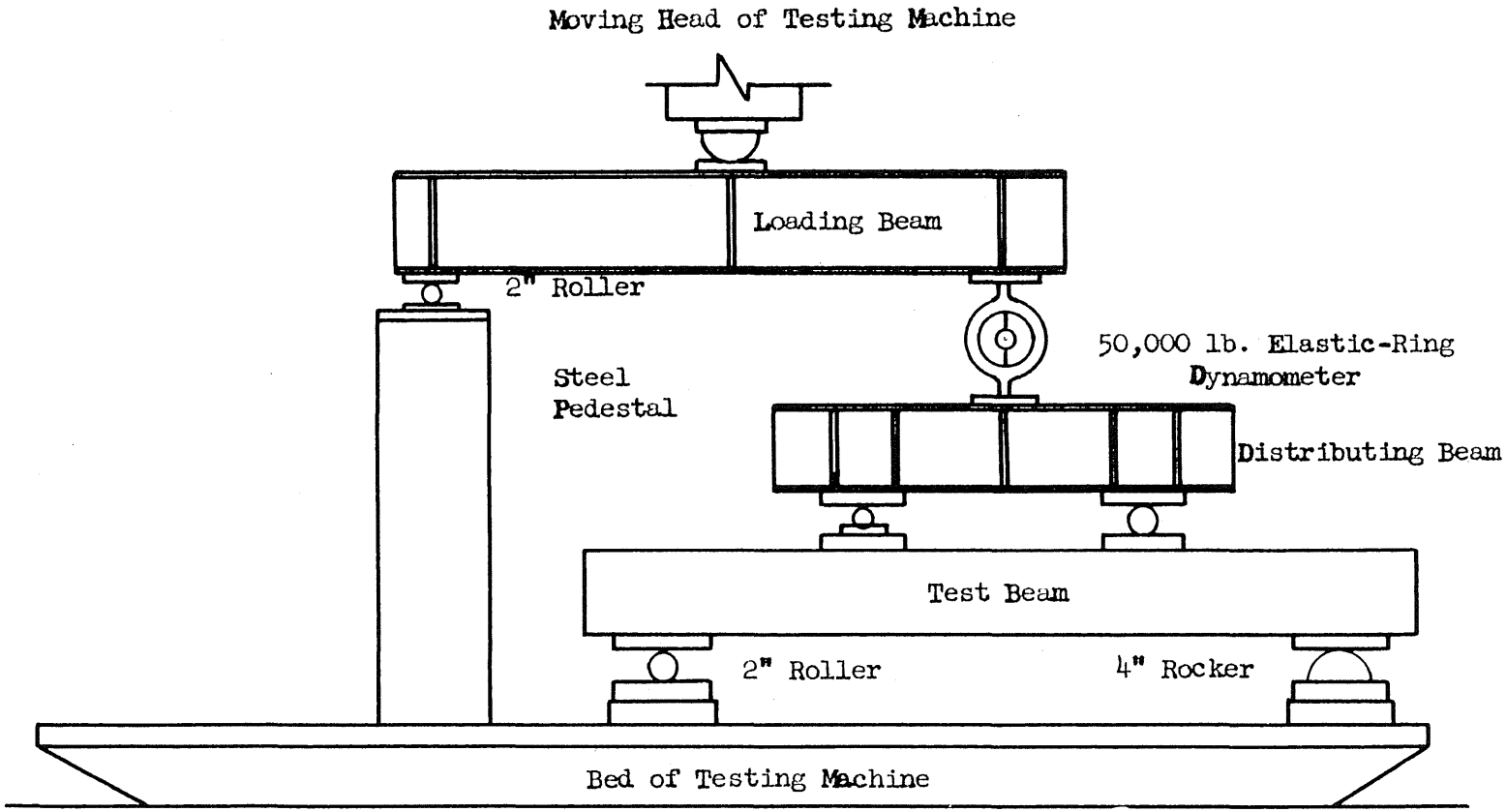

FIG. 16 SET-UP IN TESTING MACHINE

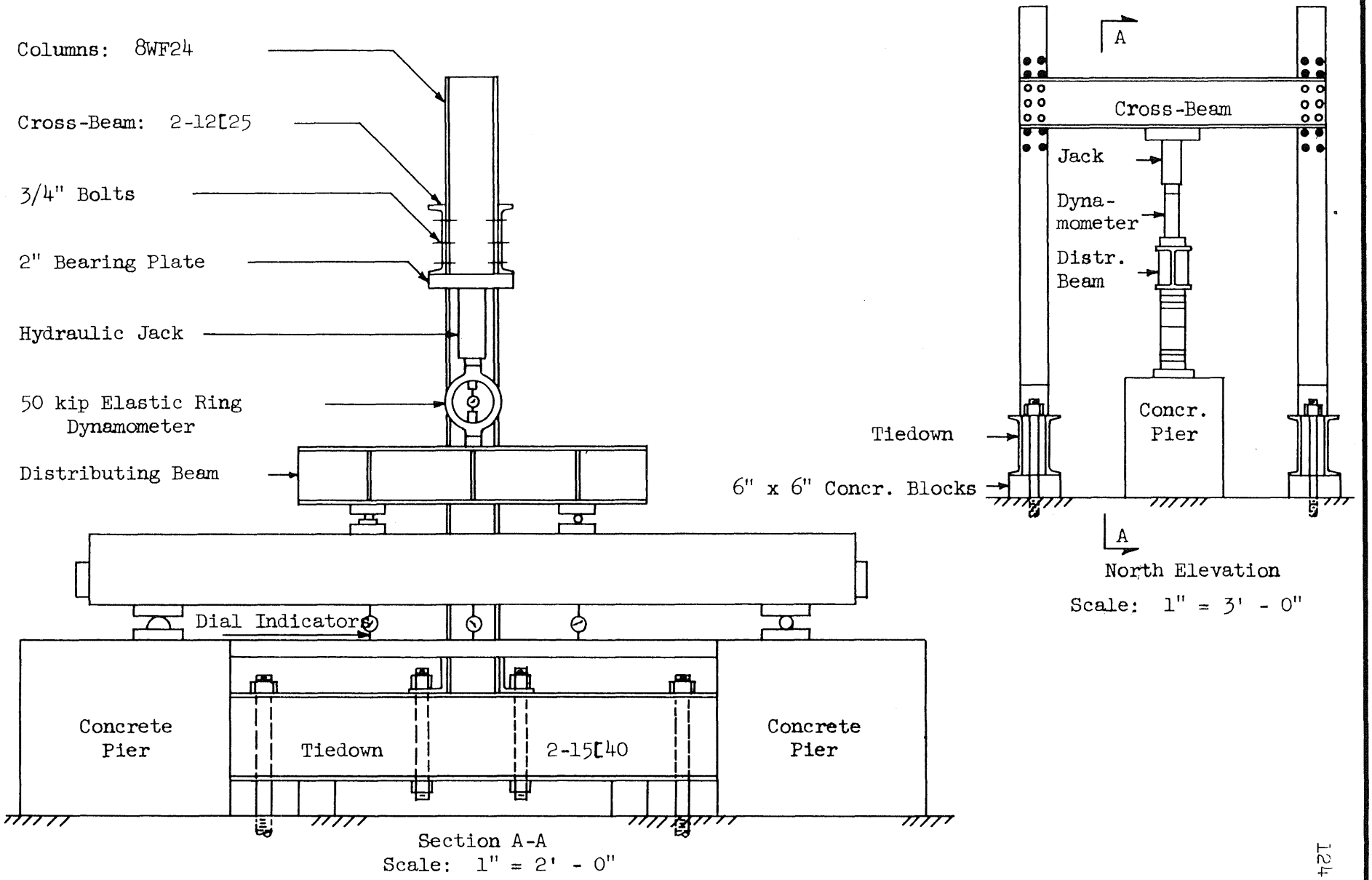

FIG. 17 SET-UP IN LOADING FRAME

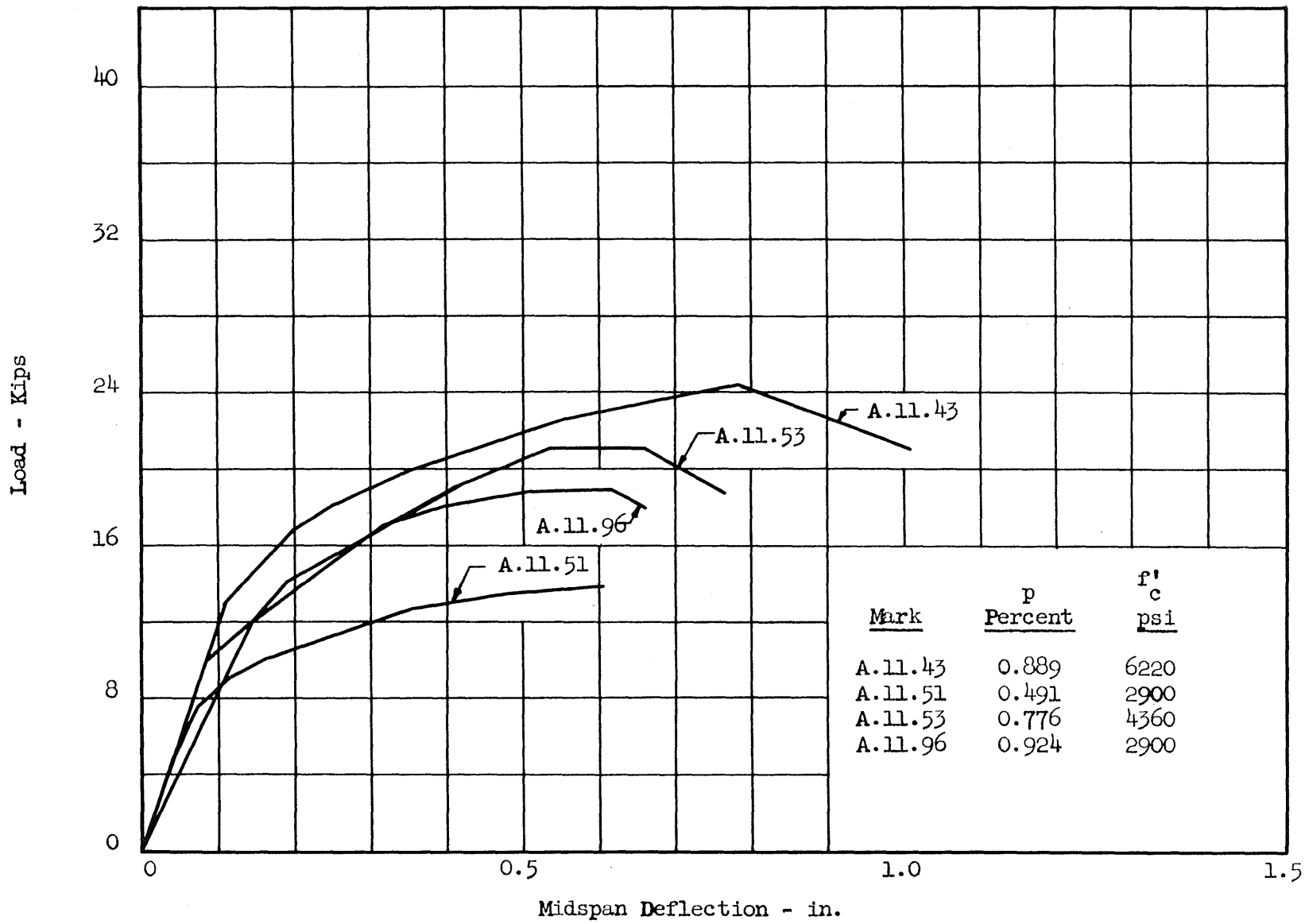

FIG. 18 LOAD-DEFLECTION CURVES FOR RECTANGULAR BEAMS LOADED AT MIDSPAN
NOMINAL PRESTRESS: 120,000 psi

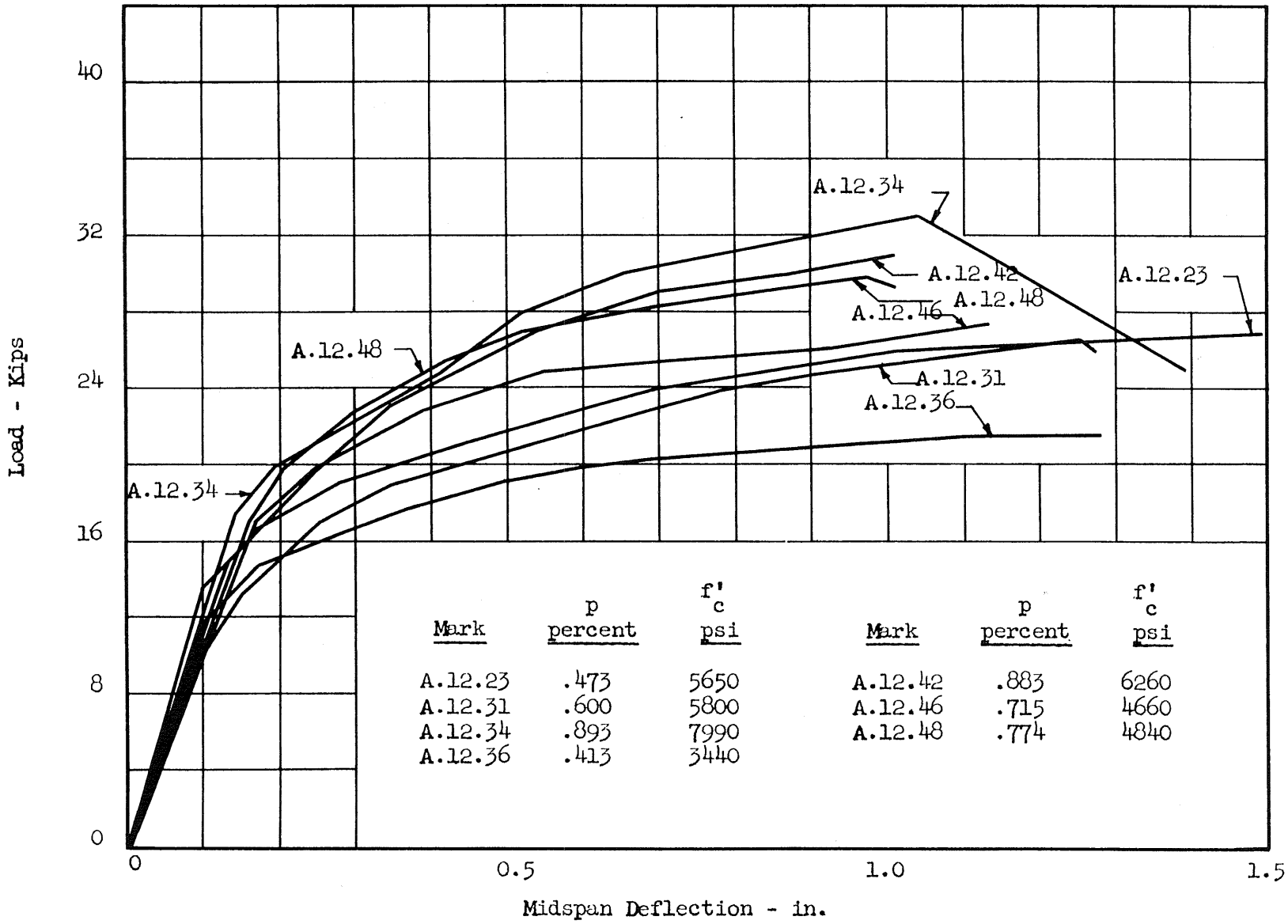

Mark	p percent	f'_c psi	Mark	p percent	f'_c psi
A.12.23	.473	5650	A.12.42	.883	6260
A.12.31	.600	5800	A.12.46	.715	4660
A.12.34	.893	7990	A.12.48	.774	4840
A.12.36	.413	3440			

FIG. 19a LOAD-DEFLECTION CURVES FOR RECTANGULAR BEAMS LOADED AT THE THIRD-POINTS
NOMINAL PRESTRESS: 120,000 psi

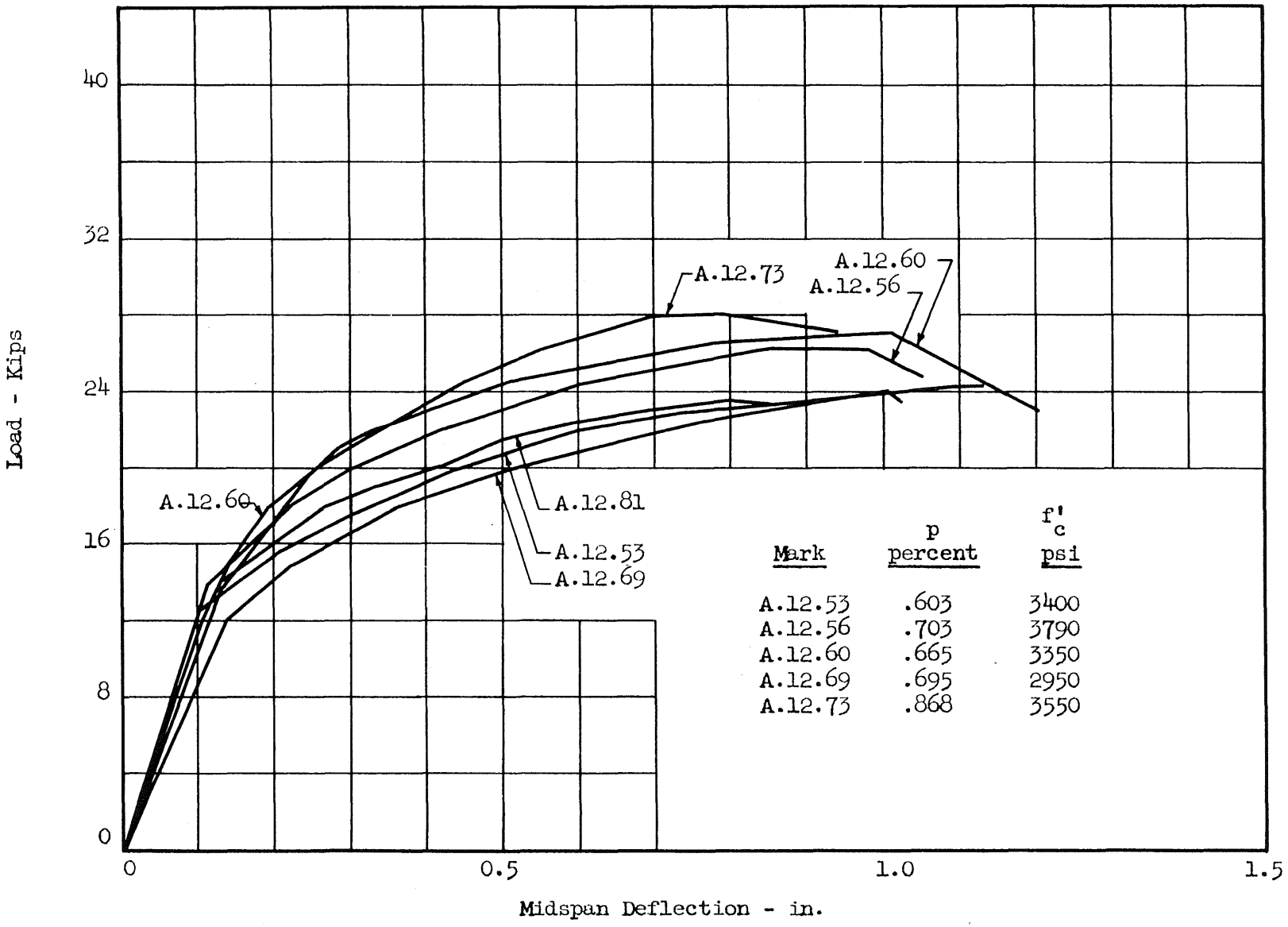

FIG. 19b **LOAD-DEFLECTION CURVES FOR RECTANGULAR BEAMS LOADED AT THE THIRD-POINTS**
NOMINAL PRESTRESS: 120,000 psi

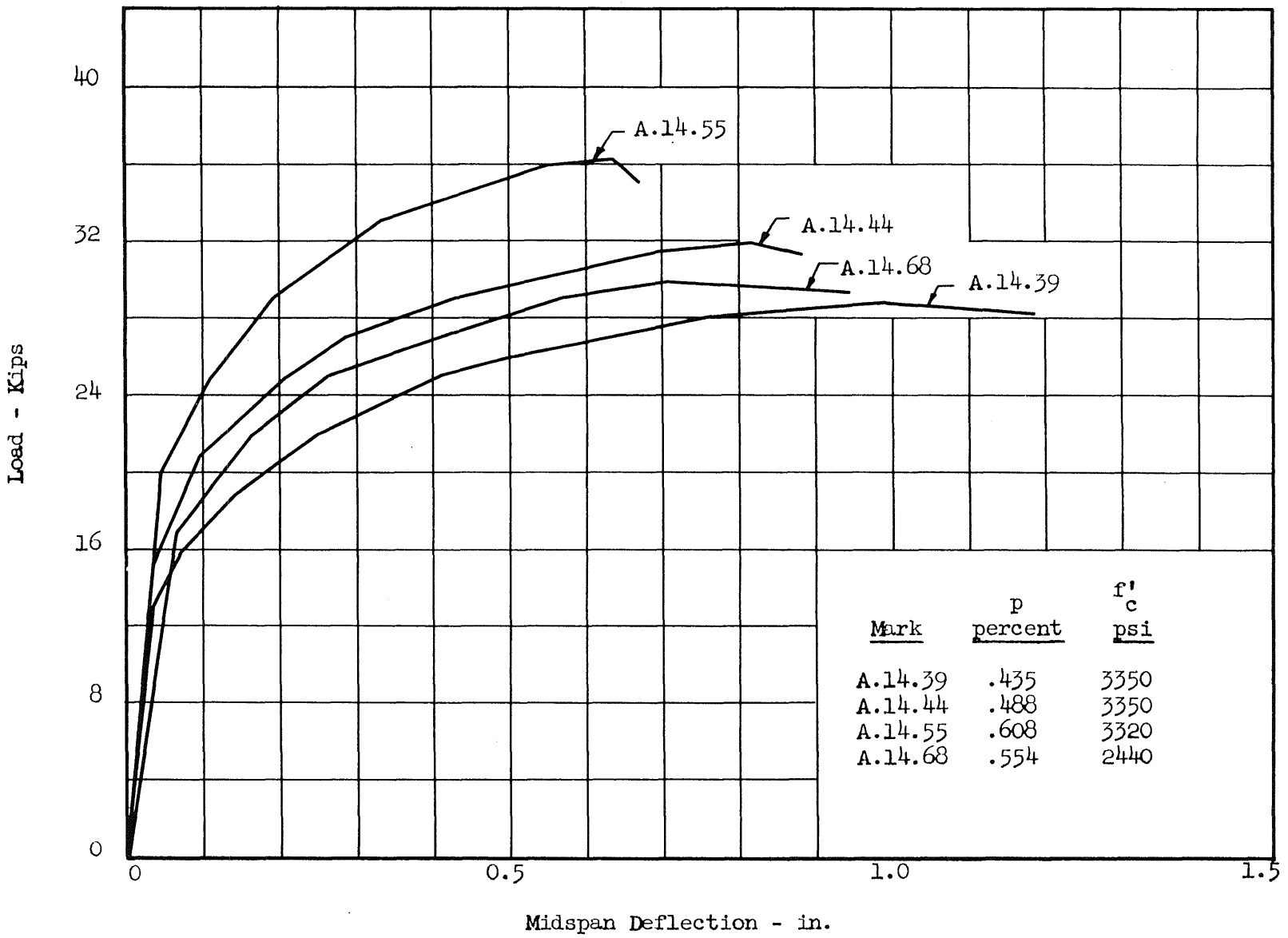

FIG. 20 **LOAD-DEFLECTION CURVES FOR RECTANGULAR BEAMS WITH 24-IN. SHEAR SPANS**
NOMINAL PRESTRESS: 120,000 psi

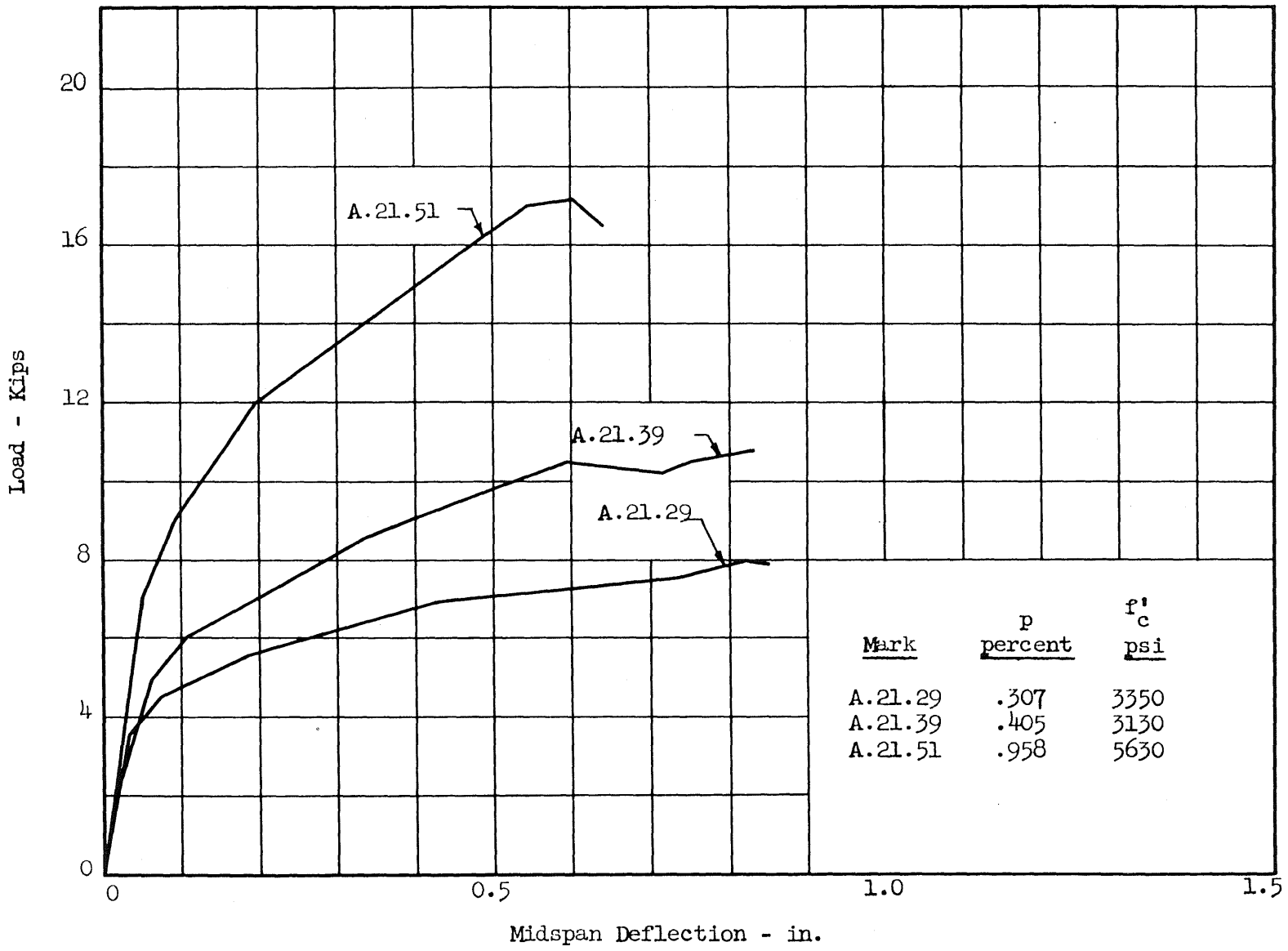

FIG. 21 LOAD-DEFLECTION CURVES FOR RECTANGULAR BEAMS LOADED AT MIDSPAN
NOMINAL PRESTRESS: 60,000 psi

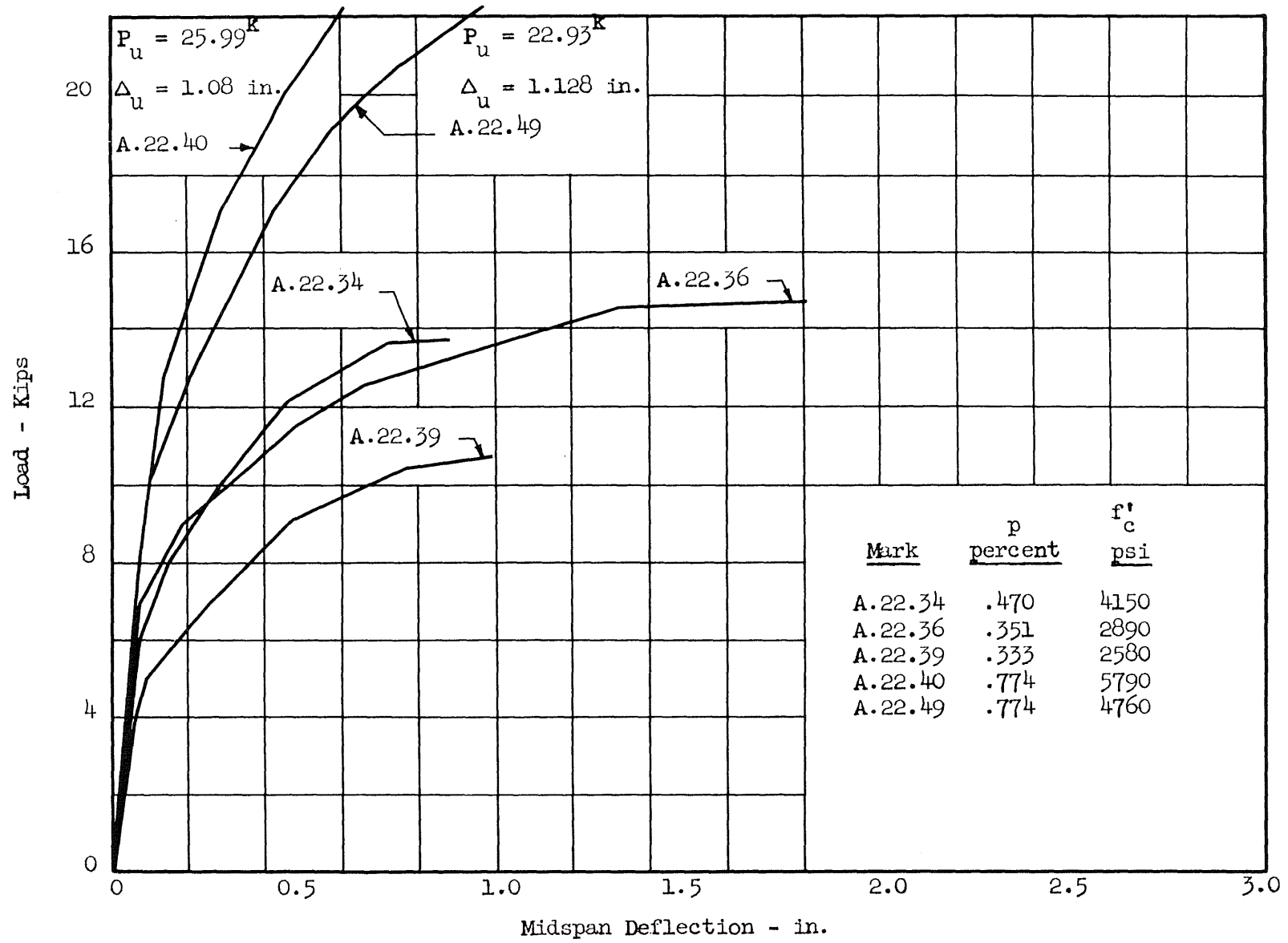

FIG. 22a LOAD-DEFLECTION CURVES FOR RECTANGULAR BEAMS LOADED AT THE THIRD-POINTS
NOMINAL PRESTRESS: 60,000 psi

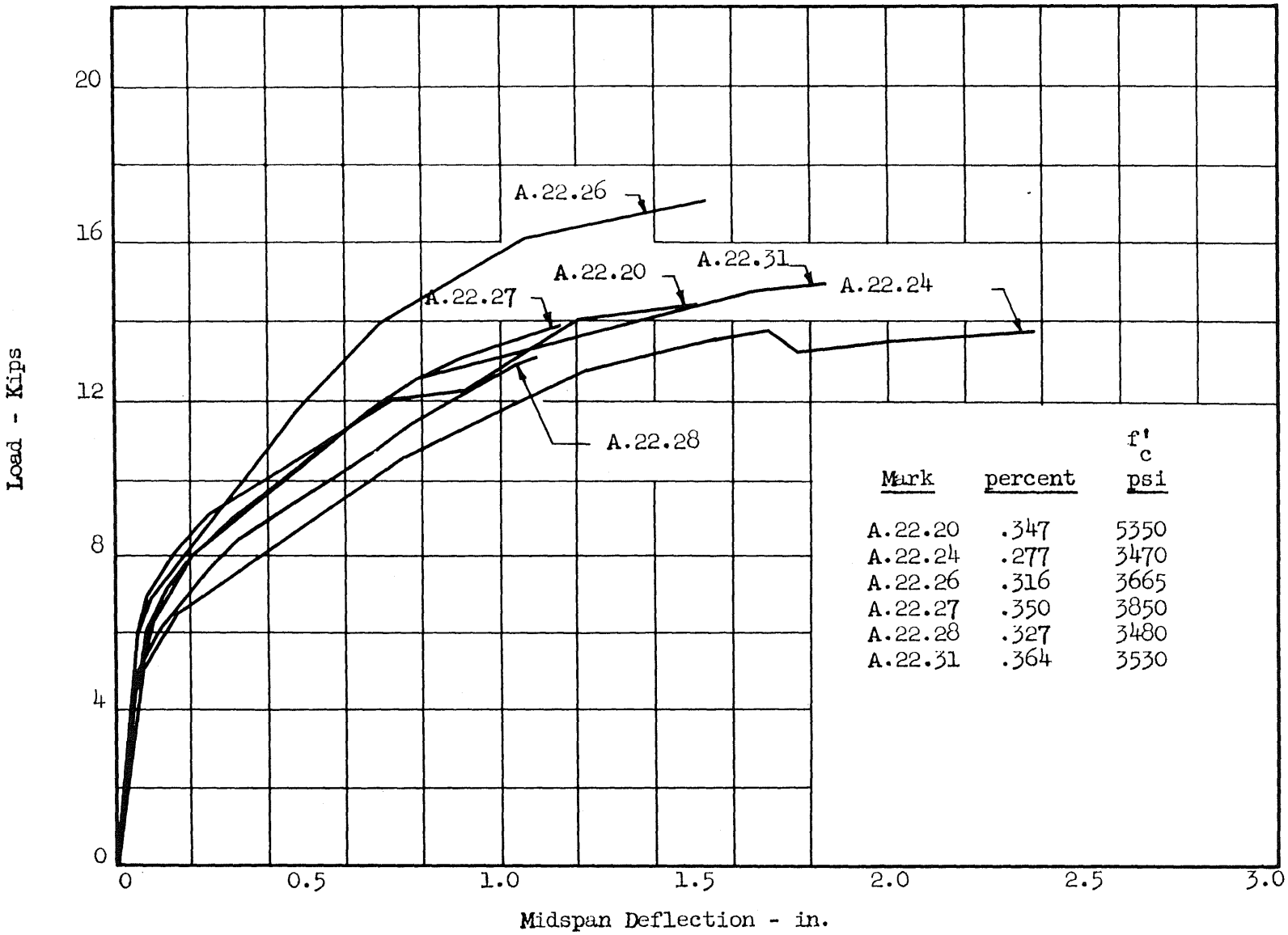

FIG. 22b **LOAD-DEFLECTION CURVES FOR RECTANGULAR BEAMS LOADED AT THE THIRD-POINTS**
NOMINAL PRESTRESS: 60,000 psi

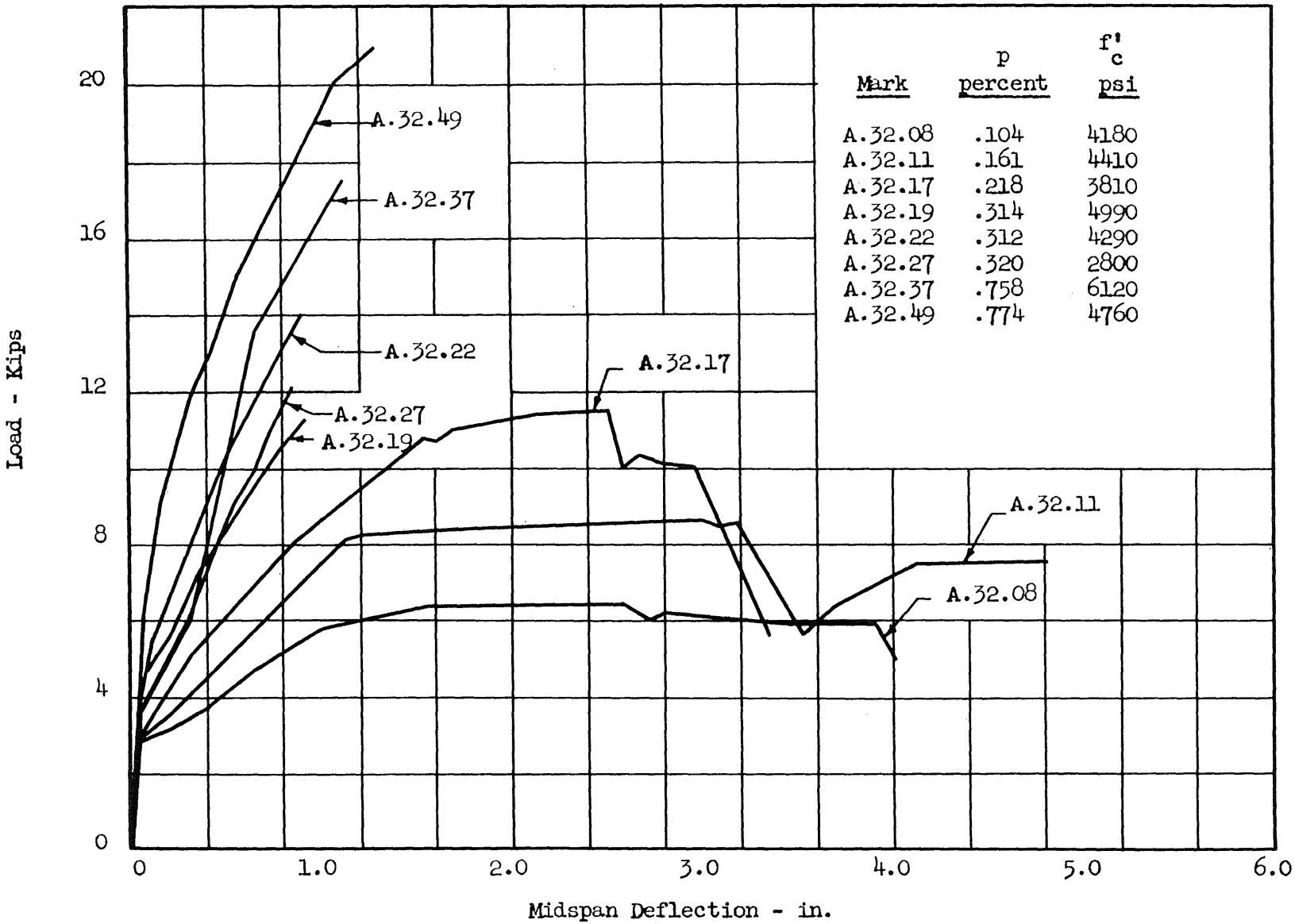

FIG. 23 LOAD DEFLECTION CURVES FOR RECTANGULAR BEAMS LOADED AT THE THIRD-POINTS
NOMINAL PRESTRESS = 0

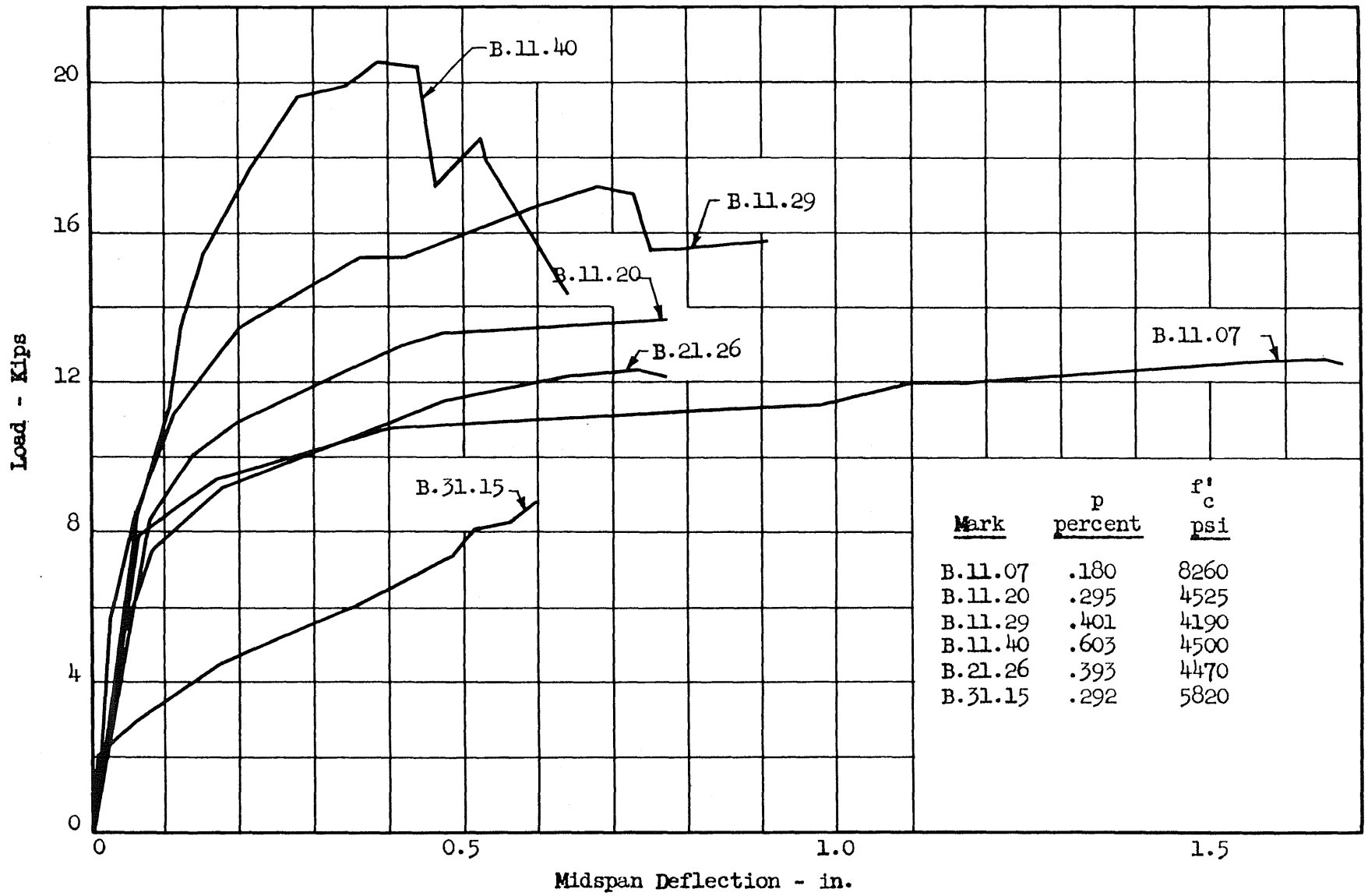

FIG. 24 LOAD-DEFLECTION CURVES FOR I-BEAMS WITH THREE-INCH WEBS LOADED AT MIDSPAN
NOMINAL PRESTRESS: ZERO

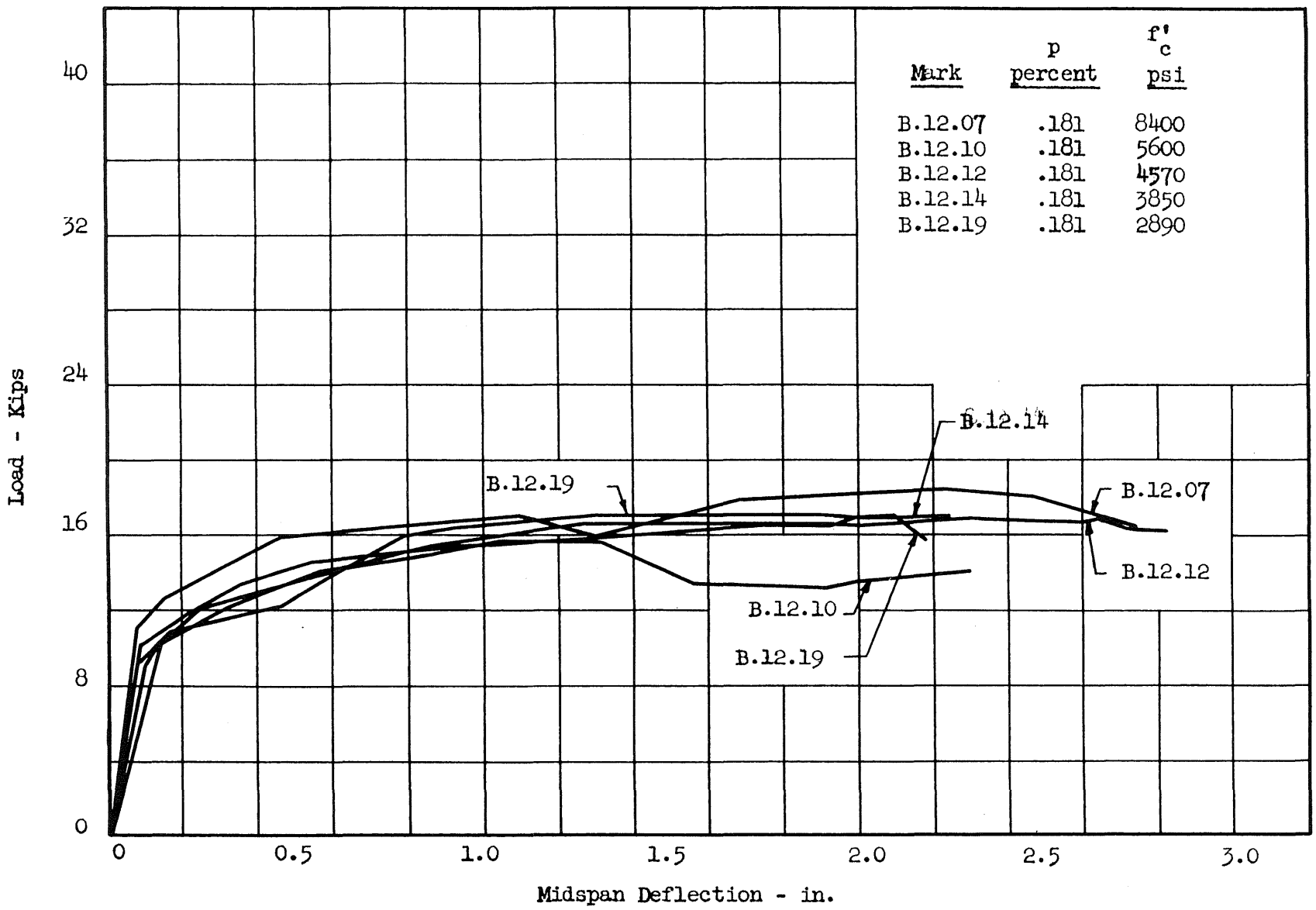

FIG. 25a LOAD-DEFLECTION CURVES FOR I-BEAMS WITH THREE-INCH WEBS LOADED AT THE THIRD-POINTS
NOMINAL PRESTRESS: 120,000 psi

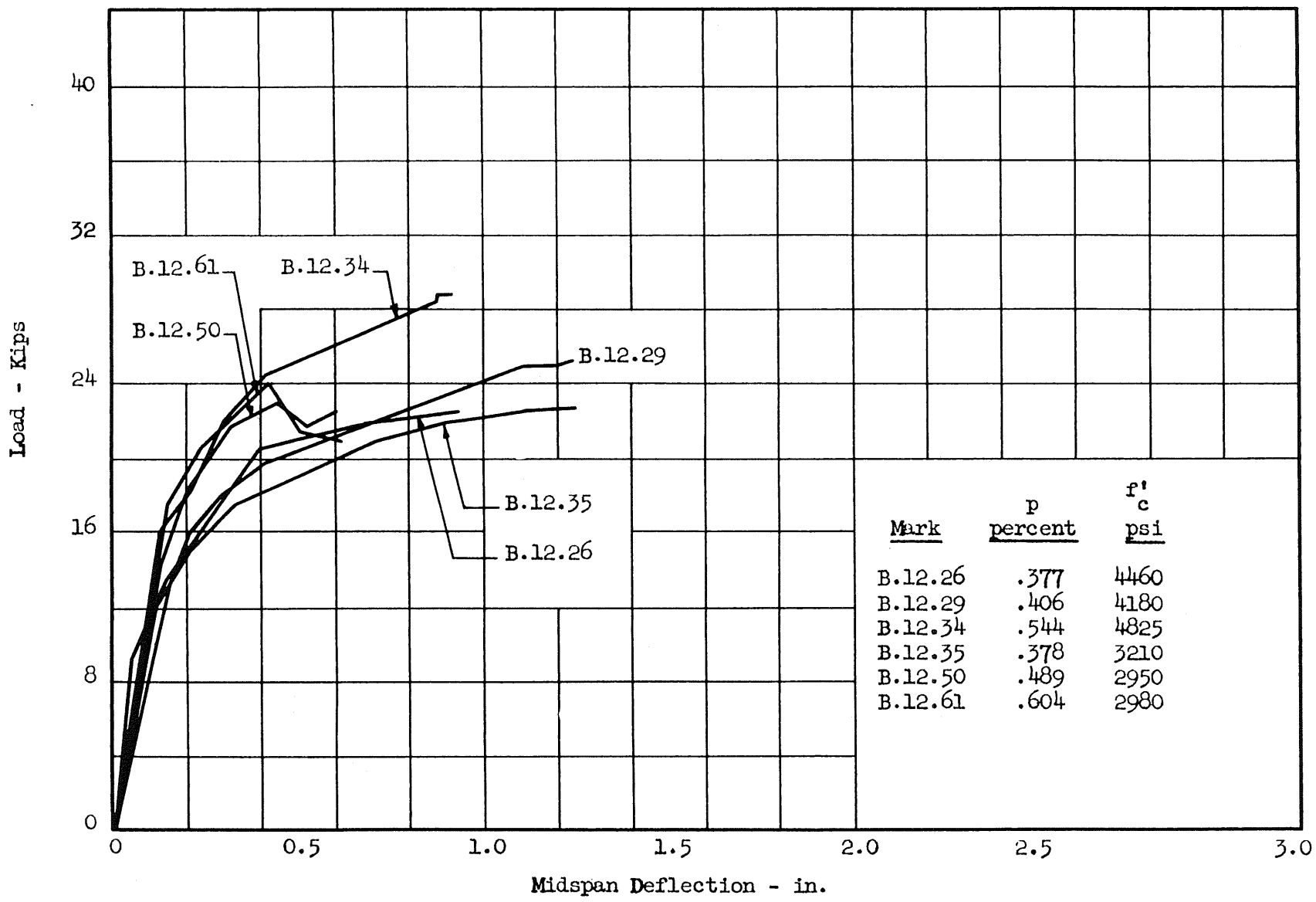

FIG. 25b **LOAD-DEFLECTION CURVES FOR I-BEAMS WITH THREE-INCH WEBS LOADED AT THE THIRD-POINTS**
NOMINAL PRESTRESS: 120,000 psi

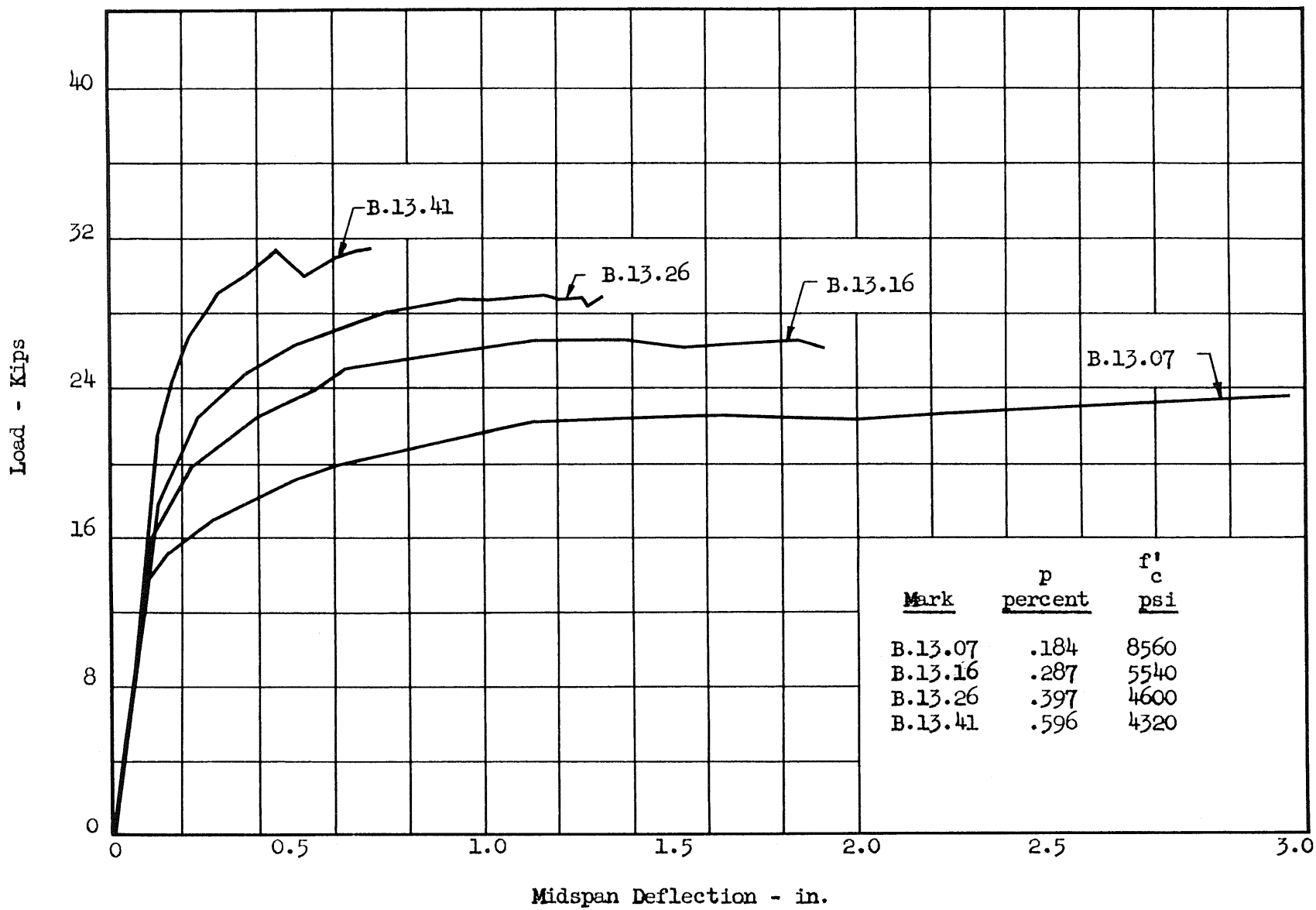

FIG. 26 LOAD-DEFLECTION CURVES FOR I-BEAMS WITH THREE-INCH WEBS AND 28-INCH SHEAR SPANS
NOMINAL PRESTRESS: 120,000 psi

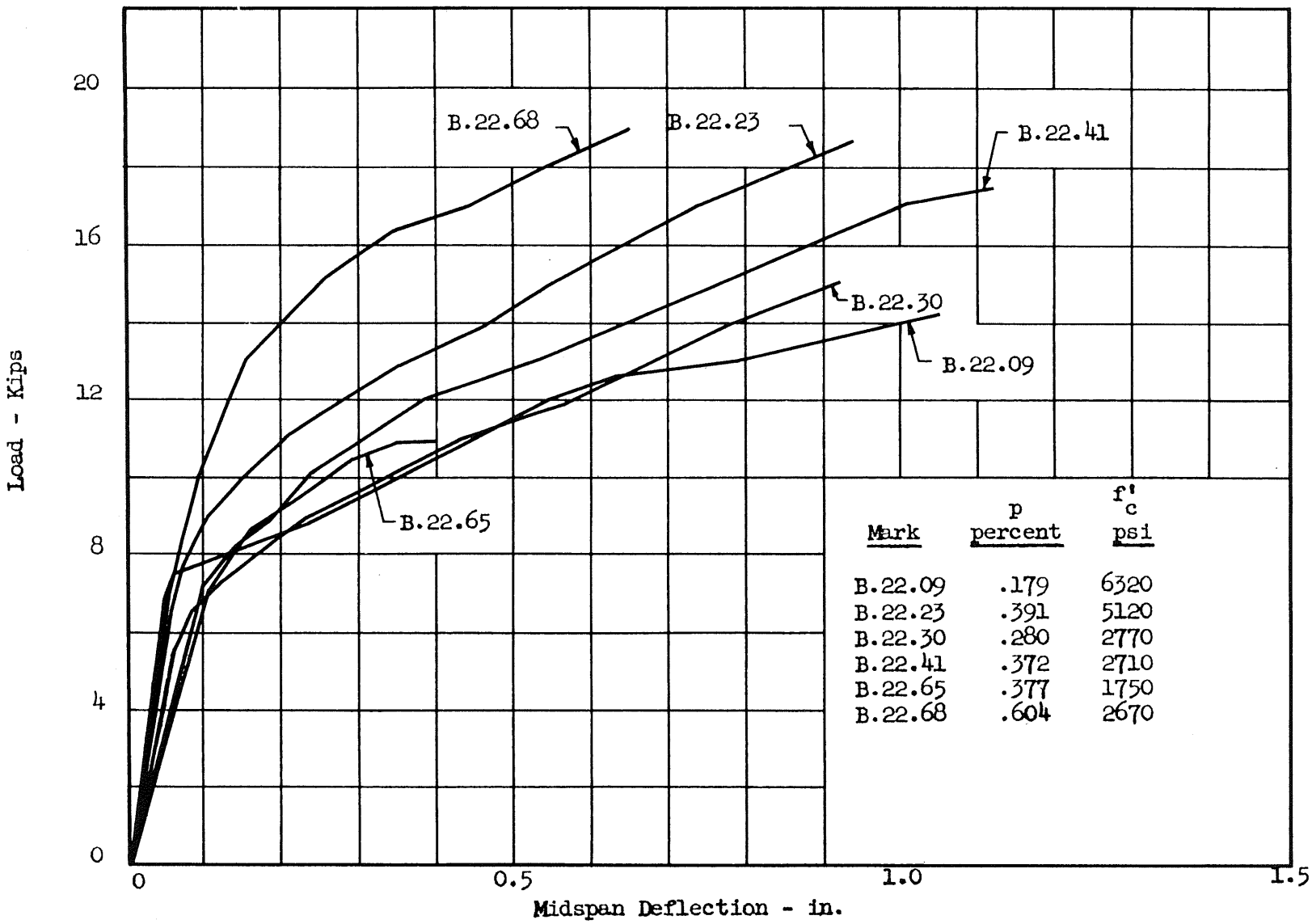

FIG. 27 LOAD-DEFLECTION CURVES FOR I-BEAMS WITH THREE-INCH WEBS LOADED AT THE THIRD-POINTS
NOMINAL PRESTRESS: 60,000 psi

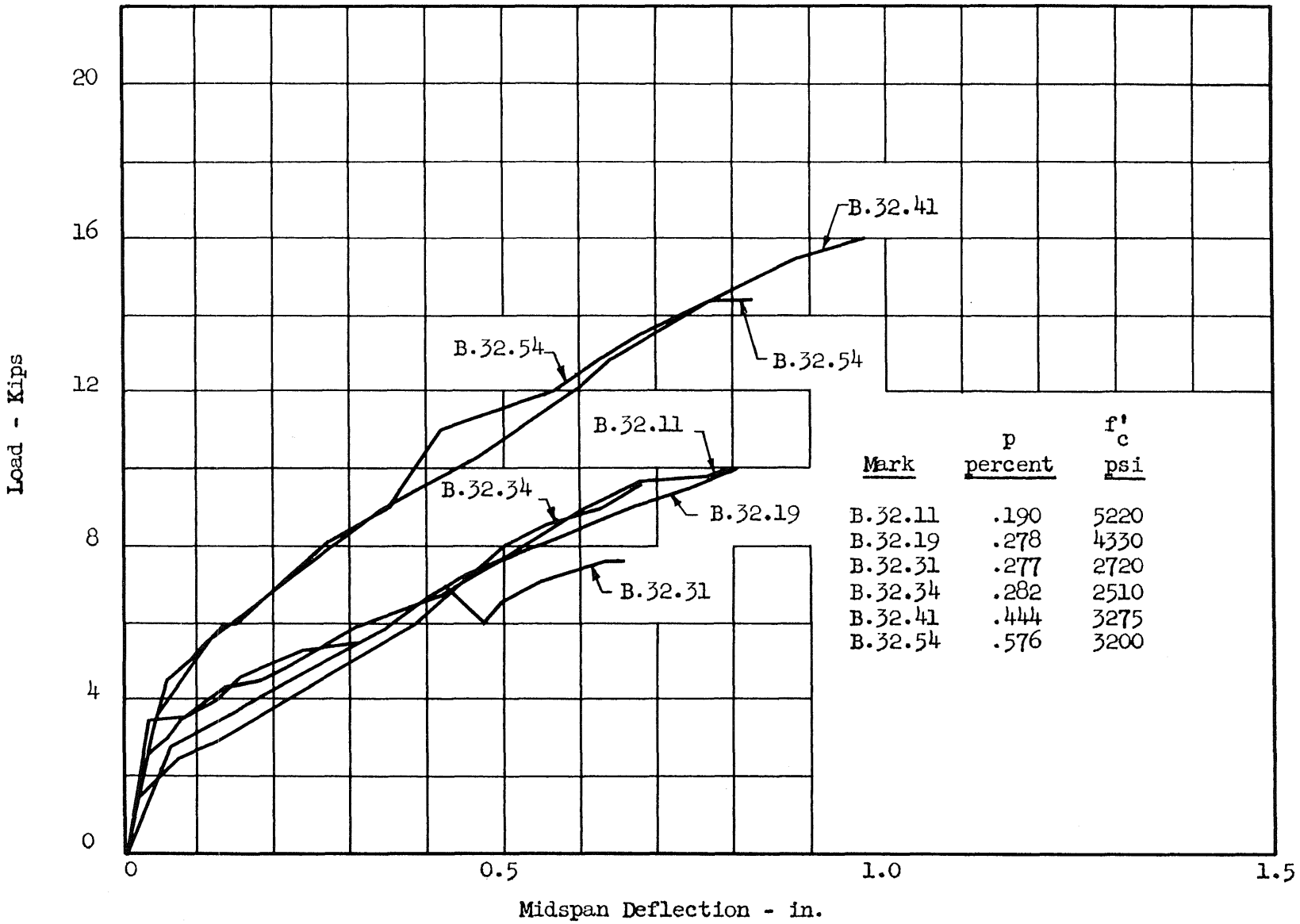

FIG. 28 LOAD-DEFLECTION CURVES FOR I-BEAMS WITH THREE-INCH WEBS LOADED AT THE THIRD-POINTS
NOMINAL PRESTRESS: ZERO

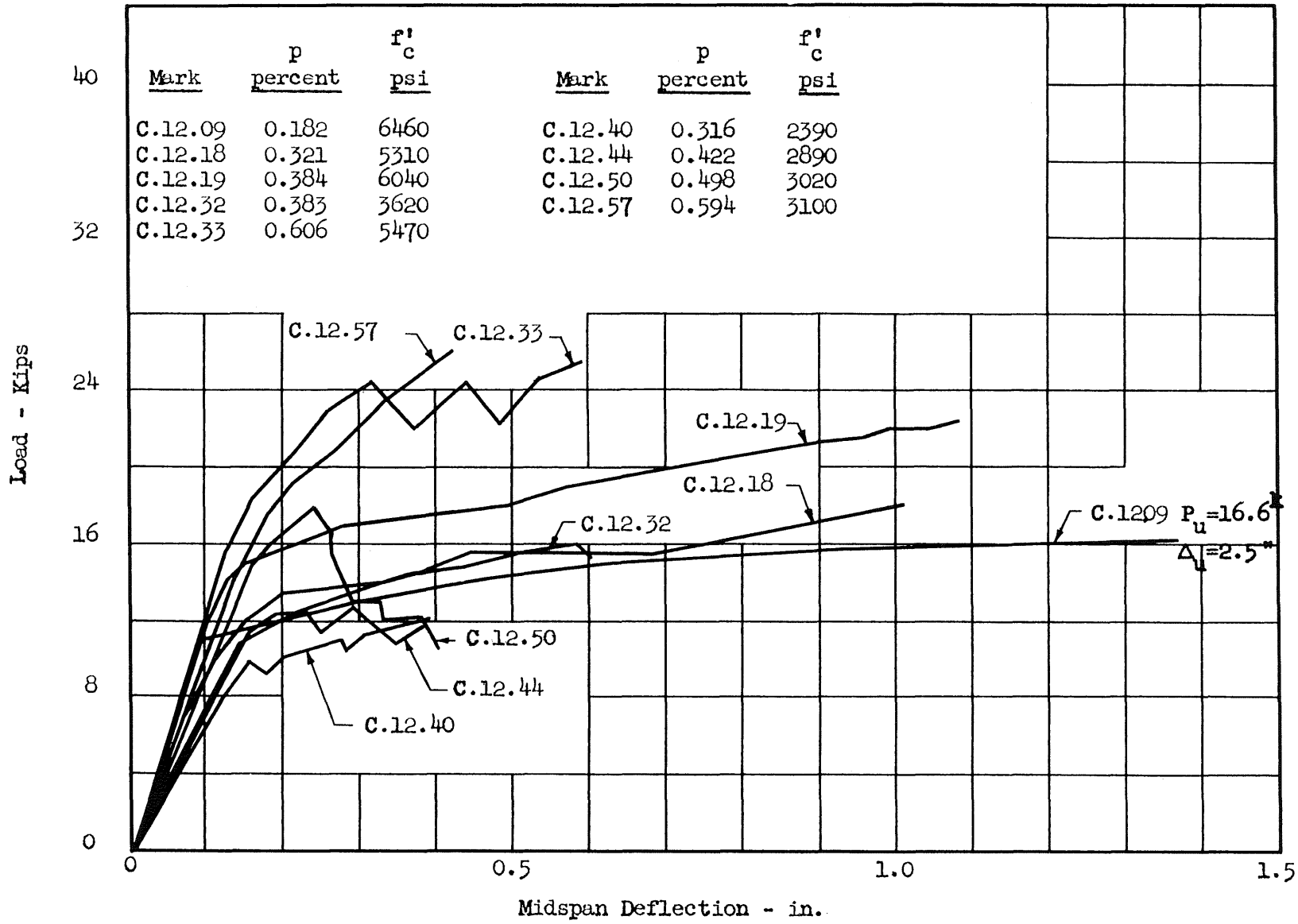

FIG. 29 **LOAD-DEFLECTION CURVES FOR I-BEAMS WITH 1 3/4-INCH WEBS LOADED AT THE THIRD-POINTS**
NOMINAL PRESTRESS: 120,000 psi

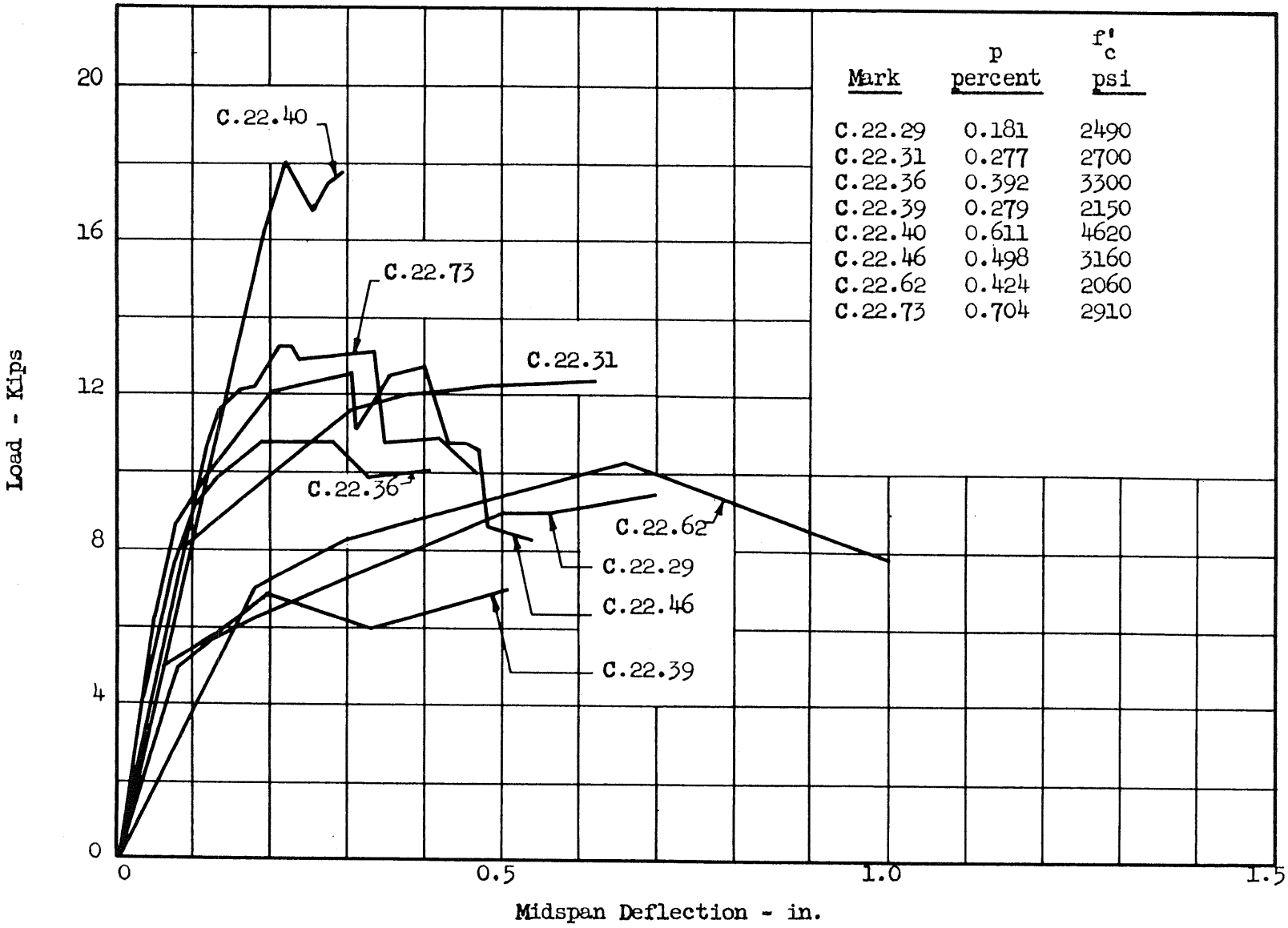

FIG. 30 **LOAD-DEFLECTION CURVES FOR I-BEAMS WITH 1 3/4-INCH WEBS LOADED AT THE THIRD-POINTS**
NOMINAL PRESTRESS: 60,000 psi

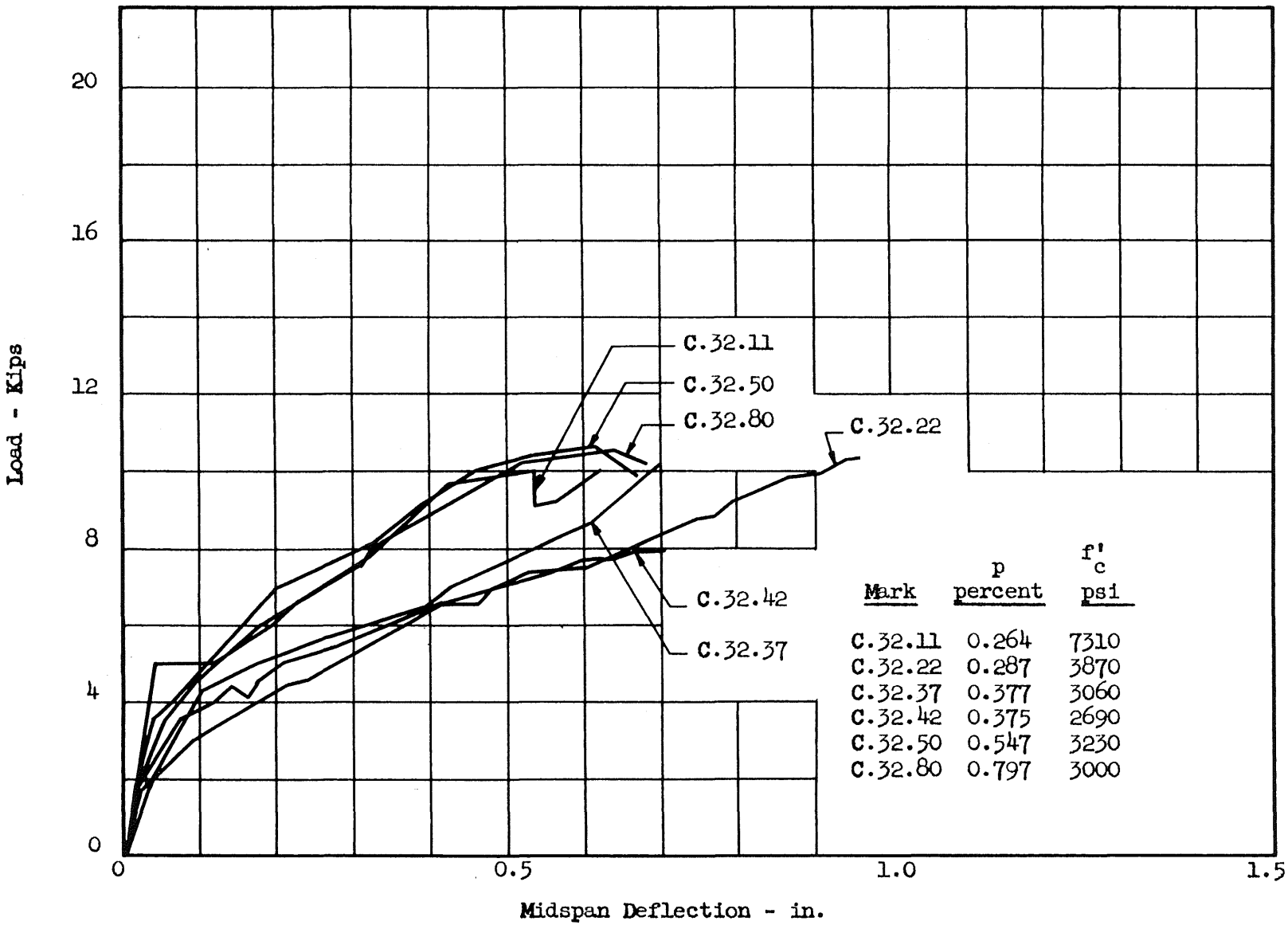

FIG. 31 LOAD-DEFLECTION CURVES FOR I-BEAMS WITH 1 3/4-INCH WEBS LOADED AT THE THIRD-POINTS
NOMINAL PRESTRESS = 0

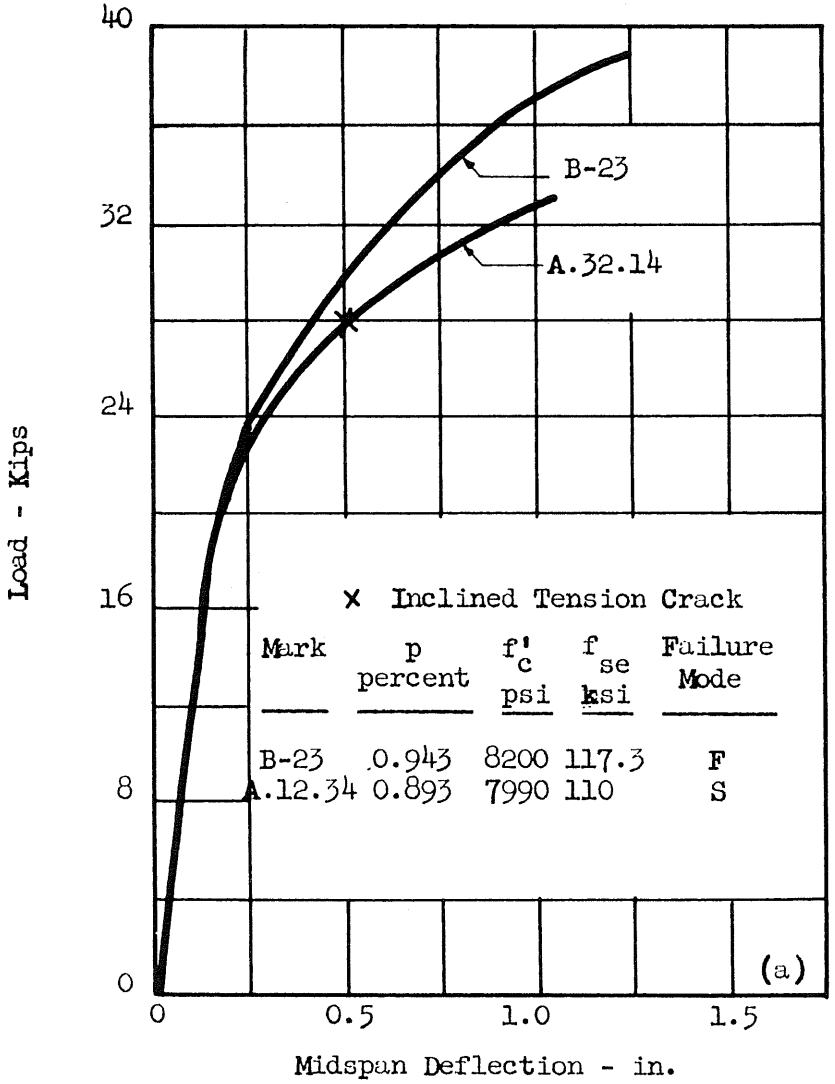

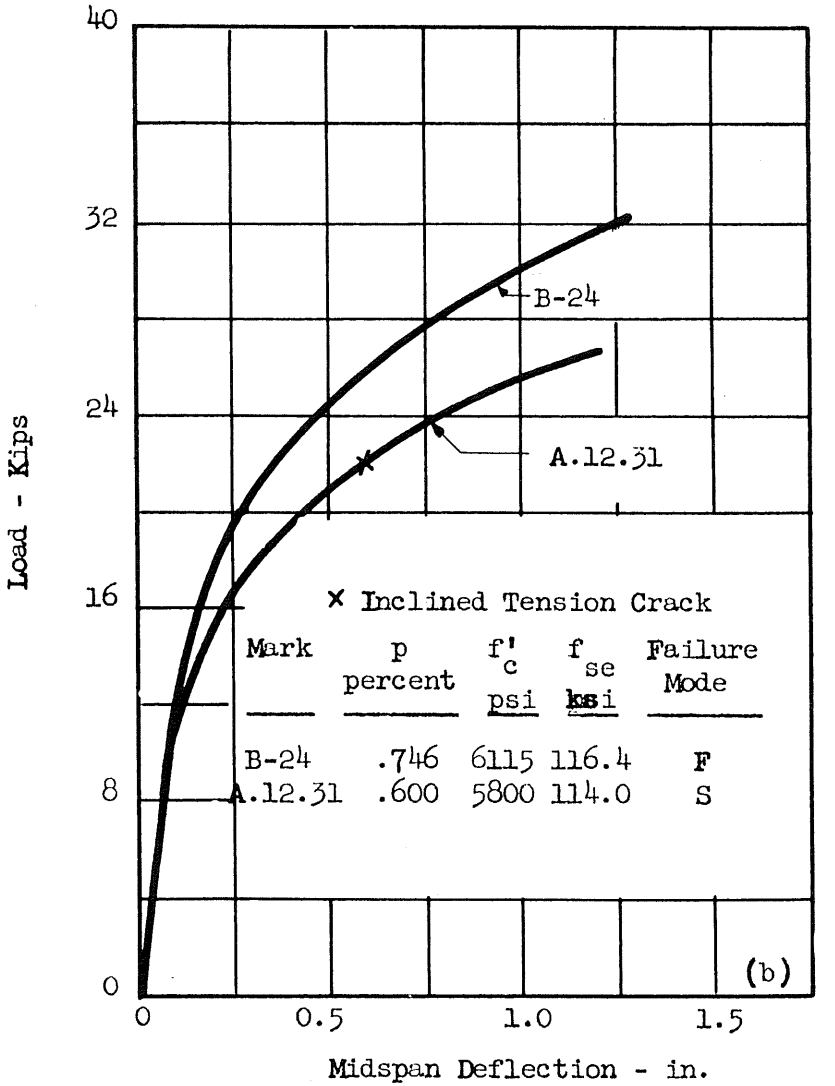

FIG. 32 COMPARISON OF LOAD-DEFLECTION CURVES FOR RECTANGULAR BEAMS FAILING IN SHEAR AND FLEXURE

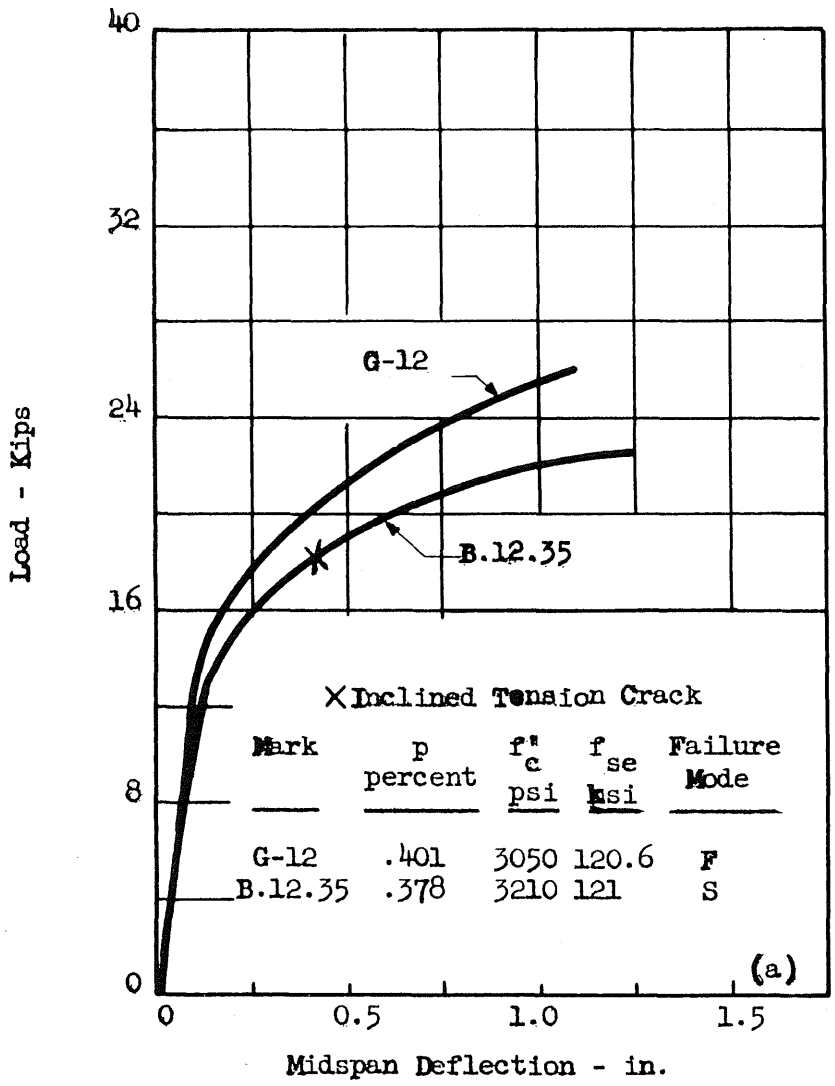

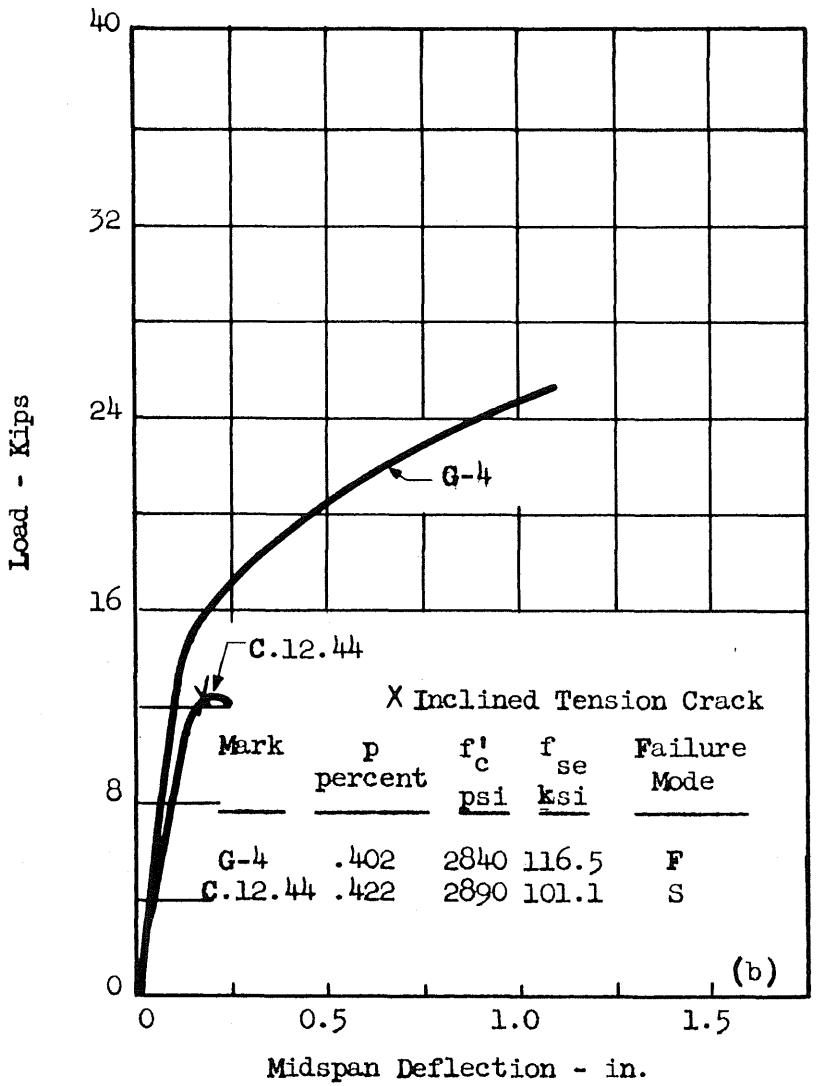

FIG. 33 COMPARISON OF LOAD-DEFLECTION CURVES FOR I-BEAMS FAILING IN SHEAR AND FLEXURE

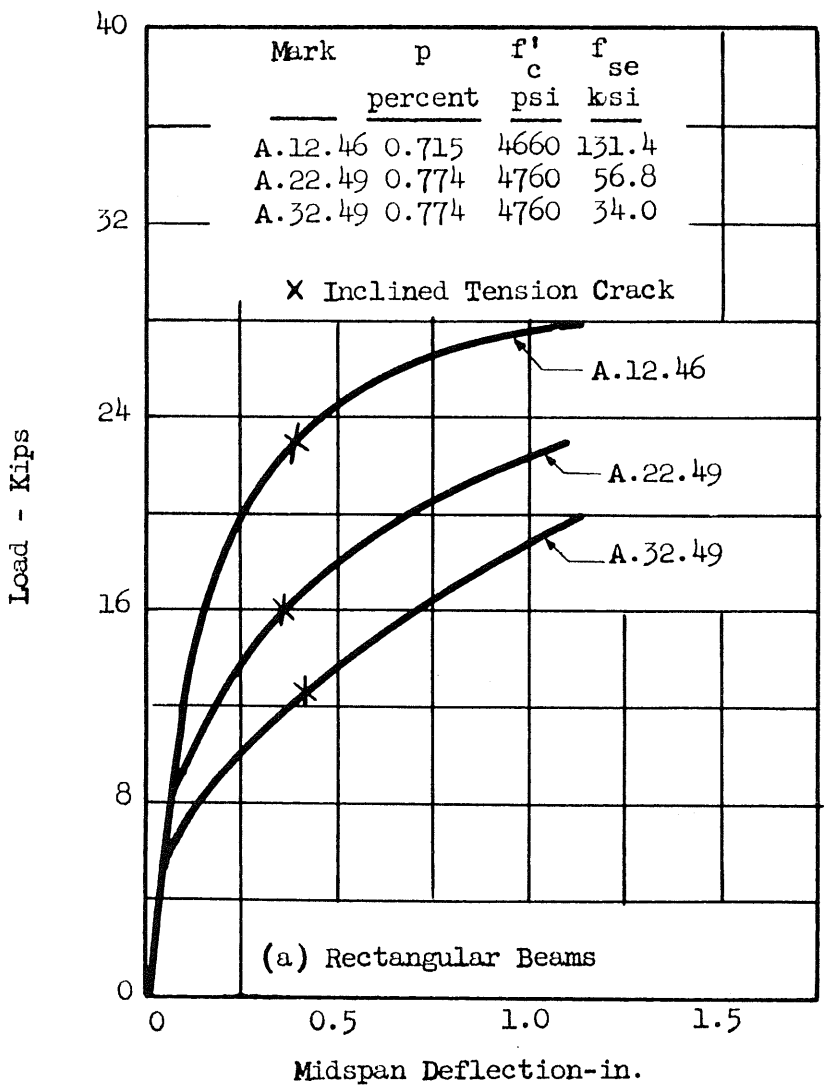

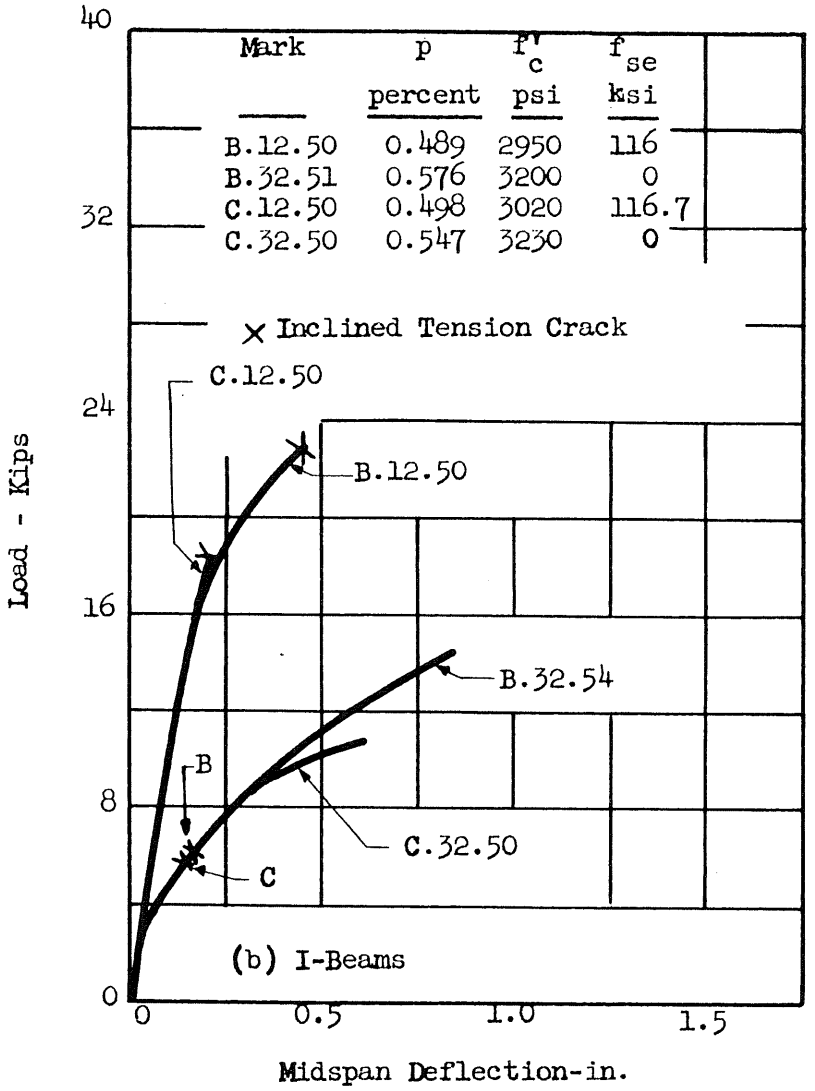

FIG. 34 EFFECT OF PRESTRESS LEVEL AND WEB THICKNESS ON LOAD-DEFLECTION CURVES

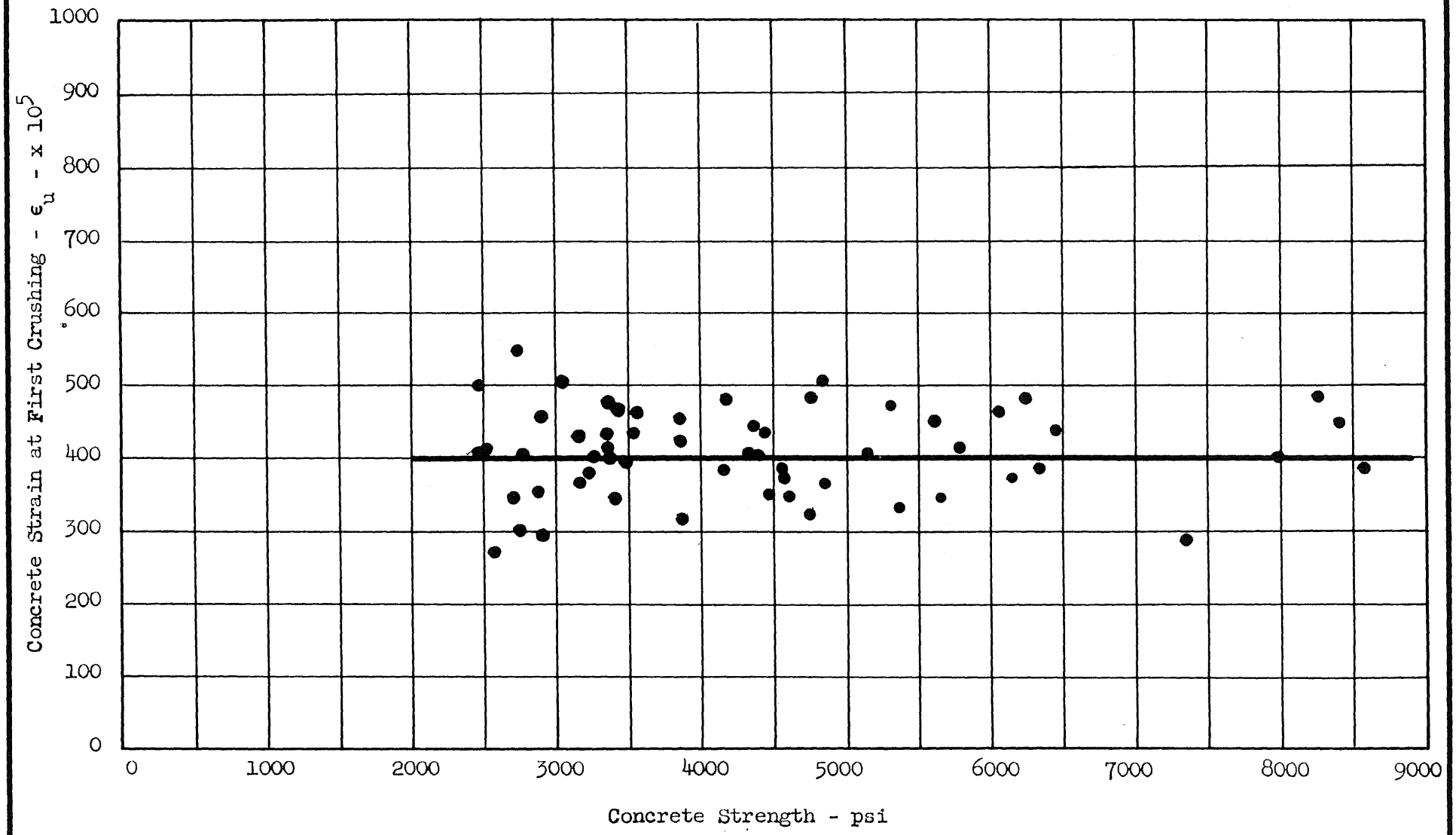

FIG. 35 MEASURED VALUES OF CONCRETE STRAIN AT FIRST CRUSHING

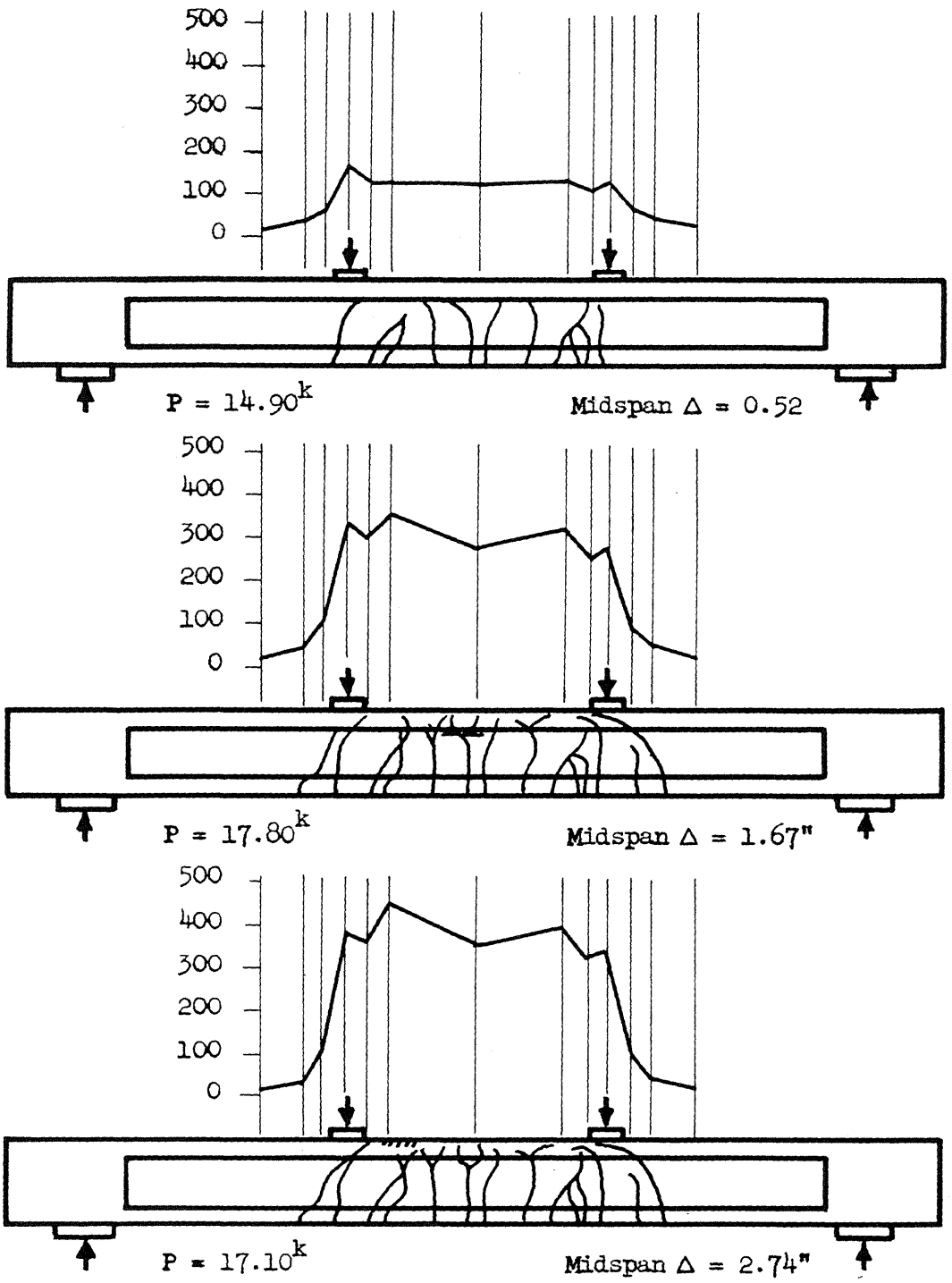

FIG. 36 DEVELOPMENT OF CRACK PATTERN AND RELATED CHANGES IN THE DISTRIBUTION OF STRAIN ON TOP SURFACE OF BEAM B.12.07

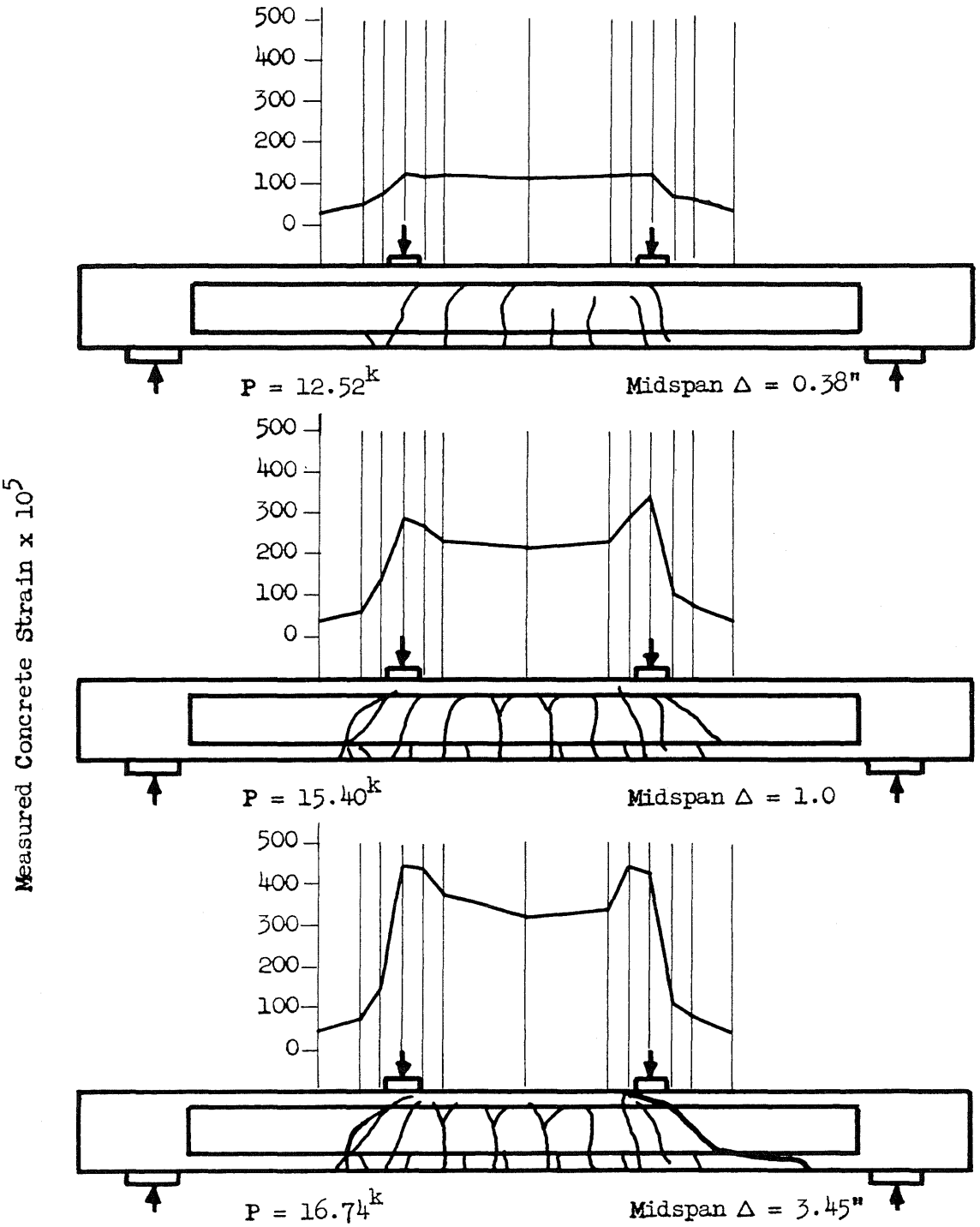

FIG. 37 DEVELOPMENT OF CRACK PATTERN AND RELATED CHANGES IN THE DISTRIBUTION OF STRAIN ON TOP SURFACE OF BEAM B.12.14

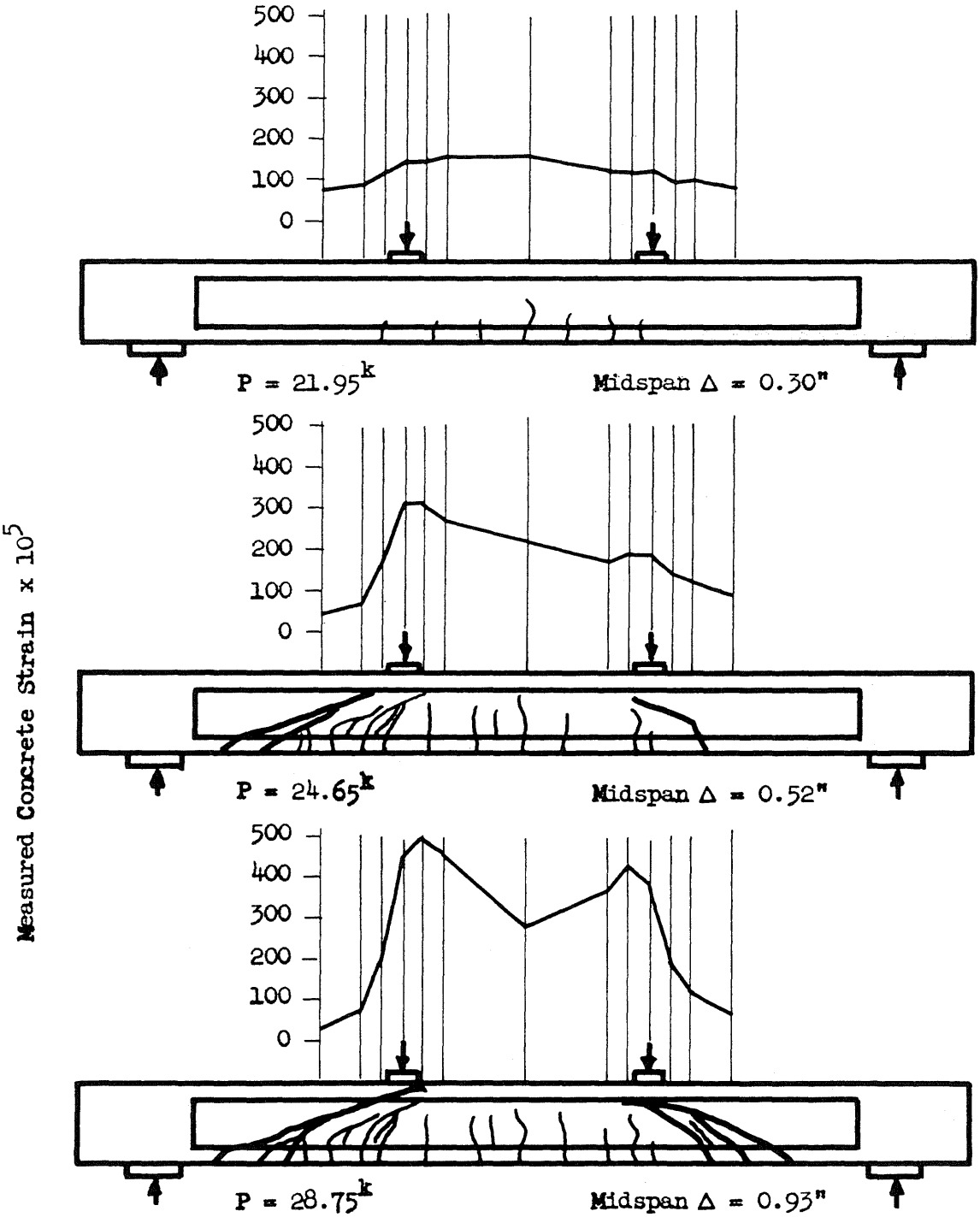

FIG. 38 DEVELOPMENT OF CRACK PATTERN AND RELATED CHANGES IN THE DISTRIBUTION OF STRAIN ON TOP SURFACE OF BEAM B.12.34

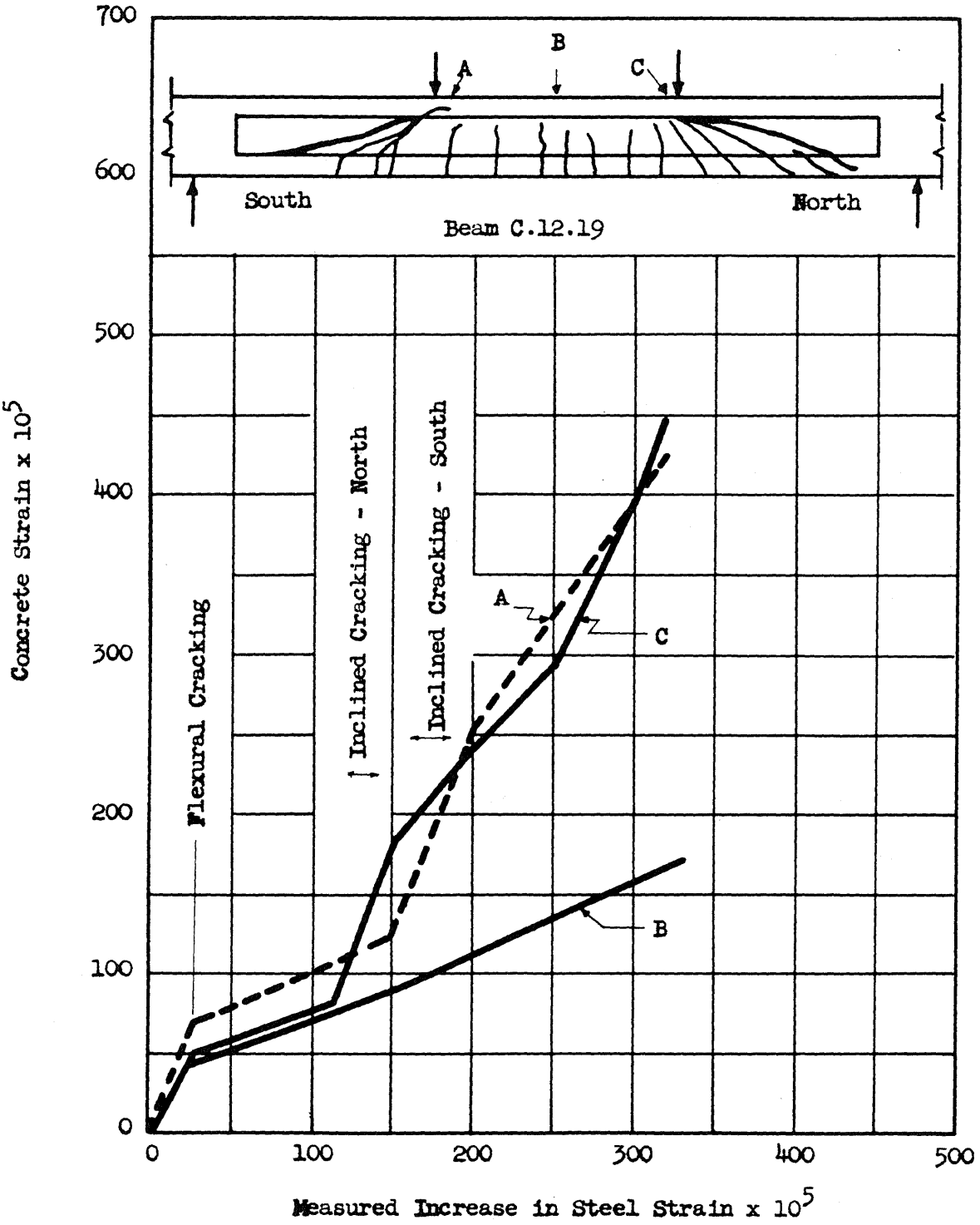

FIG. 39 RELATION BETWEEN CRITICAL CONCRETE AND STEEL STRAINS

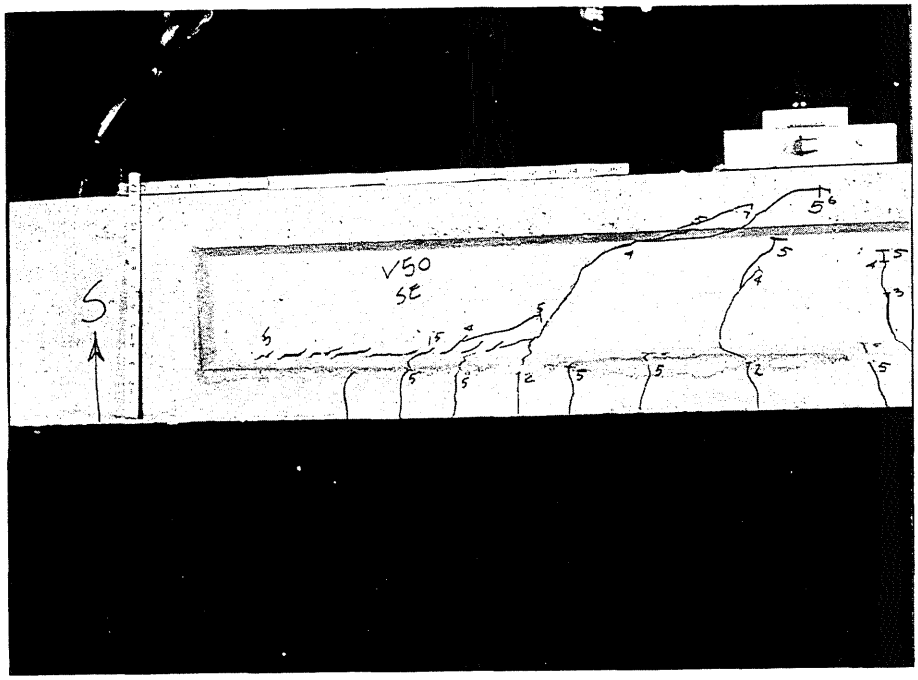

FIG. 40 INCLINED TENSION CRACK ORIGINATING FROM FLEXURE CRACK

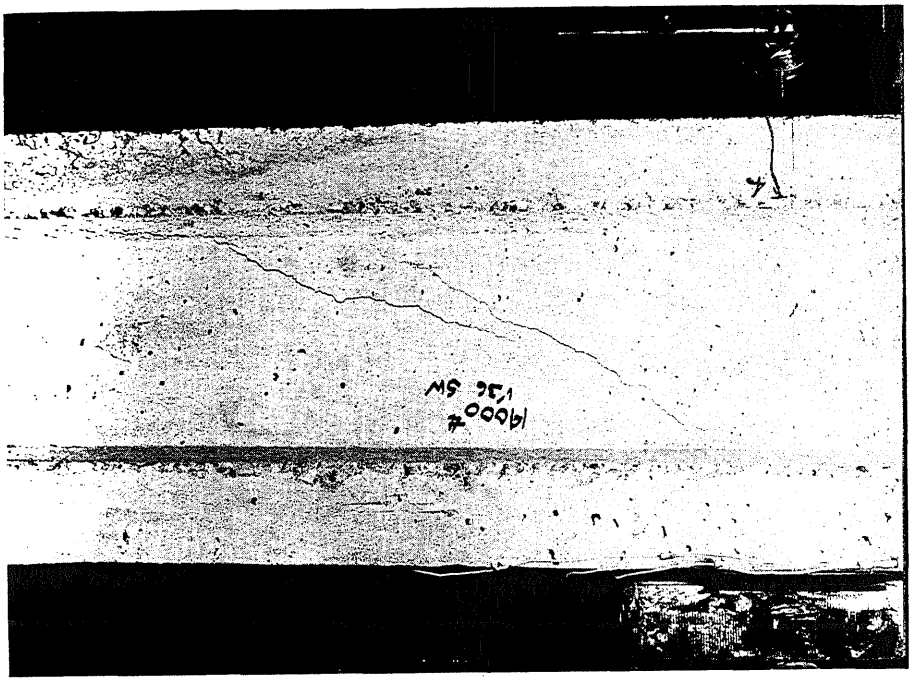

FIG. 41 INCLINED TENSION CRACK ORIGINATING IN WEB

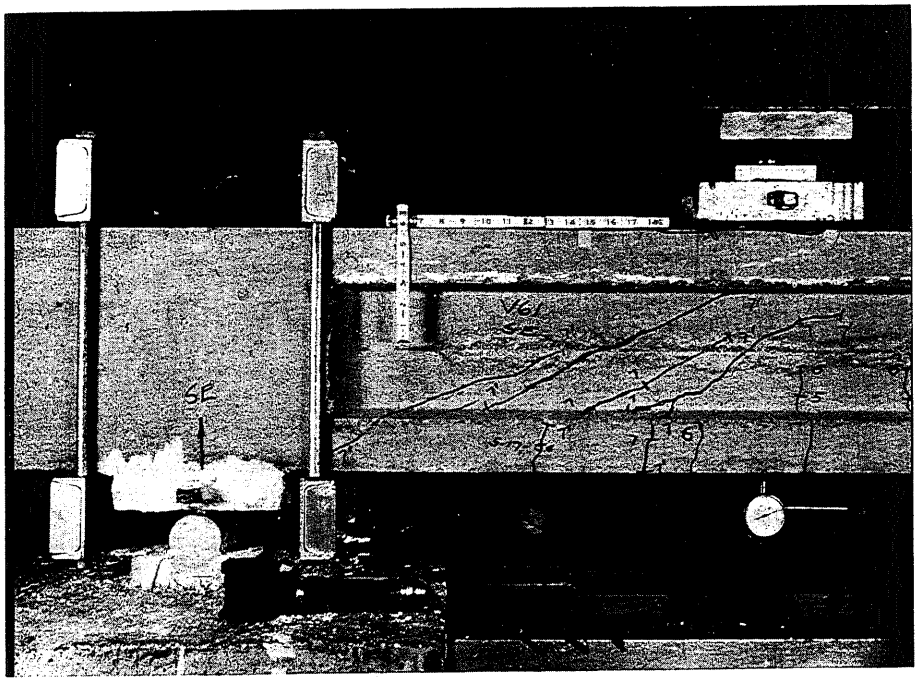

FIG. 42 INCLINED TENSION CRACKING IN BEAM B.13.41

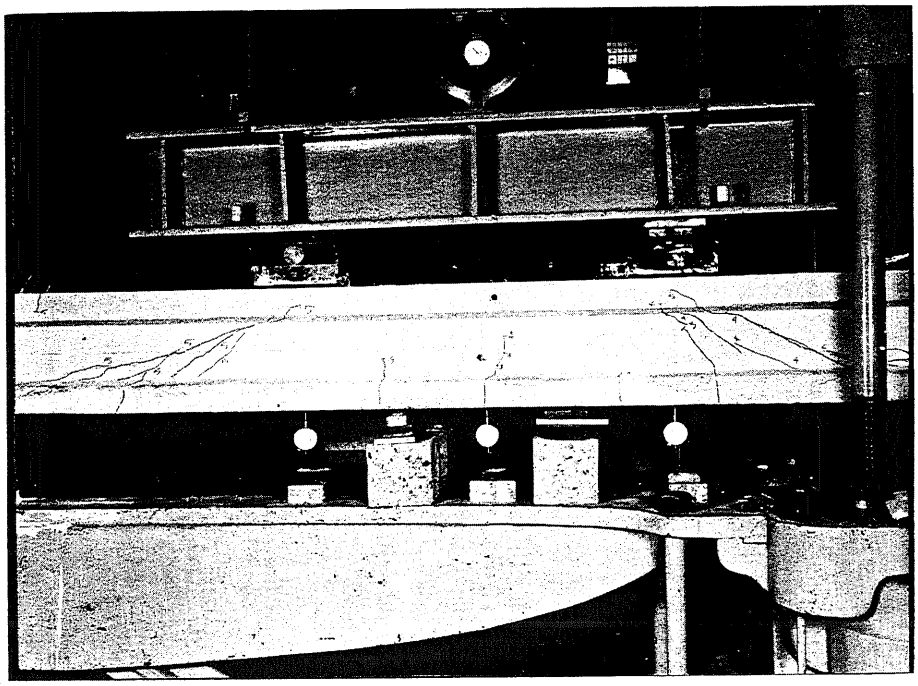

FIG. 43 INCLINED TENSION CRACKING IN BEAM C.22.39

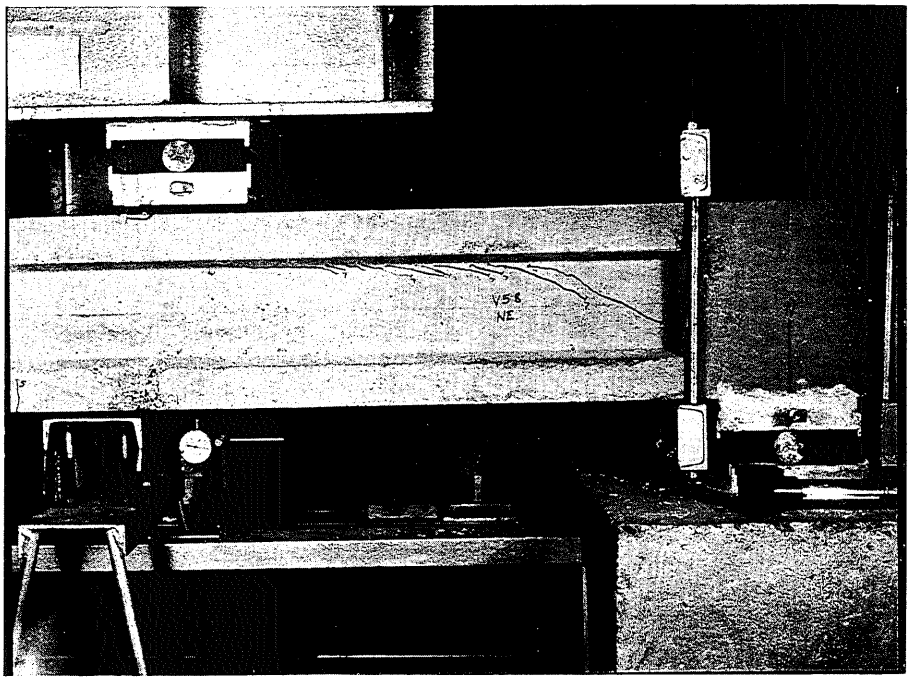

FIG. 44 SECONDARY INCLINED TENSION CRACKING

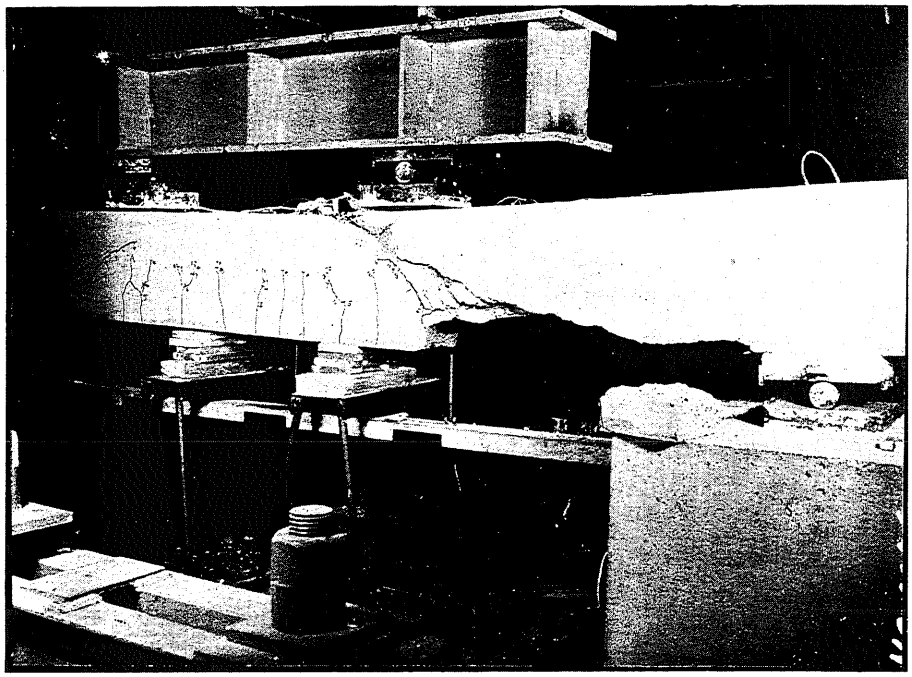

FIG. 45 SHEAR-COMPRESSION FAILURE IN A RECTANGULAR BEAM

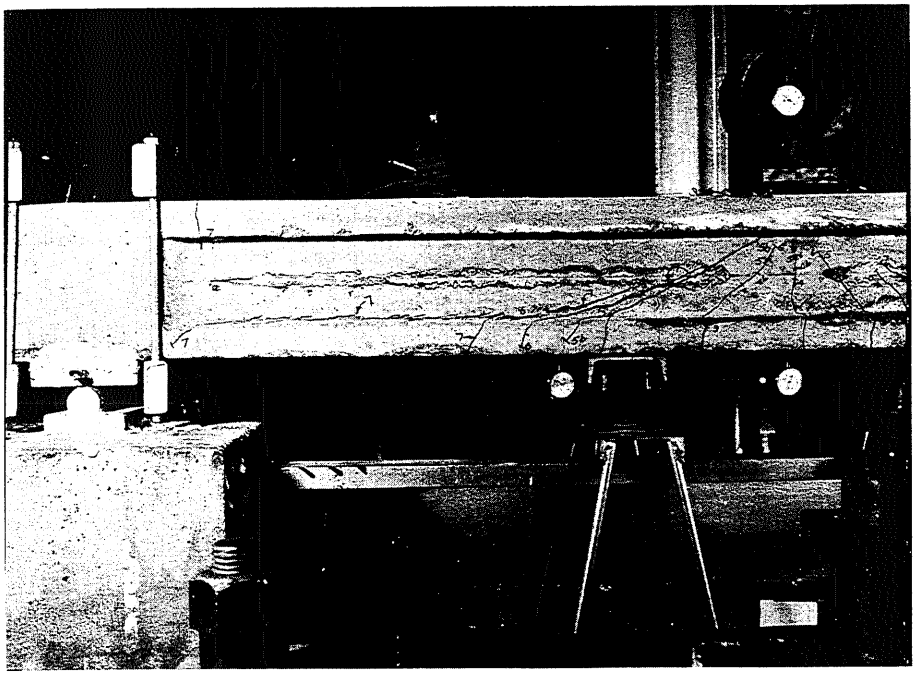

FIG. 46 CRACKS SEPARATING TENSION FLANGE FROM WEB

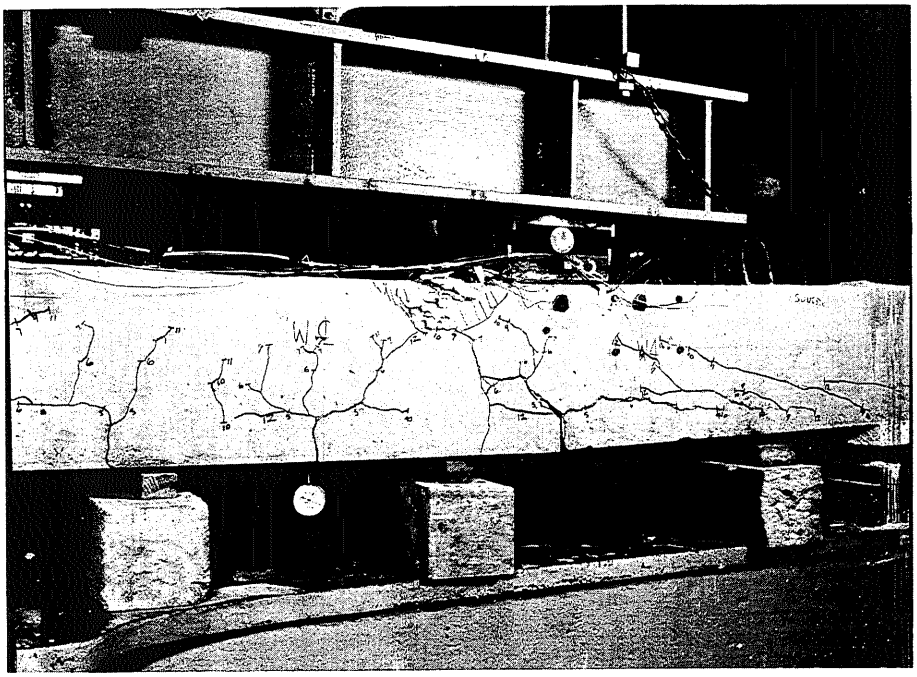

FIG. 47 RECTANGULAR BEAM "UNBONDED" AS A RESULT OF INCLINED TENSION CRACKING

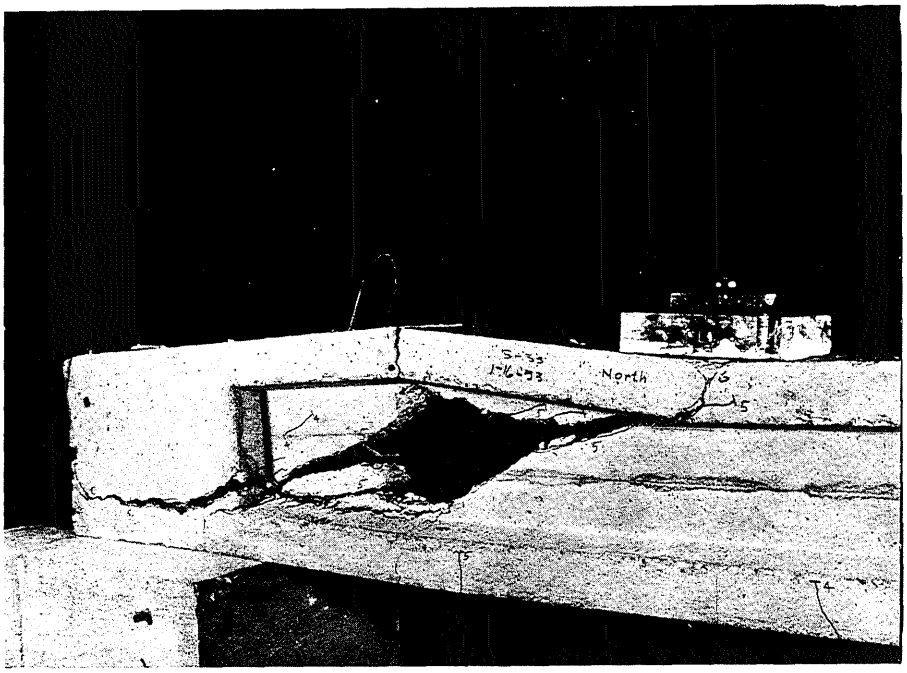

FIG. 48 FAILURE OF I-BEAM WITHOUT EXTERNAL STIRRUPS ON END-BLOCK

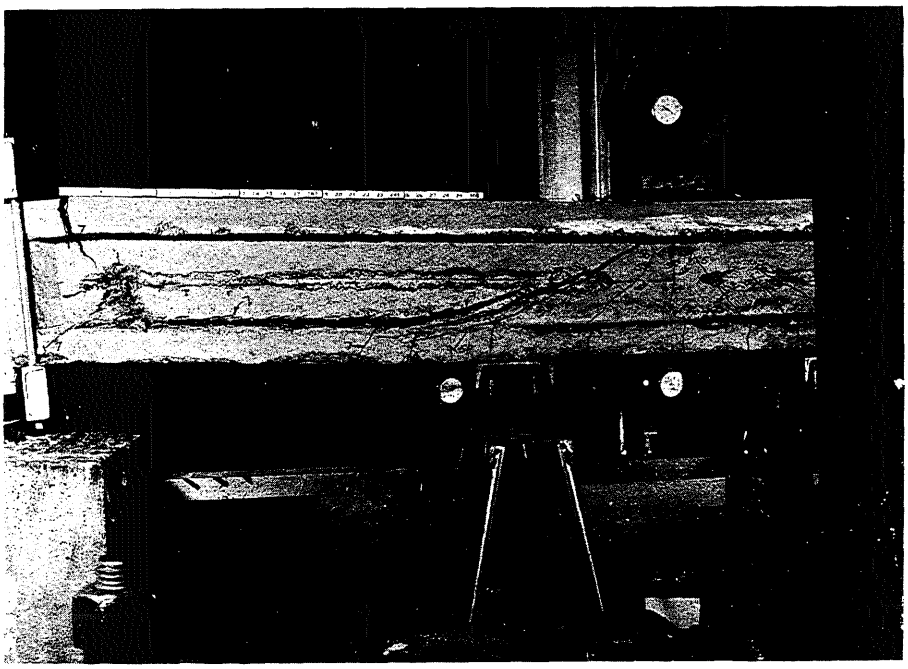

FIG. 49 WEB CRUSHING

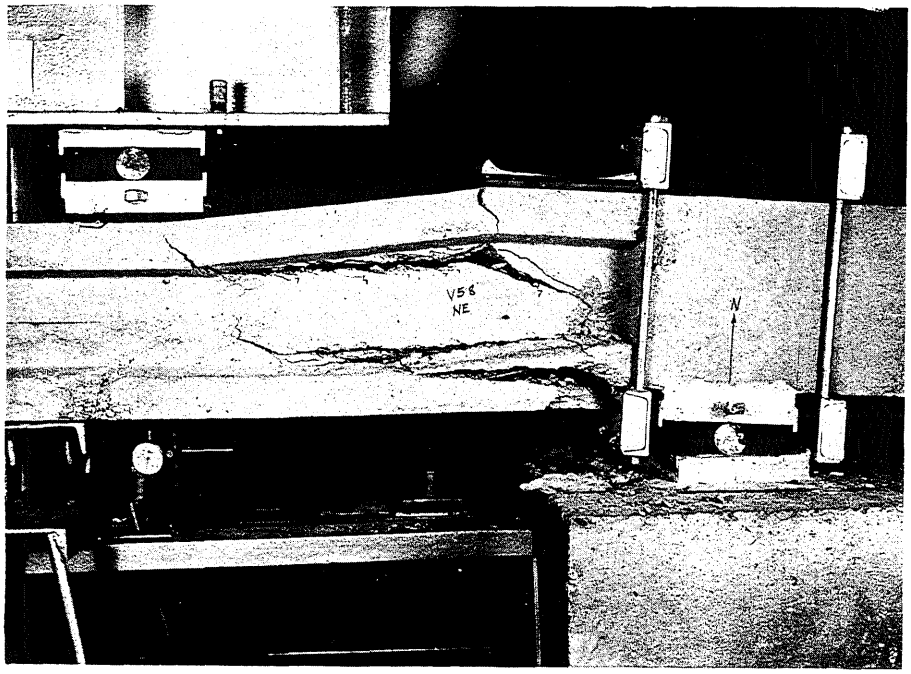

(a)

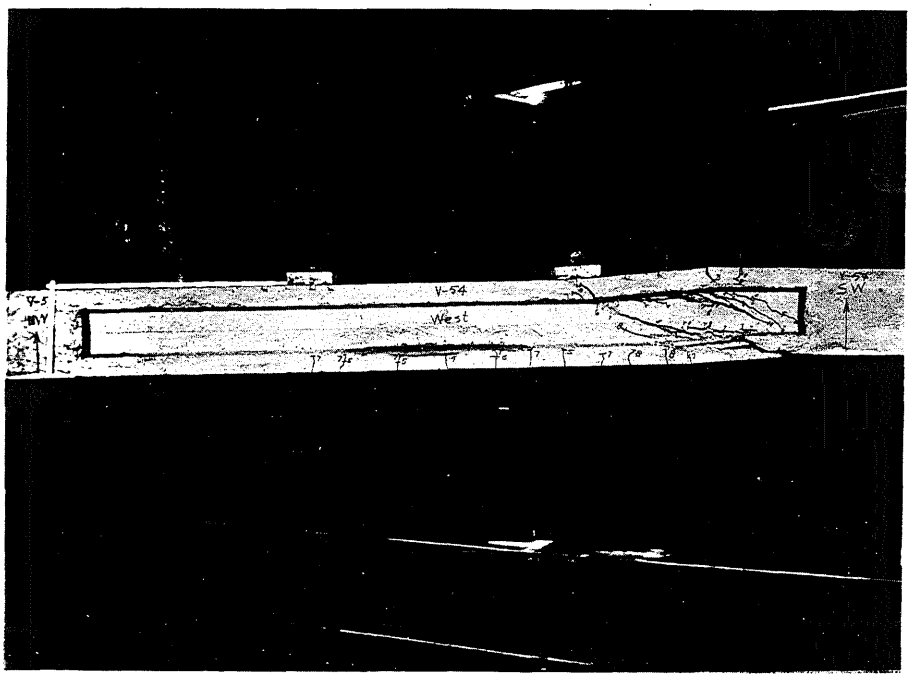

(b)

FIG. 50 FAILURE AS A RESULT OF SECONDARY INCLINED TENSION CRACKING

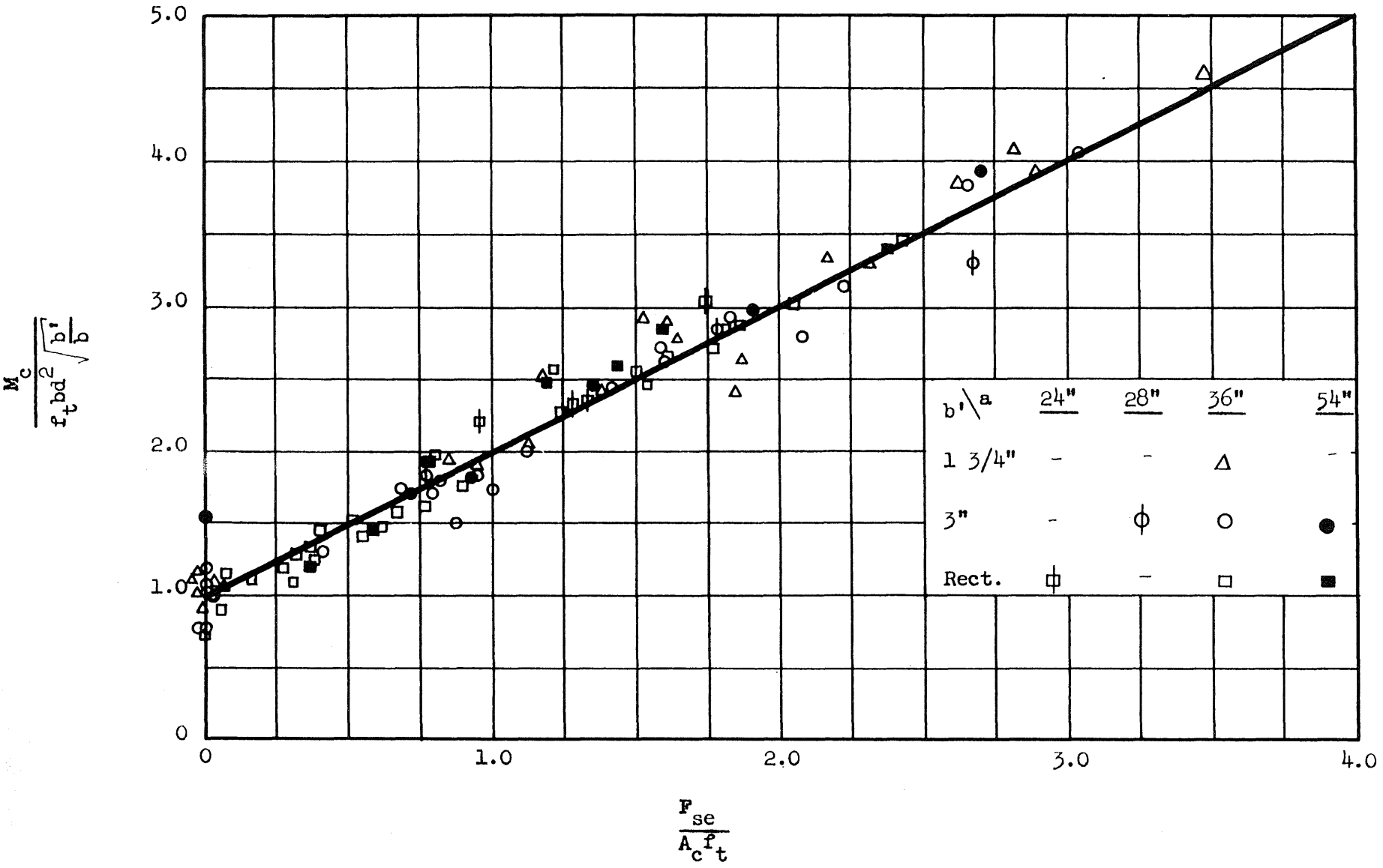

FIG. 51 COMPARISON OF MOMENT AT INCLINED TENSION CRACKING WITH MEAN COMPRESSIVE PRESTRESS

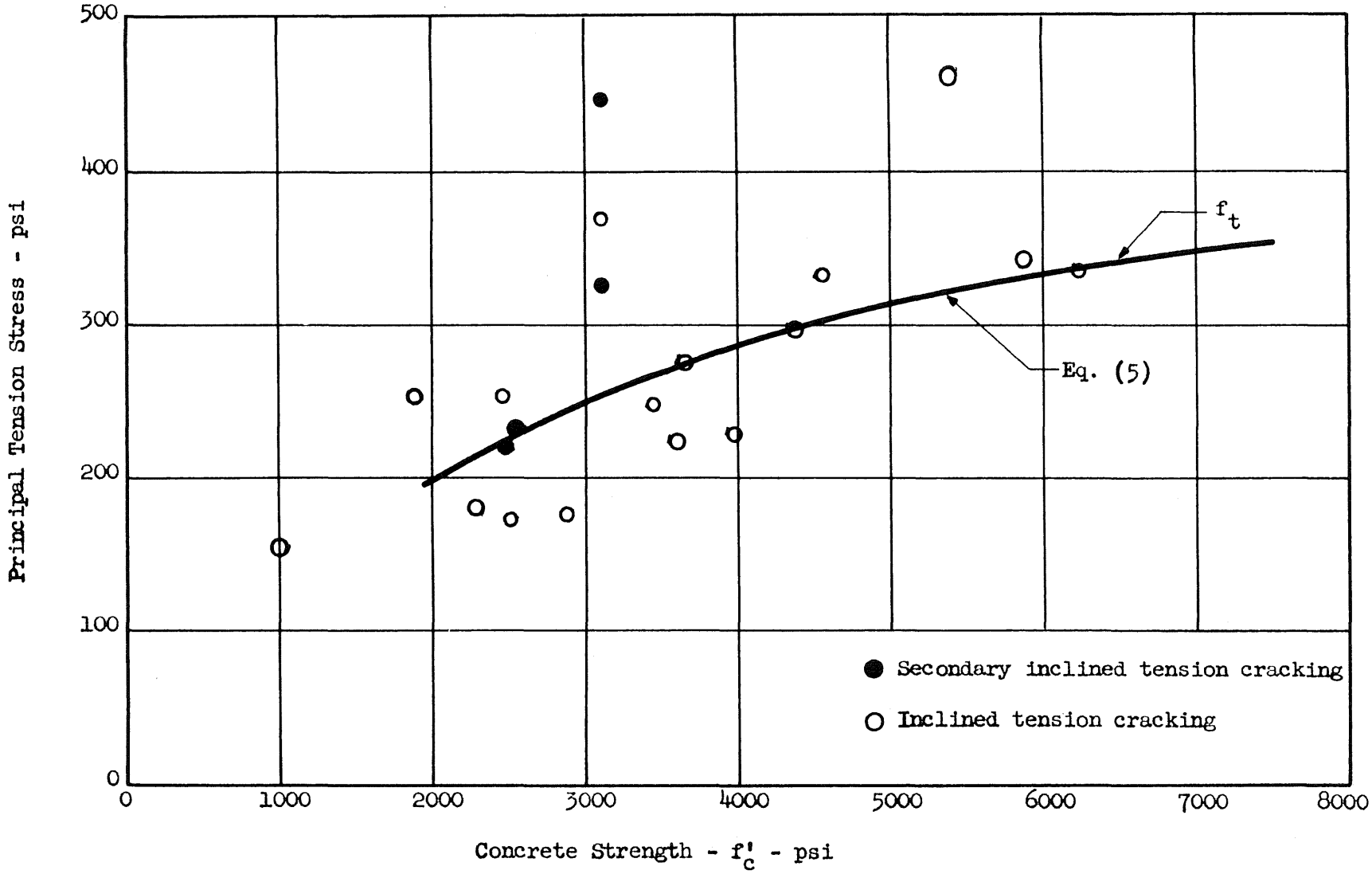

FIG. 52 COMPUTED PRINCIPAL TENSION STRESSES AT MID-HEIGHT CORRESPONDING TO INCLINED TENSION CRACKING FOR I-BEAMS WITH 1 3/4 - INCH WEBS

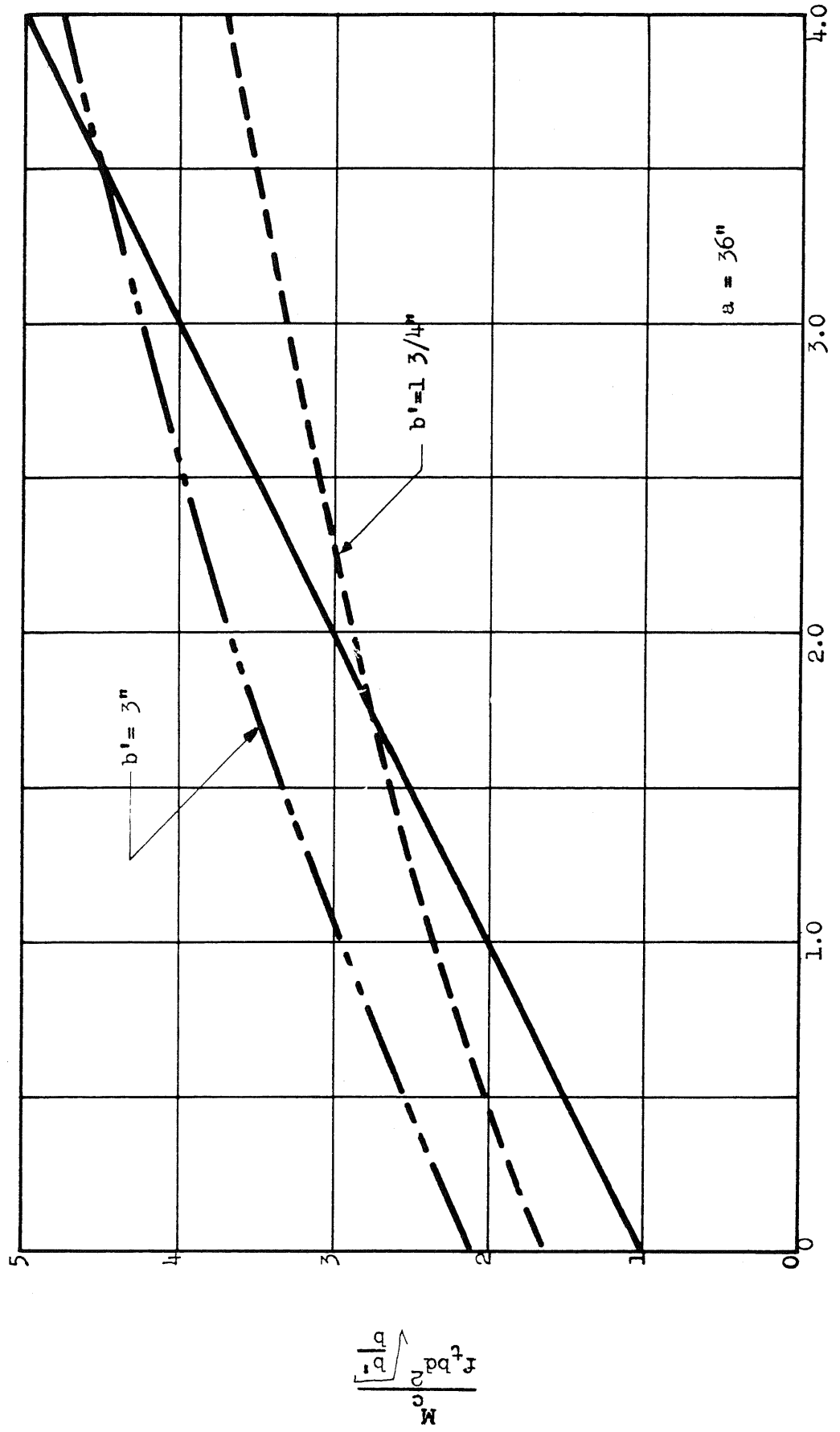

FIG. 53 HYPOTHETICAL COMPARISON OF PRIMARY AND SECONDARY INCLINED TENSION CRACKING

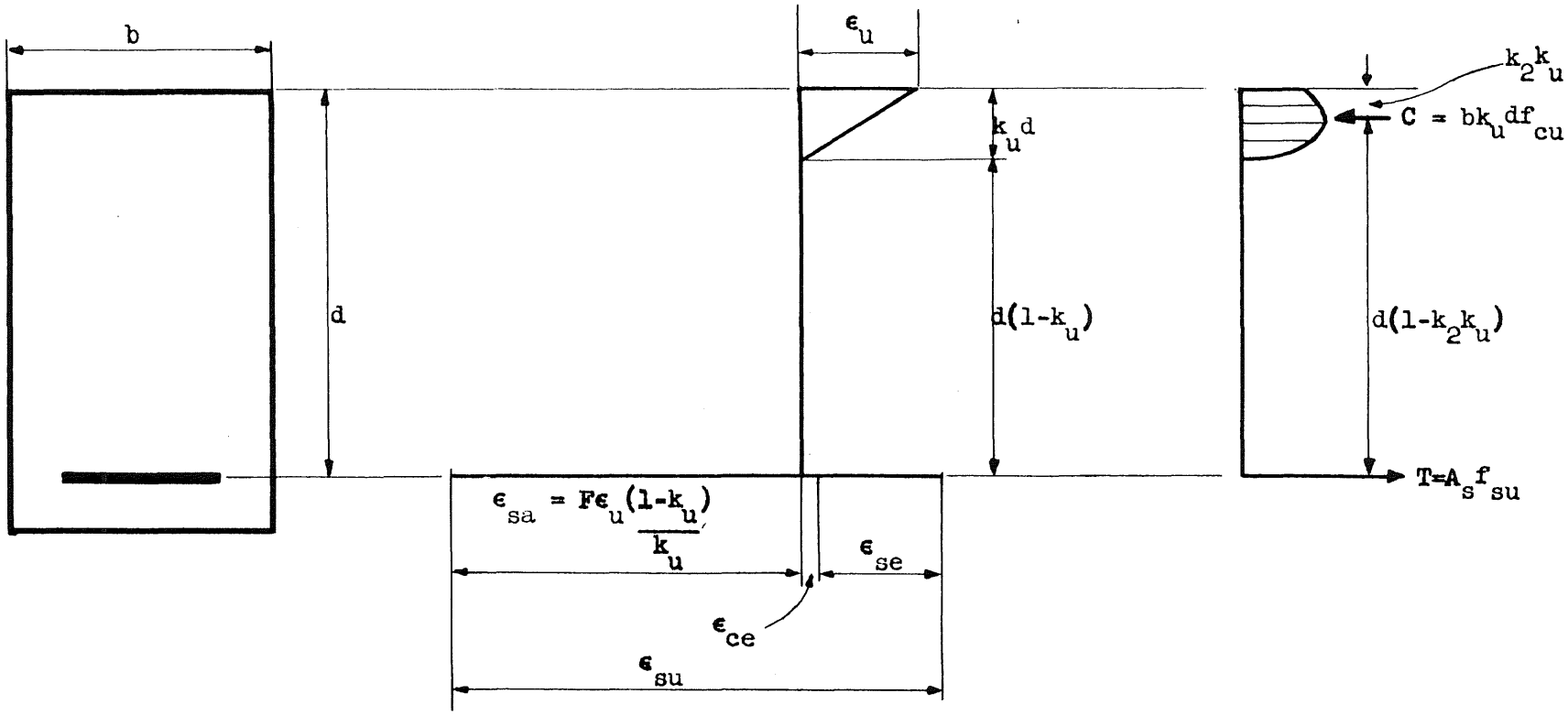

(a) Strain Distribution

(b) Stress Distribution

FIG. 54 ASSUMED STRAIN AND STRESS CONDITIONS AT ULTIMATE FOR FLEXURAL FAILURES IN PRESTRESSED CONCRETE BEAMS

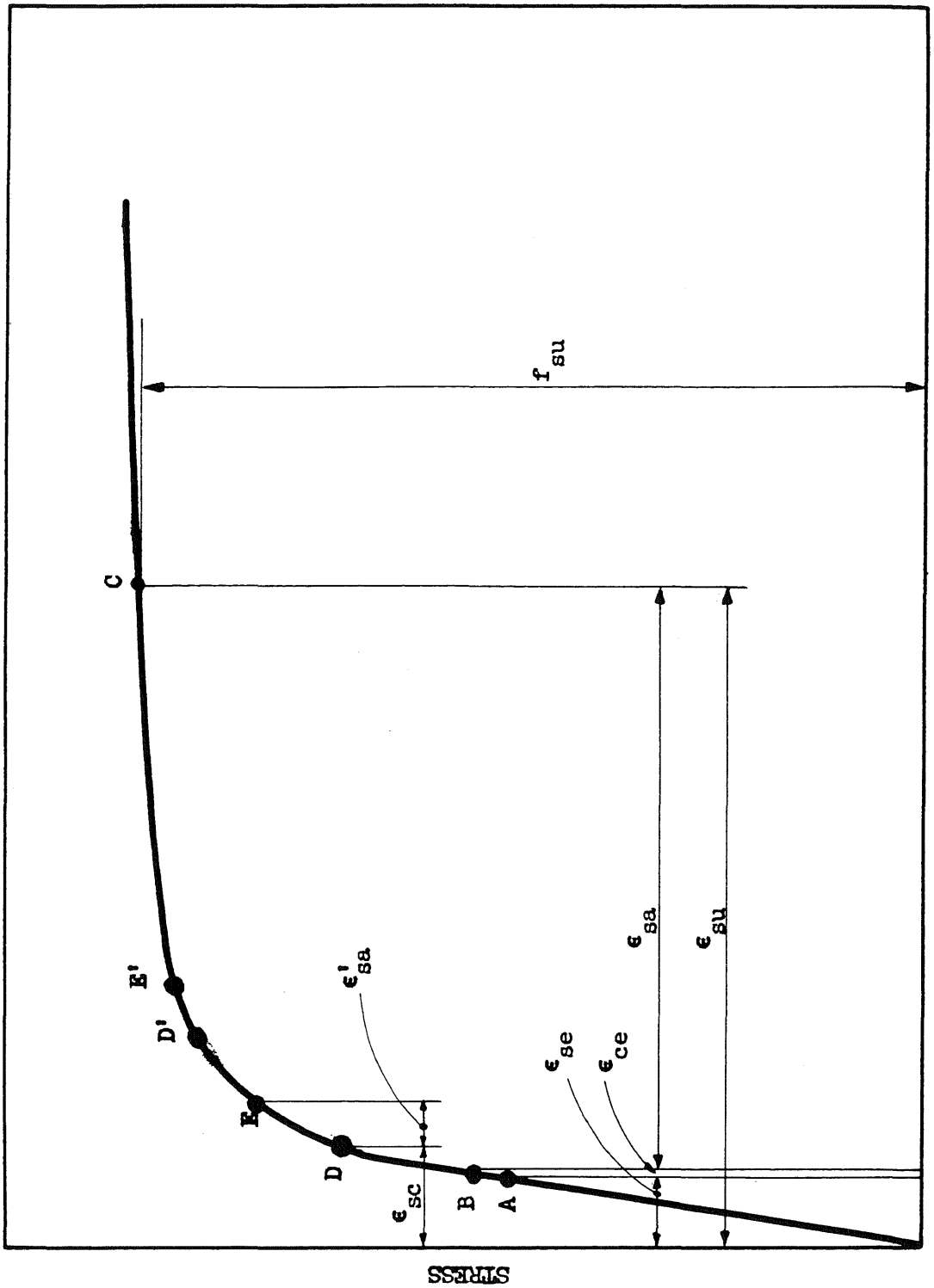

FIG. 55 STEEL STRESSES AT FAILURE

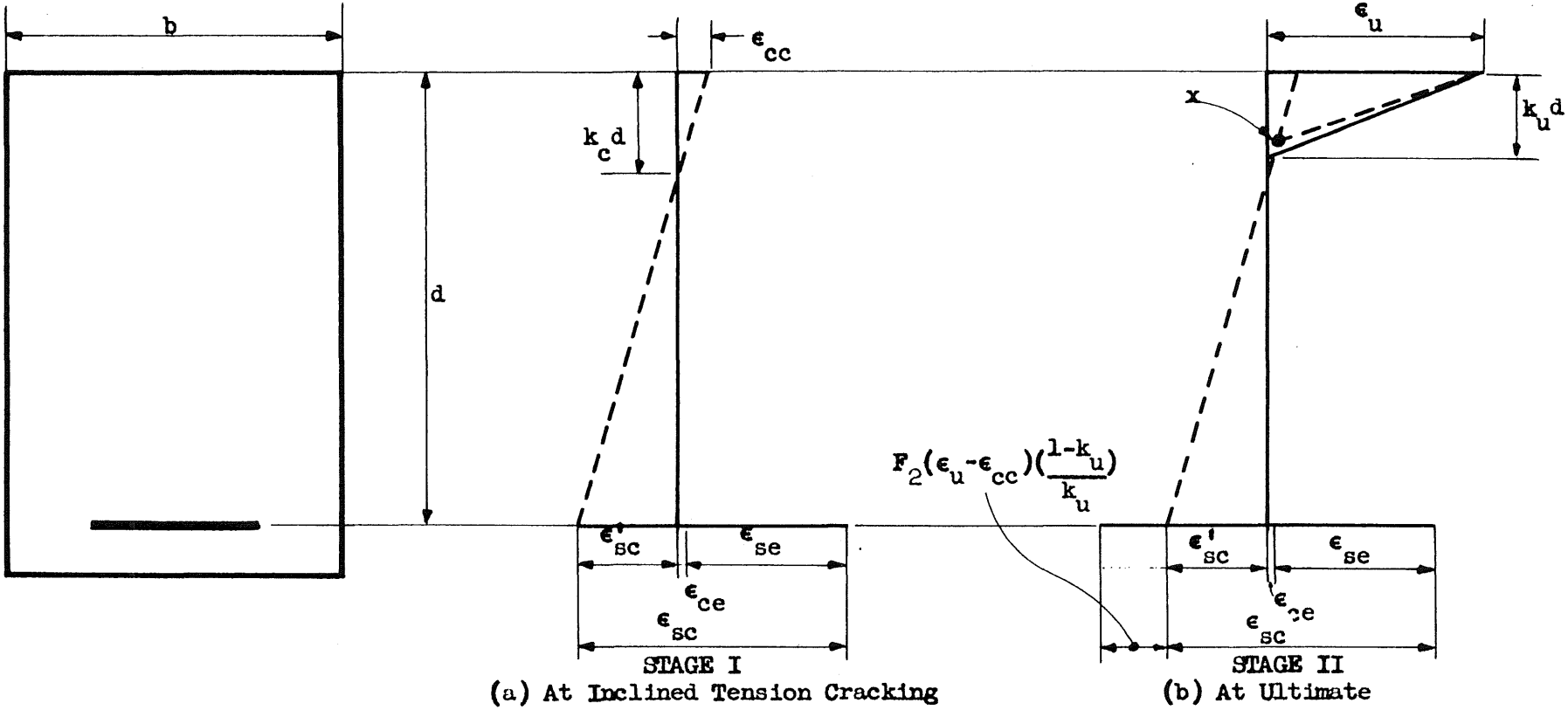

FIG. 56 IDEALIZED RELATIONSHIPS OF CRITICAL STEEL AND CONCRETE STRAINS FOR BEAM FAILING IN SHEAR COMPRESSION

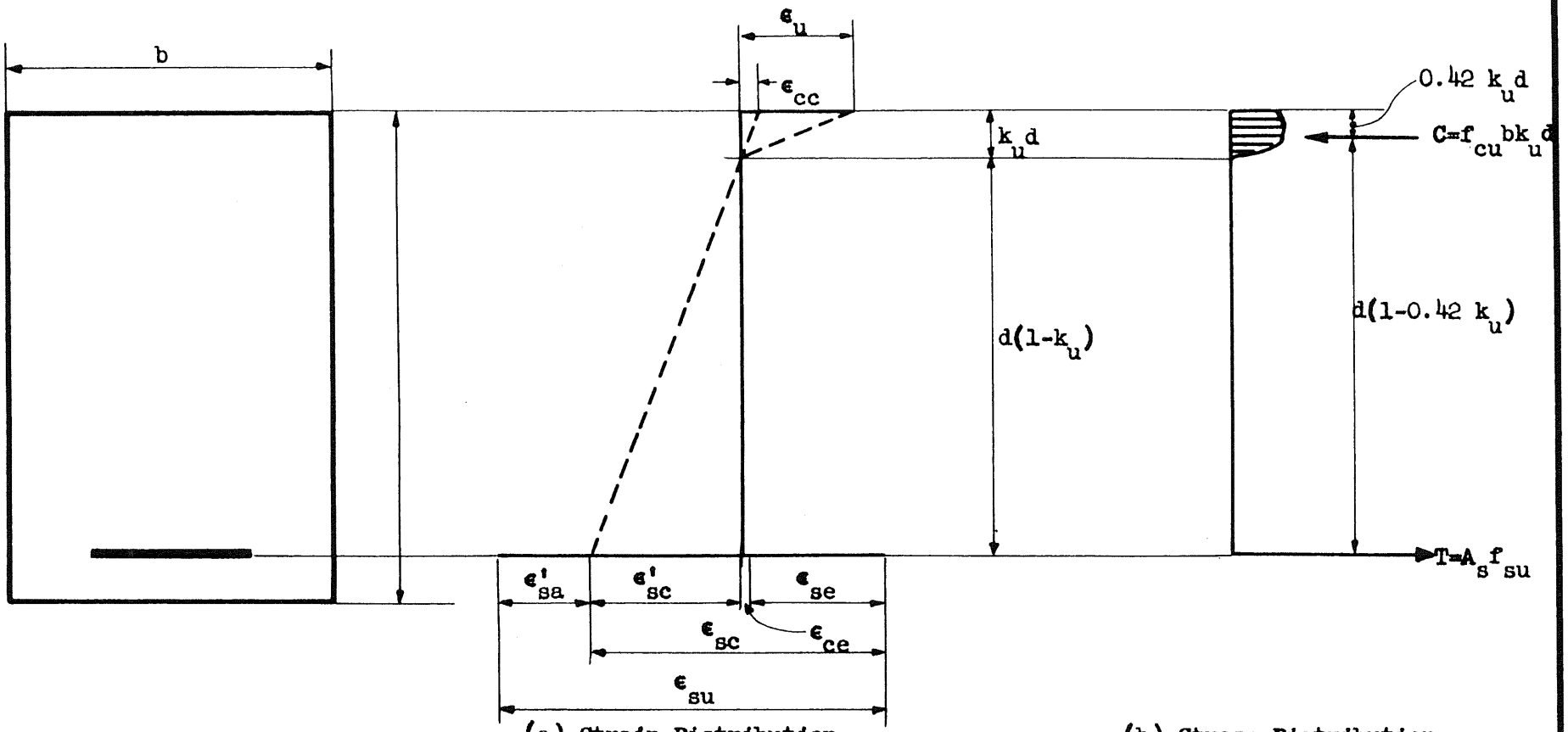

FIG. 57 ASSUMED STRAIN AND STRESS DISTRIBUTIONS AT ULTIMATE FOR BEAMS FAILING IN SHEAR COMPRESSION

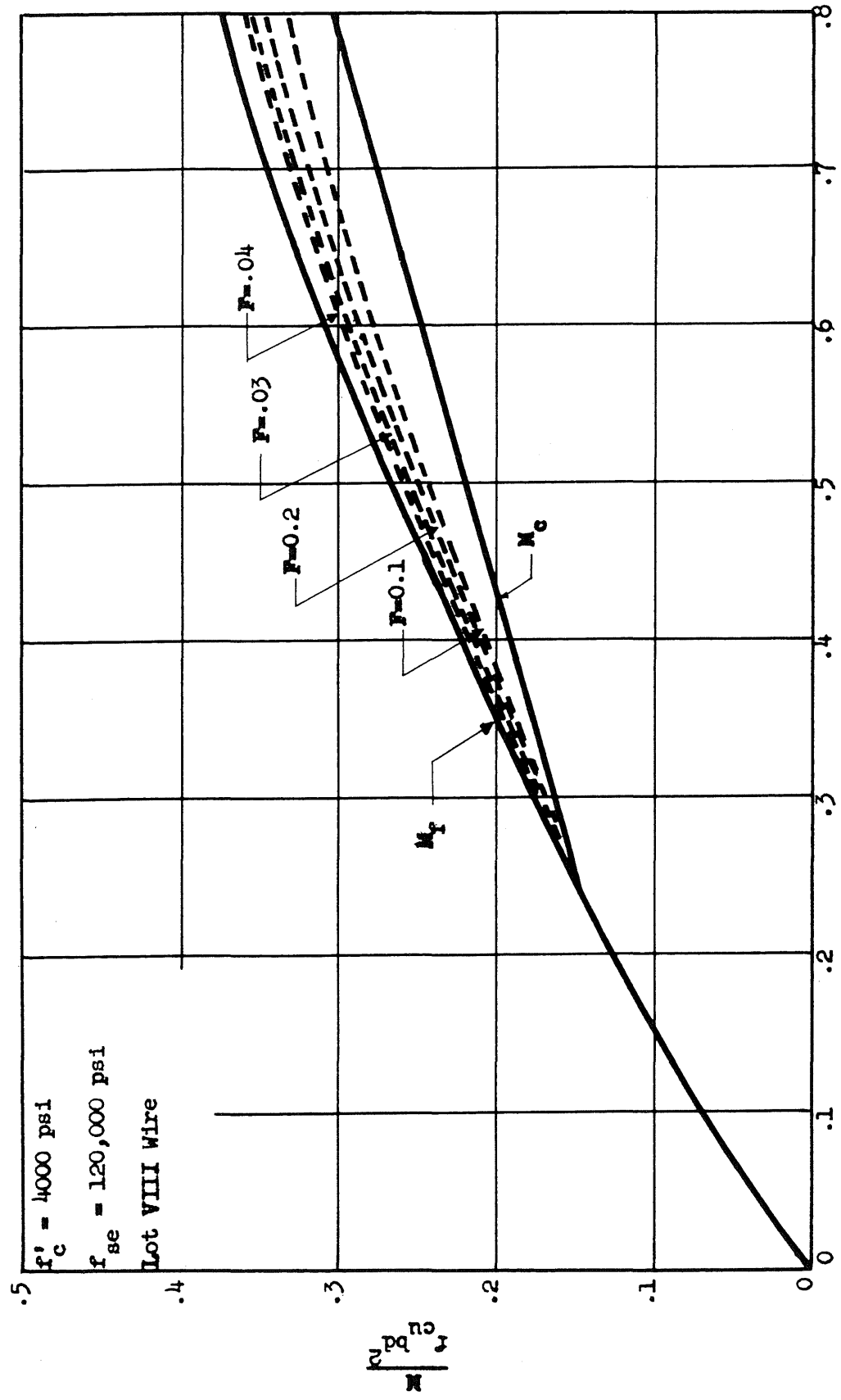

FIG. 58 VARIATION OF MOMENT CAPACITY WITH THE COMPATIBILITY FACTOR, F
RECTANGULAR BEAM

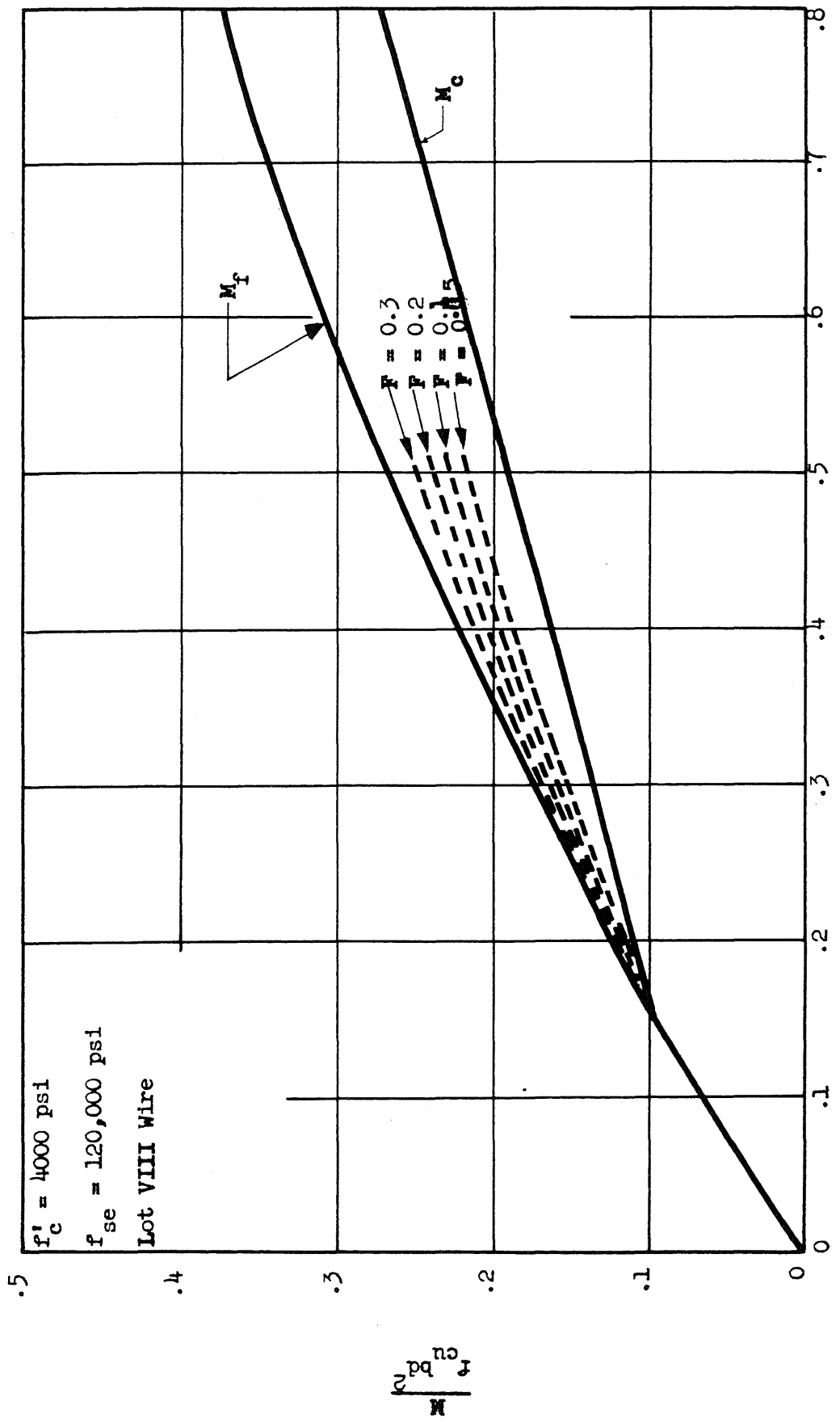

FIG. 59 VARIATION OF MOMENT CAPACITY WITH THE COMPATIBILITY FACTOR, F
I - BEAM WITH THREE-INCH WEB

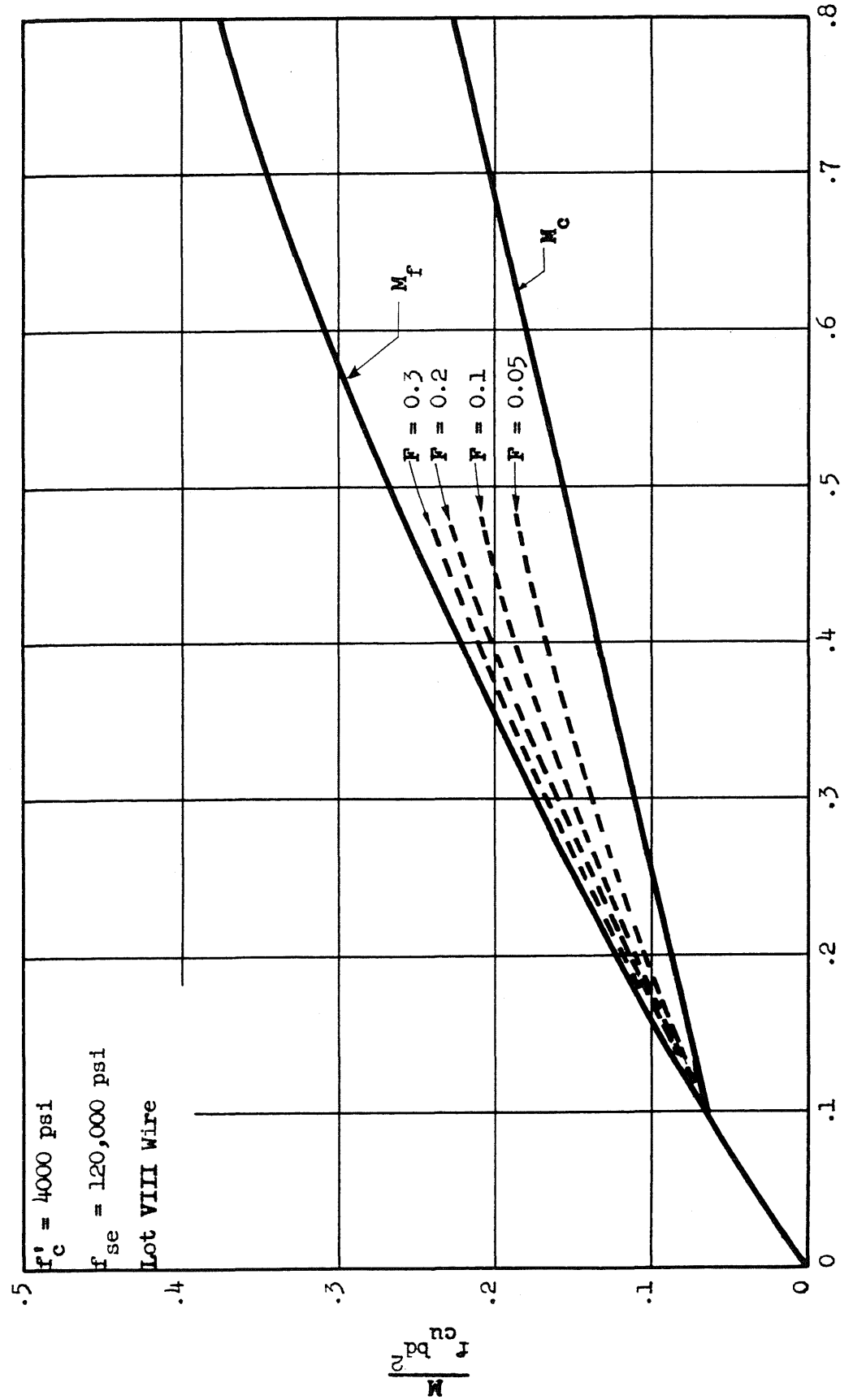

FIG. 60 VARIATION OF MOMENT CAPACITY WITH THE COMPATIBILITY FACTOR, F
I - BEAM WITH 1 3/4 - INCH WEB

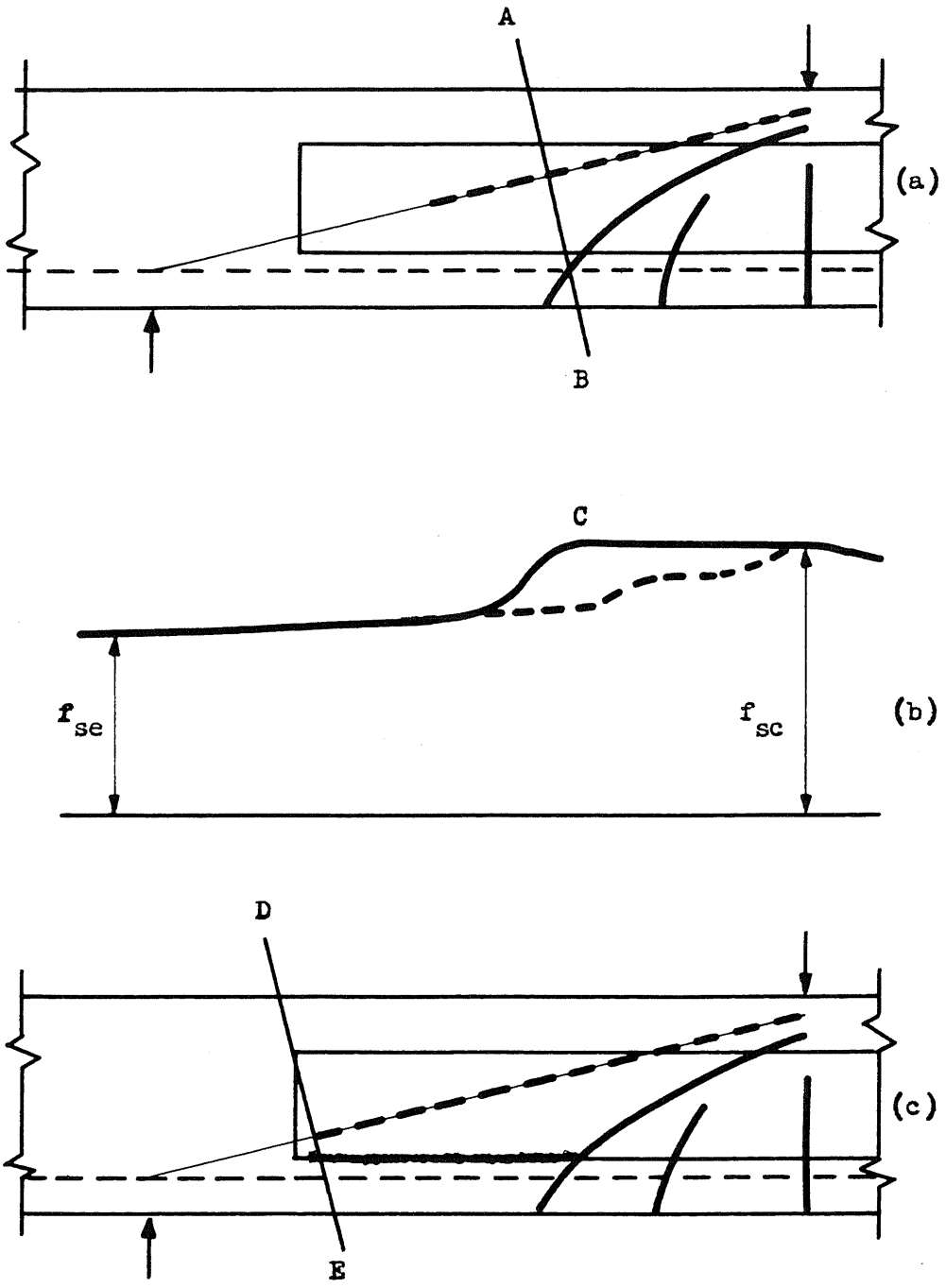

FIG. 61 IDEALIZED CONDITIONS FOR WEB FAILURES

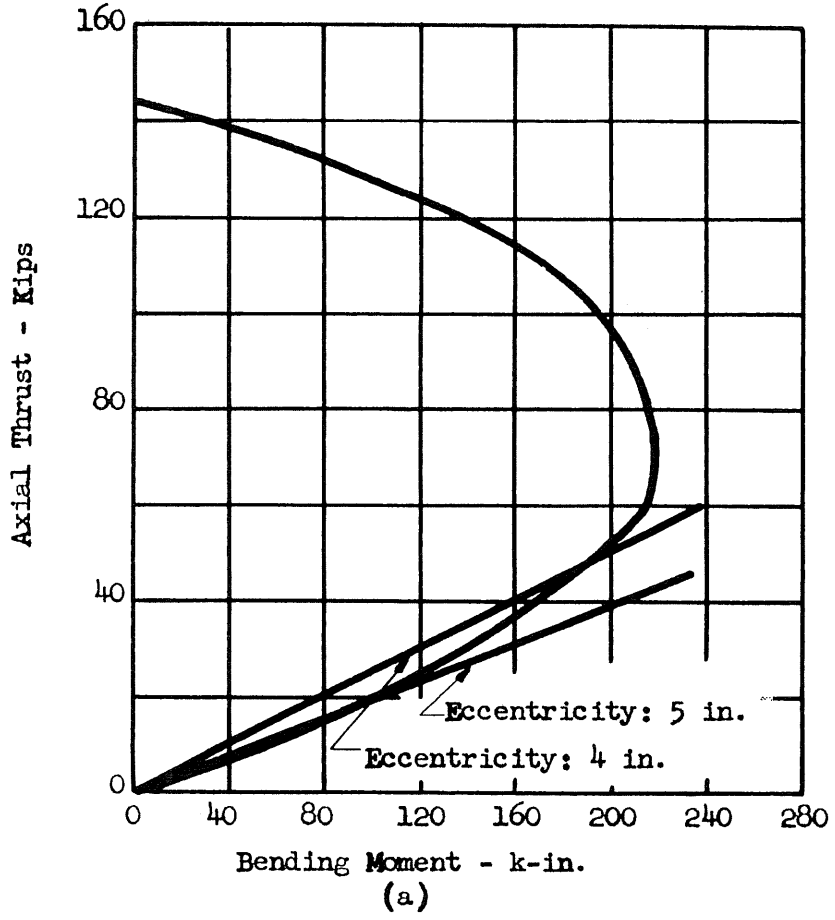

(a)

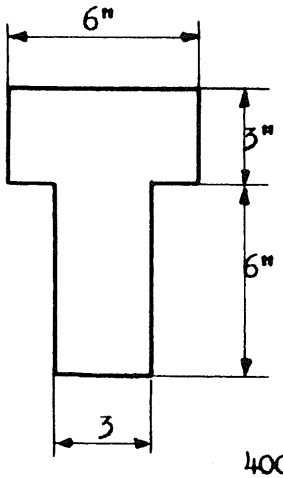

(b)

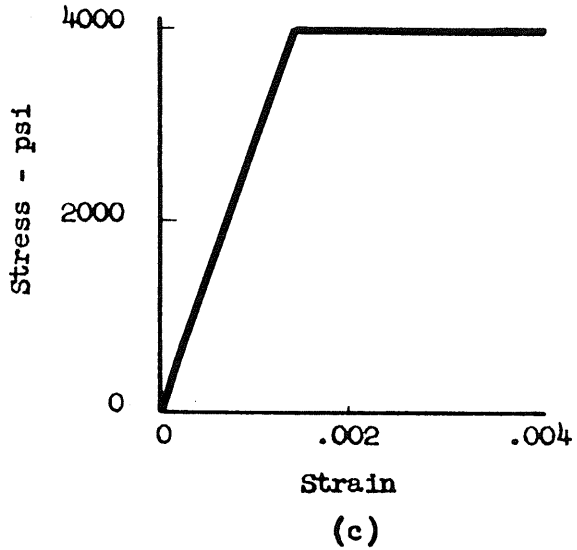

(c)

FIG. 62 INTERACTION CURVE BASED ON IDEALIZED PROPERTIES OF BEAM SECTION

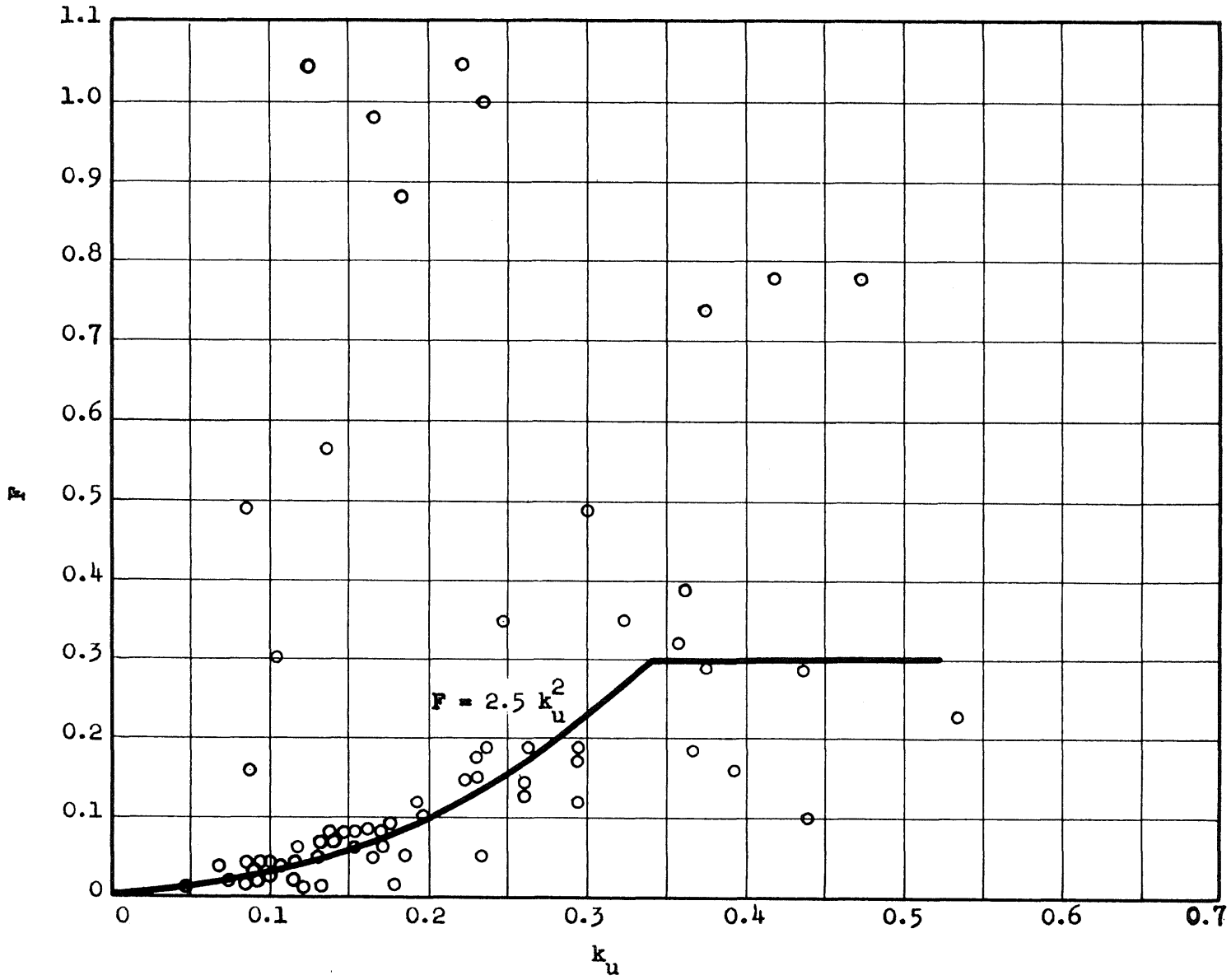

FIG. 63 COMPARISON OF THE DERIVED STRAIN COMPATIBILITY FACTOR WITH THE DEPTH TO THE NEUTRAL AXIS

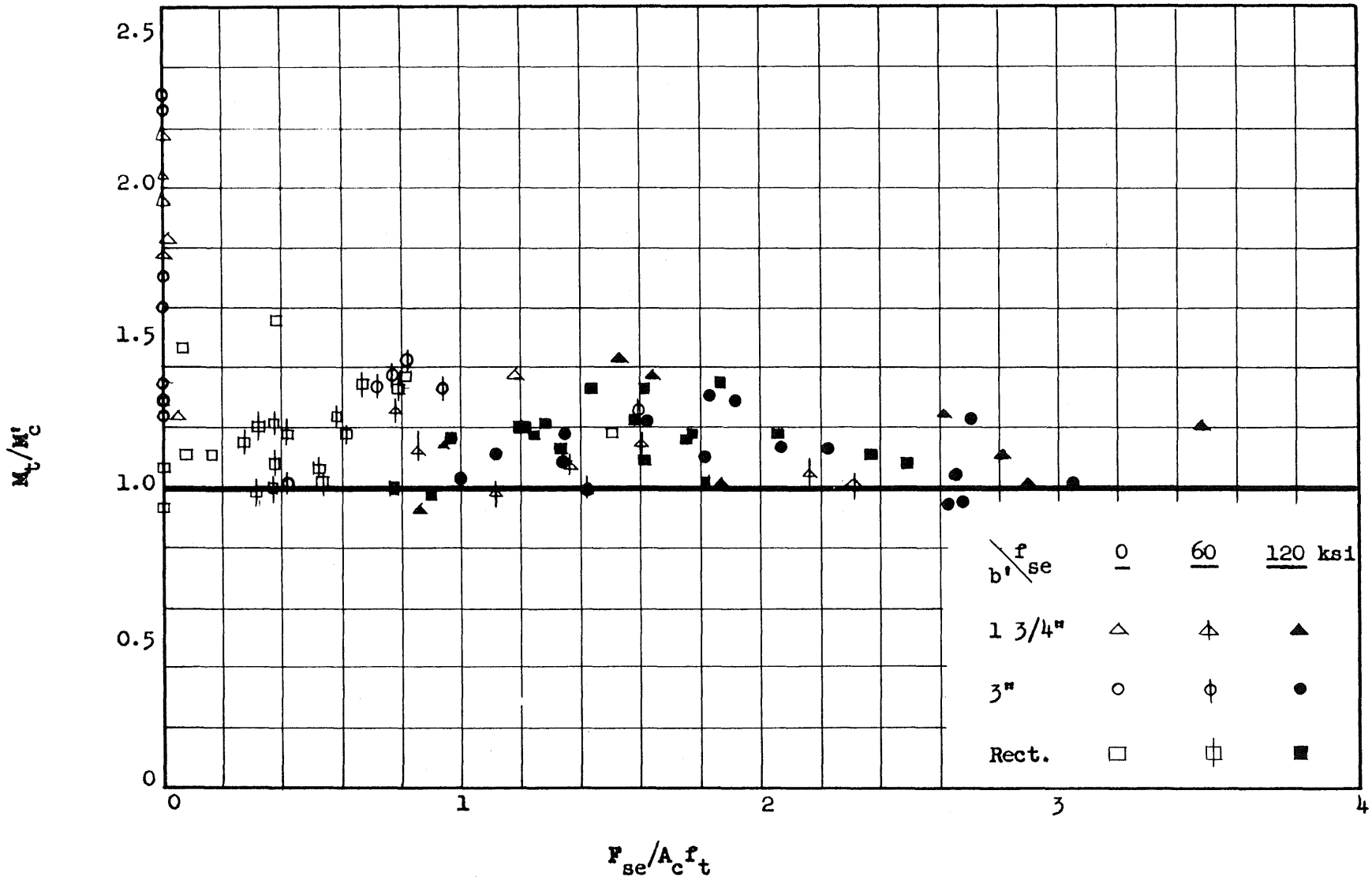

FIG. 64 COMPARISON OF MEASURED ULTIMATE MOMENT WITH COMPUTED INCLINED TENSION CRACKING MOMENT

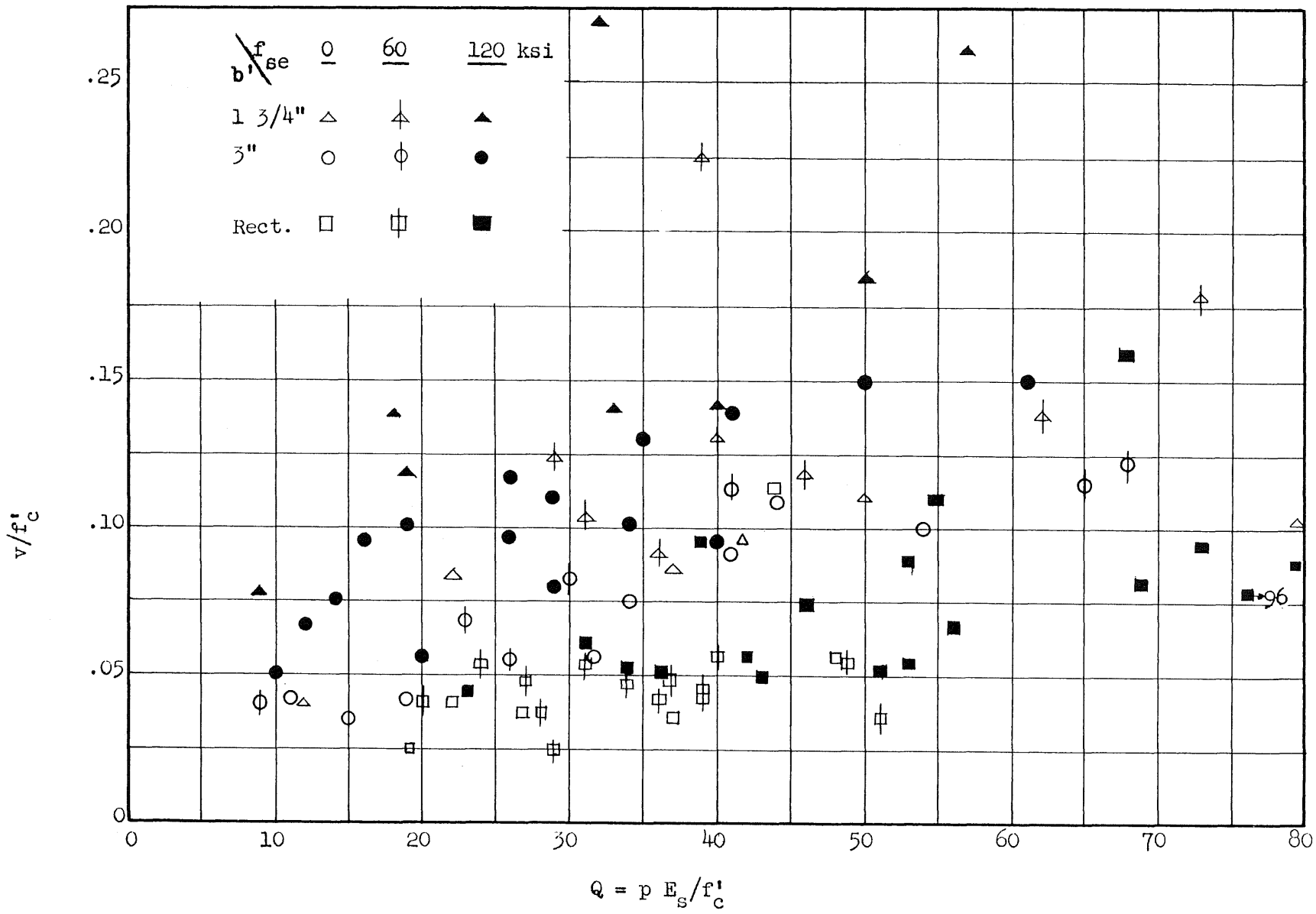

FIG. 65 RATIOS OF ULTIMATE NOMINAL SHEAR STRESS TO CONCRETE STRENGTH FOR BEAMS FAILING IN SHEAR